

# UC San Diego

## UC San Diego Electronic Theses and Dissertations

### Title

Cost of Adaptation in Power Control of Communication Systems

### Permalink

<https://escholarship.org/uc/item/6971v077>

### Author

Ha, Minh Hong

### Publication Date

2015

Peer reviewed|Thesis/dissertation

UNIVERSITY OF CALIFORNIA, SAN DIEGO

**Cost of Adaptation in Power Control of Communication Systems**

A dissertation submitted in partial satisfaction of the  
requirements for the degree  
Doctor of Philosophy

in

Engineering Sciences (Mechanical Engineering)

by

Minh Hong Ha

Committee in charge:

Professor Robert R. Bitmead, Chair  
Professor Massimo Franceschetti  
Professor William M. McEneaney  
Professor Mauricio de Oliveira  
Professor Bhaskar D. Rao

2015

Copyright  
Minh Hong Ha, 2015  
All rights reserved.

The dissertation of Minh Hong Ha is approved, and it is acceptable in quality and form for publication on microfilm and electronically:

---

---

---

---

---

---

Chair

University of California, San Diego

2015

## DEDICATION

To God, my Lord, for His unfailing love and knowledge granted to me.

To my mom, dad and brother, for their unparalleled love and support.

## EPIGRAPH

*Trust in the Lord with all thine heart; and lean not unto thine own understanding.*

*In all thy ways acknowledge Him, and He shall direct thy paths.*

—Proverbs 3:5-6

## TABLE OF CONTENTS

Signature Page	. . . . .	iii
Dedication	. . . . .	iv
Epigraph	. . . . .	v
Table of Contents	. . . . .	vi
List of Figures	. . . . .	viii
List of Tables	. . . . .	ix
List of Acronyms	. . . . .	x
Acknowledgements	. . . . .	xi
Vita	. . . . .	xiii
Abstract of the Dissertation	. . . . .	xiv
Chapter 1	Introduction . . . . .	1
	1.1 Adaptive control and power control . . . . .	1
	1.2 Literature review . . . . .	4
	1.3 Structure . . . . .	6
	1.4 Summary . . . . .	7
	1.4.1 Energy cost of adaptation in power control . . . . .	7
	1.4.2 Power control as a dual adaptive control problem . . . . .	9
	1.5 Contributions . . . . .	10
Chapter 2	Cost of Adaptation in Power Control of Communication Systems . . . . .	13
	2.1 Introduction and literature review . . . . .	13
	2.2 Some definitions . . . . .	18
	2.3 SNR estimation in communication systems . . . . .	20
	2.3.1 System model . . . . .	21
	2.3.2 Channel estimation by least squares . . . . .	24
	2.3.3 SNR estimation . . . . .	27
	2.4 Examination of the SNR estimate . . . . .	33
	2.5 Results in the real-channel case . . . . .	36
	2.6 Link quality and formulation of energy cost . . . . .	39
	2.7 Examination of the total energy cost . . . . .	46
	2.8 Total energy cost with MS mobility . . . . .	49
	2.9 Blind adaptation via hypothesis testing . . . . .	56

	2.10 Conclusion . . . . .	59
Chapter 3	Optimal Mobile Wireless Power Control as a Dual Adaptive Control Problem . . . . .	62
	3.1 Introduction . . . . .	62
	3.2 Literature review . . . . .	65
	3.3 Solution to optimal dual adaptive control . . . . .	71
	3.3.1 Problem formulation and information state . . . . .	72
	3.3.2 Information state update . . . . .	74
	3.3.3 Dynamic programming and control policy . . . . .	75
Chapter 4	ODAC Solutions to the Power Control Problem . . . . .	77
	4.1 Description of the problem . . . . .	77
	4.2 Implementation of the SDP algorithm . . . . .	83
	4.2.1 Information state and its update . . . . .	83
	4.2.2 Duality of the power control problem . . . . .	85
	4.2.3 Dynamic programming and control policy . . . . .	87
	4.3 Heuristics and alternative control laws . . . . .	92
	4.3.1 Heuristics . . . . .	92
	4.3.2 Alternative control laws . . . . .	93
	4.4 Computational results . . . . .	94
	4.4.1 Performance and computation time . . . . .	95
	4.4.2 Examination of control laws . . . . .	97
	4.5 Conclusion . . . . .	100
Chapter 5	Conclusion & Future Direction . . . . .	105
	5.1 Conclusion . . . . .	105
	5.2 Future direction . . . . .	108
Bibliography	. . . . .	113



## LIST OF FIGURES

Figure 2.1:	Communication system structure . . . . .	21
Figure 2.2:	An example of pdf of the SNR estimate, as $\mathcal{F}$ distribution . . . . .	34
Figure 2.3:	Pdf of SNR estimate in both complex-channel and real-channel cases	38
Figure 2.4:	90% confidence interval curves for SNR estimate as $F$ -distribution .	39
Figure 2.5:	Total energy cost: Simulation 1. . . . .	47
Figure 2.6:	Total energy cost: Simulation 2. . . . .	48
Figure 2.7:	Total energy cost: Simulation 3. . . . .	49
Figure 2.8:	Total energy cost with MS mobility . . . . .	56
Figure 2.9:	Number of errors to reject the null hypothesis with 95% confidence	58
Figure 2.10:	Power-of-test values for the first hypothesis test . . . . .	59
Figure 2.11:	Power-of-test values for the second hypothesis test . . . . .	60
Figure 4.1:	Power control problem from the perspective of dual adaptive control	79
Figure 4.2:	Energy cost as a quadratic function . . . . .	86
Figure 4.3:	Histograms of control values. Real fade is equal to $-3\text{dB}$ . . . . .	98
Figure 4.4:	Histograms of control values. Real fade is equal to $-17\text{dB}$ . . . . .	99
Figure 4.5:	Histograms of control values. Real fade is equal to $-7\text{dB}$ . . . . .	100
Figure 4.6:	Histograms of control values. Real fade is equal to $0\text{dB}$ . . . . .	101
Figure 4.7:	Evolution of the information state averaged over 10 realizations of the noise for each adaptive control scheme vs. sample time. Upper plot: real fade is $f[3]$ . Lower plot: real fade is $f[4]$ . . . . .	103
Figure 4.8:	Evolution of the information state averaged over 10 realizations of the noise for each adaptive control scheme vs. sample time. Upper plot: real fade is $f[1]$ . Lower plot: real fade is $f[2]$ . . . . .	104
Figure 5.1:	More complete power control problem in communications . . . . .	108
Figure 5.2:	Full-scale power control in mobile wireless communications in the framework of stochastic cooperative game theory . . . . .	111

## LIST OF TABLES

Table 2.1:	Summary of simulation results . . . . .	50
Table 4.1:	Average empirical performance of the control policies . . . . .	96
Table 4.2:	Computation time of the control laws . . . . .	96

## LIST OF ACRONYMS

- AWGN: Additive white gaussian noise.
- BER: Bit-error-rate.
- BPSK: Binary phase shift keying.
- BS: Base station.
- CDMA: Code-division multiple access.
- CE: Certainty equivalence.
- DAC: Dual adaptive control.
- GSM: Global system for mobile communications.
- LS: Least squares.
- ML: Maximum likelihood.
- MMSE: Minimum mean-square error.
- MS: Mobile station.
- ODAC: Optimal dual adaptive control.
- OFDM: Orthogonal frequency-division multiplexing.
- QAM: Quadrature amplitude modulation.
- QPSK: Quadrature phase shift keying.
- SDAC: Suboptimal dual adaptive control.
- SDP: Stochastic dynamic programming.
- SER: Symbol-error rate.
- SNR: Signal-to-noise ratio

## ACKNOWLEDGEMENTS

Thanks must first be directed to God, my Lord, for Your unfailing love even in the darkest hours of my life, and for Your infinite wisdom, a tiny portion of which has been granted to me to make this work possible and to help me become a much better person than I was before I knew You. Thank You, Lord, for saving my soul!

For mortals, my most sincere thanks must be given to Professor Robert Bitmead at MAE Department, my first ever mentor and chair of my doctoral committee. Bob, you have set a great example of how a mentor should be and you will remain among the best I have and will have ever worked with. Your knowledge, patience, support and dedication have been invaluable over the past five years of my doctoral study. This work could never have been possible without the uncountable hours you have spent on meeting with, teaching and advising me, both as an academic advisor and as a friend. You have also taught me a great deal on the philosophy of being an engineer. I really wish I could work longer with you because I know there are still many things, engineering or otherwise, that I could learn from you. I truly appreciate your unparalleled efforts to keep me funded even in the most difficult time, your patience with such an average student as myself and your help with preparing me and influence in looking for my first job in the industry.

I would also like to thank the personnel at the University of California, San Diego for the help over the past five years. Thanks are also given to Professor James Friend, a new faculty member of MAE Department, who helped get me to where I am now by believing I could walk on waters. I would also like to acknowledge the world-class faculty of my doctoral committee members: Professor William McEneaney, Professor Mauricio de Oliveira, Professor Bhaskar Rao, and Professor Massimo Franceschetti.

Thanks must also be given to my family for their unconditional love and supports. I could never have gone this far without you, Mom. You have been taking care of me in almost everything, from the encouragement you have given me to even the visa paperwork

when I first set out to go to Australia for college. Thanks to Dad, for your enormous effort and strange way to teach me to become a better person. Thanks to Tú, my Brother, for the countless hours of fun and great memories, and for being the best brother I could have personally.

Chapter 2 and Chapter 4, in full, are currently being prepared for submission for publication of the material, by M. H. Ha and R. R. Bitmead. The dissertation author was the primary investigator and author of this material.

## VITA

- 2009 Bachelor of Science in Mechanical Engineering, Monash University, Melbourne, Victoria, Australia.
- 2011 Master of Science in Mechanical Engineering, University of California, San Diego.
- 2015 Doctor of Philosophy in Mechanical Engineering, University of California, San Diego.

## PUBLICATIONS

M. H. Ha and R. R. Bitmead, "Performance cost of adaptation in mobile wireless power control," in *IEEE 2013 European Control Conference*, Zurich, Switzerland, July 2013, pp. 2257-2262.

ABSTRACT OF THE DISSERTATION

**Cost of Adaptation in Power Control of Communication Systems**

by

Minh Hong Ha

Doctor of Philosophy in Engineering Sciences (Mechanical Engineering)

University of California, San Diego, 2015

Professor Robert R. Bitmead, Chair

Power control has become an important aspect of any communication system such as cellular networks, wireless LANs and DSL modems. Power control offers many benefits: optimizing the SNR in the link, conserving the battery life and minimizing the interference between the transmitter terminals. Power control is recognized as adaptive control. Here, we consider solely the optimization of the battery life and assessing the total energy cost in power control. The power control problem is formulated in a communication link with a static complex gain and a single transmitter, corrupted by complex normal noise. The channel estimate is computed by least squares using pilot tones. Then the signal power and noise power estimates are calculated, and ultimately the

SNR estimate and its statistical properties. Based on this SNR estimate, an appropriate power level can be chosen for data transmission. The total energy cost of the power control process is formulated with aid of the statistics of SNR estimate. The cost is found to exhibit a pathological behavior, where a transmitter should send an infinite number of pilot tones at zero transmitted power to minimize the non-zero total energy cost of power control. When the transmitter is moving, however, this pathological behavior disappears.

Next we look at the power control problem from the perspective of ODAC. The dual feature of the problem is that to probe the link effectively, the transmitter must use a large power level, but this affects the control process negatively as it increases the overall energy cost. A balance between the two aspects must be obtained. Assuming some *a priori* information about the fade is known, we use SDP, with aid of the information state that describes the evolution of the fade's statistics as measurements are obtained and controls applied, thus acquiring ODAC solutions to the power control problem. The solutions are found to depend greatly on what we know beforehand about the channel, a feature that is not present in current power control algorithms. We also develop heuristics that help reduce the computational demand due to SDP algorithm.



# Chapter 1

## Introduction

### 1.1 Adaptive control and power control

In everyday language, “to adapt” is to change a behavior to conform to new circumstances. An adaptive system is one that can modify its behavior in response to changes in the dynamics of the process and the character of the disturbances. Therefore, adaptive control is a variation of feedback since the latter also attempts to reduce the effects of disturbances and uncertainties [1]. However there appears to be a consensus that a constant-gain feedback system is not an adaptive system. Over the year, despite many attempts to define adaptive control formally, an exclusive definition of adaptive control still does not exist. Even expert committees failed to settle on an unanimous definition. For the purposes of this work, an adaptive controller is defined as a controller with adjustable parameters and a mechanism for adjusting the parameters. Because of the adjustment mechanism, an adaptive controller exhibits nonlinear behaviors, that are hard to analyze in general. The adjustment mechanism can be achieved in several ways, such as gain scheduling, auto-tuning, self-tuning control and dual control. A control engineer should have sufficient knowledge about adaptive systems because they possess useful

properties that can be used to design control systems with improved performance and functionality. It has also been found that adaptive techniques can also be used to provide automatic tuning of controllers.

Generally speaking, adaptive systems are dynamic systems which involve an explicit learning or adjustment component in which a number of parameters are adapted based on input-output data. The dynamics of adaptation or learning have been studied by many researchers in dynamic systems theory and in static machine learning contexts and focus on the evaluation of a learning rate characterizing the convergence properties of the parameter estimates as the number of training data increase, and the dependence of this rate on the complexity of the parametrized class of functions, the desired probabilistic accuracy of the estimate, the data quality, and the properties of the underlying target system dynamics. Within adaptive systems, adaptive control is perhaps the most difficult to characterize because of its extraordinarily nonlinear behavior and the potential loss of stability due to adaptation.

Power control in mobile communication systems fits well under the framework of adaptive control, where a transmitted power for the transmitter is to be selected with aid of channel estimation. Power control algorithms are used in contexts such as cellular networks, wireless local area networks and digital subscriber line modems. The benefits of adaptation in power control are many: optimizing the SNR in the communication link, increasing spectral efficiency, protecting against fading, conserving the transmitter's battery life and reducing the interference between neighboring transmitters, increasing the link data rate and network capacity, and maximizing geographic coverage and range. Here, the fading in the communication link can be viewed as the variability of the process due to the mobility of the MS. The adjustable parameter is the transmitted power level of the transmitter, and the adjustment mechanism is the power control algorithm. In this thesis, we focus solely on the energy question and explore the determination of the

correct transmission power at, say, the MS transmitter using feedback information from its serving BS receiver. The central question is the estimation of the appropriate operating SNR at the receiver and then the subsequent selection of the appropriate transmission power to maintain the BER at the receiver at a sufficiently low level (e.g.  $10^{-2}$  [2]) so as to permit error detection and correction codes to recover the message reliably.

The process of adaptation in power control, however, comes at a cost. Usually, the adaptation in power control of communication system depends mostly on the pilot, or training, sequences. Pilot sequences are deterministic signals that are known to both the transmitter and the receiver. For example, in mobile wireless communications, a pilot sequence can be a BPSK signal stream that is known to both the MS and the BS. In fax machines, a pilot sequence is a sequence of tones that is also known to both the transmitter and the receiver machines; this is the source of the familiar signature tones that are heard in every fax machine upon startup. The purpose of the pilot sequence, in general, is to estimate the communication channel quality (in the case of the fax machine), or to mitigate the effects of interference between transmitting terminals, or both (in the case of mobile phones). Channel estimation allows the transmitters to choose an appropriate transmitted power level to acquire the aforementioned benefits. Intuitively, the cost of this adaptation process can be seen as the energy spent on the information-free pilot sequences to probe the communication links, the time it takes for the links to be estimated, and the reduction in the channel capacity, as the pilot sequences are often embedded into the data stream in the mid-amble or pre-amble section. A good power control algorithm must strike a balance between the said benefits and drawbacks based on the performance criteria that are most important to the designer and end-users.

## 1.2 Literature review

Research on adaptive control can be traced back to the early 1950s. It was motivated by design of autopilots for high performance aircraft that operate over a wide range of velocities and altitudes [3]. It was found that while an ordinary constant-gain linear feedback controller may perform well, difficulties may arise when operating conditions change. This necessitated a more complicated control algorithm, which is found to be adaptive in nature. At the time, interest in the area was diminished due to lack of insights and a disaster in a flight test [4]. The effort was re-kindled in the 1970s, when the progress in research on control theory from previous decades helped improve the knowledge about adaptive control. This was further expedited by the rapid development of microelectronics that allowed the implementation of adaptive control policies in simple and cheap ways. Nowadays, as adaptive control gains more attention because of its many significances and benefits and advantages, a significantly large portion of the literature is dedicated to adaptive control. There are so many works on adaptive control that the review of them all would not fit into this thesis. For surveys, the readers are referred to [5, 3, 6, 7, 8, 9, 10].

As an adaptive system that changes its behavior according to the current condition of the communication link, power control in communication systems has become significant because of the benefits stated previously. There are many algorithms to perform power control process, which depends on the purposes and performance criteria of the network in consideration. For example, in GSM-1900, also known as PCS-1900, the MS is instructed to change the transmitted power level in steps of 2dBm [11, 12] to maintain a certain criterion regarding the SNR in the communication link while reducing the interference between the MS terminals to ensure quality of service.

More examples in power control research can be found in [13], where the au-

thors investigate the power control problem in a single-cell CDMA wireless data system with many users in a viewpoint of game theory and Pareto efficiency, where each user minimizes its own utility. In [14, 15], an approach to power control in wireless systems is proposed based on an economic model, where the service preference for each terminal is presented by a utility function—the level of satisfaction a user gets from using the system resources. In [16], the power control-based multiple access algorithm for contention-based wireless *ad hoc* networks is analyzed via investigating the similarities and differences between problems previously solved for cellular networks. In [17], the problem of cross-layer design of joint multi-user detection and power control is tackled in the setting of non-cooperative game theory to optimize the energy efficiency for CDMA system. Numerous other papers are also dedicated to the subject because of its importance. A good survey of power control algorithms in wireless communication can be found in [18, 19].

The cost of adaptation in power control, however, has not been fully investigated nor appreciated. There are a few texts that have a remotely similar theme in a multiuser context, such as [20] where the authors present an approach to estimating SNR using a pilot sequence. They however go no further in applying the algorithm to an adaptive power control context, or quantifying the cost associated with the channel estimation scheme. Goldsmith [21] includes solutions to variable modulation and coding problems and power control based on SNR (or signal-to-interference-noise ratio in the case of multiuser networks) but does not formalize the uninformative energy required to carry out the algorithms. Various studies [22, 23, 24] also deal with many types of adaptation problems such as rate, modulation, power and coding adaptations but none has taken into account the tradeoffs in terms of energy. Chi et. al. [25] also aim to design an optimal training sequence in OFDM system with minimum mean square error criterion and examine the tradeoffs that are inherited in OFDM such as peak-to-average power

ratio and phase noise. However the paper considers a fixed amount of transmitted energy and is not concerned with finding the optimal amount.

### 1.3 Structure

The structure of the thesis is as follows. In Chapter 2, the investigation of the cost of adaptation in power control of communication systems with static channels is presented. This includes the formulation of channel estimation using LS and the resulting link SNR estimate, followed by the formulation and investigation of the total energy cost of power control, which is an adaptation process. Next, the case where then transmitter is moving, making changes in the channel, is analyzed. In the end of Chapter 2, a blind adaptation technique based on hypothesis testing is also proposed to compare to the current data-aided techniques using pilot sequences.

In Chapter 3, we reformulate the power control problem from the perspective of dual adaptive control. In order to solve the problem from the viewpoint of dual adaptive control, in this chapter, we present the preliminaries regarding the SDP algorithm that includes Bellman's equation. The optimal control policy is then formulated based on the SDP algorithm.

In Chapter 4, the power control problem in communication networks from the perspective of dual adaptive control is formally formulated, with reduced complexity where the MS and BS can share their information about the system. Then, application of the SDP algorithm to obtain the solutions to the problem is presented. Next, some heuristics are recognized and consequent control laws proposed. In the end of the chapter, a simulation is investigated which includes the implication of the solutions of the system's performance as well as the computational burden that the problem bears.

In Chapter 5, we conclude our results in the thesis and formulate the more

complete optimal power control problem where we remove the assumption that the transmitter and receiver can share their information. Next, we highlight some interesting areas that possess connection to the problems we have considered, that can offer alternative solutions to our problems.

## **1.4 Summary**

This section summarizes the results found during our investigation of the problem of identifying the cost of the adaptation process in power control of communication networks.

### **1.4.1 Energy cost of adaptation in power control**

The first problem we shall analyze is regarding the energy spent on power control of communication systems. For simplicity and investigation purposes, we only consider the context of a single-user in a static channel setting (e.g block fading), where the signal is corrupted by circularly symmetric complex AWGN. For channel estimation purposes, first we assume the use of pilot tones. Based on a number of pilot tones, we use the LS estimation technique to examine the condition of the communication link between the transmitter and the receiver stations. Then, based on the channel estimate, the noise and signal power estimates can be found, followed by the estimate of the SNR of the link and its probabilistic properties. The SNR estimate computed by our proposed technique is found to be distributed as an  $\mathcal{F}$  distribution, familiar from the analysis of variance, with parameters as functions established through the available information of the communication link. Following the statistics of the SNR estimate, an optimal transmitted power level for the data stream can be chosen to meet a criterion regarding a certain reference value of the BER in the link. This is to ensure the quality of service.

Regarding the SNR estimate, we find that to minimize its variance, the optimal strategy is to let the transmitted power for pilot tones go to zero, and then to use an infinite number of pilot tones to estimate the channel.

The total energy cost of the adaptation process of the power control algorithm described above is then formulated. This includes the energy spent on the pilot tones as well as on the data symbols. However, when the transmitted power for the data stream is selected wrongly, either the energy spent has an overhead as wasted energy due to higher-than-necessary power, or, in the case of insufficient power, the energy has to take into account the retransmission of the data symbols as a result. These energy terms can all be computed as functions of the SNR estimate.

It is found that in the case under consideration, where the link is static and characterized by a single complex channel gain, the total energy cost of adaptation exhibits a pathological behavior. The pathological behavior is that in order to minimize the total energy cost, the transmitter should use an infinitely large number of pilot tones at zero power to work out the link conditions, just like the optimal strategy to minimize the variance of the SNR estimate, because the total energy cost is actually a function of the SNR estimate. The result implies a conundrum in the methodology to minimize the cost of adaptation in static channels. When the channel does not change, one can spend an infinite amount of time to investigate the link condition at minimal energy cost.

However, when the MS transmitter is assumed to have a velocity, the total energy cost is modified to take into account the change in the channel condition due to the MS mobility. The above pathological behavior of the total energy cost disappears when the MS mobility is introduced. In this case, there exists an optimal pilot length  $K$  and pilot transmitted power  $P_0$  that results in the smallest minimum of the total energy cost across the range of the pilot transmitted power.

We also propose a non-data-aided, known as blind adaptation, technique to apply



to the power control problem. It is, however, found that in the setting of mobile wireless communication, the blind adaptation algorithm takes too long to compute the BER of the link, making it unimplementable.

### 1.4.2 Power control as a dual adaptive control problem

In the next part of the thesis, we look at the power control problem from the viewpoint of DAC, which is a subclass of adaptive control. Here, the data-aided technique using pilot tones is employed once more in a AWGN channel with a constant gain (fading coefficient). Further, we assume that the transmitter and the receiver can share their knowledge. This greatly simplifies the problem, even though finding the solution is still tedious labor. The optimal stochastic power control algorithm in fact exhibits the behavior of a dual adaptive control system. First, in order to probe the communication link as precisely as possible, the transmitter has to inject a large power level into the pilot tones. However, in so doing, the energy cost increases, which is undesirable. A good power control algorithm must strike a balance between probing the link and minimizing the total energy spent, or regulating the system. This is the essence of DAC. The balance can be accomplished by applying the SDP algorithm that is notoriously demanding in computational power due to its *curse of dimensionality* in solving the Bellman equation. This is demonstrated in our simulation example where, with a time horizon of 4 and 4 state values, it takes almost an hour to complete a simulation session in `matlab`.

The solution to the power control problem as an ODAC problem is found to depend greatly on what is known about the channel's statistics before carrying out the SDP algorithm, that is, the *a priori* information about the fading of the channel. The probability distribution of the fade changes when a measurement and a control have been produced, and is known as the *information state* of the system. We develop the formulation to update the information state using the data accumulated over time when

controls are applied and measurements received. Hence, a significant distinction between non-dual control and dual control is the dependence of the future information about the communication link upon the control signal applied. This further enhances the estimate of various parameters of the channel, which consequently improves the regulation process and performance of the system.

In the work, we investigate both the control (the selected transmitted power level) and the evolution of the information state, both of which depend greatly on the controls applied and measurements acquired over time. This complicated relation is embedded in the recursive equations of the SDP algorithm. Based on these findings, we establish some heuristics about the power control process and compare the ODAC solution to the certainty equivalence principle and other control laws based on these heuristics. The comparison is made with regard to the cost function in terms of energy, conditioned on the measurements and controls over time as well as the noise in the channel.

The implication of our results is that the power control problem is in fact a DAC problem. When treated so and solved accordingly, the transmitted power level can be selected accurately to overcome the fading in the environment without resulting in too much energy spent. On the side line, the information about the communication link is continuously acquired over time which contributes greatly to subsequent transmission of data. This is a great improvement when compared to current power control algorithms in the industry which do not take into account the effect of the control on the evolution of the information about the channel.

## **1.5 Contributions**

The first part of the thesis, which is Chapter 2, has the following contributions.

- We propose a SNR estimation technique in in communication networks with

complex channels. This can be view as an extension from [26] who investigated the case of real channel. Our extension makes the technique appropriate for modern systems, such as OFDM.

- We pose, analyze and optimize the total energy cost of the power control algorithm, including the energy cost of adaptation.
- We expose a conundrum in SNR estimation where the channel is static, in which to optimize the total transmitter energy, the MS should use an infinite number of pilot tones at zero transmitted power. The total energy cost of power control exhibits the same behavior because it is based upon the statistics of the SNR estimate.
- We introduce MS mobility, making the channel vary as the MS moves. The total energy cost is modified to take into account the change in the channel condition due to the MS mobility. The above pathological behavior of the total energy cost disappears when the MS mobility is introduced. In this case, there exists an optimal pilot length  $K$  and pilot transmitted power  $P_0$  that results in the smallest minimum of the total energy cost across the range of the pilot transmitted power.

The rest of the thesis has the following contributions.

- We recognize that the power control problem in communication networks is a stochastic optimal control problem. We further expose its dual character and classify it as a DAC problem.
- The ODAC problem we set up and solve is associated with a practical (power control) problem and is among the first thorough analysis and computation of an ODAC problem, as opposed to adaptive control with dual aspects.
- We determine the effect of the control signal on the distribution of the varying

parameter (fading), known as the information state of the system. The update of the information state once the controls have been applied is also computed.

- We draw heuristics upon our findings: the first optimal control at time 0 can be calculated offline and the power control algorithm following CE principle, and the propagation of the *a priori* knowledge about the channel through time can be determined.
- We expose and quantize the computational intractability of the problem caused by Bellman equation in the SDP algorithm.
- We make comparison between various control policies and highlight what optimality offers and at what cost.
- We expand the problem further, considering the case where the MS and BS are no longer able to share their information. We explore the possible alternative solutions to the problem offered by other fields.

## **Chapter 2**

# **Cost of Adaptation in Power Control of Communication Systems**

In this chapter, we shall consider the cost of adaptation in power control of communication systems. First, using pilot tones, we look at the problem of estimating the channel in a communication system, which can be real (e.g. real channel with BPSK signal), or complex (e.g. in the case of OFDM system). The channel estimation allows both signal and noise power estimates to be computed. The SNR estimate can then be calculated, and an appropriate transmitted power level chosen to transmit the data stream at a desirable level of BER. Finally, the total energy cost of the whole power control process will be formulated and its behavior analyzed.

### **2.1 Introduction and literature review**

In communication networks, power control is an adaptive system that adapts to the changes in channel condition. The power control algorithm operates billions and billions of time everyday without human intervention. Power control in mobile wireless

systems is associated with the management of energy consumption in the transmitting devices and also with the interference between devices. Its many other benefits are also outlined in Chapter 1. Here we focus solely on the energy question (e.g. preserve the battery life of the transmitter) and explore the determination of the correct transmission power at, say, the MS using feedback information from its serving BS. The central question is the estimation of the operating SNR at the receiver and then the subsequent selection of the appropriate transmission power to maintain the BER at the receiver at a sufficiently low level (e.g.  $10^{-2}$  [2]) so as to permit error detection and correction codes to recover the message reliably.

Power control requires the knowledge of the communication channel which can be obtained by channel estimation techniques. A standard way to estimate the channel is to use a pilot, or training, sequence that is known to both the MS and BS. To aid the pilot-based channel estimation, much of the literature has been dedicated to optimal design and placement of the pilot symbols within the data block, which have a significant effect on the overall performance of the system [27, 28, 29]. For example, in [30], the problem of optimal design and placement of the pilot tones for channel estimation is considered, where the Cramer-Rao Bound of mean square error of the channel estimator is minimized for both single-input single-output and multiple-input multiple-output systems. In [29] and [31], the authors consider the optimization of pilot tone selection that minimizes the mean square error of the MMSE estimator for OFDM. In [32], the author analyzes the optimal performance of two pilot-assisted schemes in various aspects of CDMA. In [33], the authors look into the optimization of the pilot tone design and placement in multiple-input multiple-output OFDM systems, where LS estimator is used and the pilot tone design and placement is optimized with respect to the estimator's mean square error, with an additional analysis of LS estimator over multiple OFDM symbols and of a recursive LS algorithm to enhance the channel estimation performance.

A large portion of the research work has been on channel estimation and the design of the pilot sequence used in channel estimation of OFDM specifically. With pilot tones, channel estimation can be performed by either inserting the pilot tones into all of the subcarriers of OFDM symbols with a specific period, known as block-type pilot, or inserting them into each OFDM symbol, known as comb-type pilot [34]. Generally, block-type pilot is applicable under the assumption of slow fading channel, meaning that the channel transfer function is not changing very rapidly. There are two widely employed estimator for the block-type pilot, namely LS and MMSE. With MMSE, channel estimation is based on cascading two one-dimensional finite impulse response interpolation filters whose coefficients are based on MMSE criterion [35]. LS and MMSE are described in detail in [36] where the latter is shown to be better in terms of SNR performance for the same mean square error of the channel estimation. When the channel changes even in one OFDM block, the comb-type pilot is introduced. This kind of pilot estimates the channel at pilot frequencies and interpolates the channel. The former can be based on LS, MMSE or least mean square. The latter can make use of many interpolation techniques such as linear interpolation, second order interpolation and low-pass interpolation. There are many papers devoted to channel estimation techniques used in OFDM. In [37], the full review of well-known channel estimation techniques used in both block-type pilot and comb-type pilot is presented, with various modulation schemes such as QPSK, 16QAM, BPSK and differentially encoded QPSK. A study of iterative channel estimators for mobile OFDM systems is presented in [38]. Also in [39], a thorough comparison of various pilot-aided channel estimation methods is made. Here the ML estimator is found to be simpler to implement than the MMSE estimator, because it does not require knowledge of channel statistics and SNR. But MMSE performs better when prior information about the channel is available. In [40], a low-rank approximation of the linear MMSE estimator for block-type pilot is considered,

by utilizing the frequency correlation of the channel to eliminate the major drawback of MMSE which is computational complexity. In [41], the complexity of the MMSE estimator in comb-type pilot is also reduced by deriving an optimal low-rank estimator with singular-value decomposition. The authors also show that the 2nd order interpolation performs better than the linear interpolation. In [42], time-domain is shown to give lower BER compared to linear interpolation. In [43], the authors use piecewise constant and piecewise linear interpolations between pilots, that are easy to implement but need large number of pilots, thus affecting channel capacity. The MMSE estimator is also studied in [44] that exploits channel correlations in time and frequency domains, that require knowledge of channel statistics and SNR. In [45], channel estimation is performed by 2D interpolation between pilots, which is robust to Doppler shifts even though the performance is reduced with lower Doppler frequencies. The ML estimator is also investigated in [31]; it does not need any information on the channel statistics or the operating SNR. In [46], the authors propose another channel estimation technique with iterative filtering and decoding in a flat fading environment for a single-carrier BPSK modulation scheme. The idea is to feed the information from the output back to the estimation stage that improves the performance by collecting information from both pilots and coded bits.

Much effort is also devoted to SNR estimation in communication networks, as this is very important to improve system performance, such as adaptive coding and modulation [47], soft decoding procedures [48] and channel assignment [49]. One of the first to examine channel estimation is [50] in the context of real-channel with BPSK pilot signal, using the ML estimator, later perfected by [26]. The formulation of the split-symbols moments estimator algorithm proposed by Simon and Mileant [51] assumes BPSK modulation in a wide-band AWGN channel. The application of second- and fourth-order moments to the separate estimation of carrier strength and noise strength



in real AWGN channels to estimate channel SNR appears in [52, 53, 54]. An excellent overview of SNR estimation techniques can be found in [55]. In [56], under the context of multi-input multi-output OFDM, Boumard estimates the signal power by the channel coefficients available in the channel estimation, where the coefficients of the adjacent subcarriers are assumed to be the same. The assumption however is invalid in highly frequency selective multi-path channels, leading to the degradation of the performance. In [57], the authors use a subspace-based method to estimate the SNR using the estimated coefficients of the pilot subcarriers in the OFDM packet. The method possesses high complexity and the overall performance relies greatly on the number of pilot tones. In [57], the properties of the correlation of pilot data in time-domain is utilized to estimate the average SNR. This method also depends much on the number of pilots. In [58], using pilot tones in frequency selective channels, a SNR estimation technique is proposed, where, to be able to estimate the noise variance, it is required that the preamble contains two or more symbols with the same structure or one symbol with many identical parts. In [59], the authors develop a SNR estimation technique that estimate the colored noise variance instead of the usual assumption of white noise. In [60], another pilot-based SNR estimation technique is proposed based on periodically used subcarriers and the time domain periodic preamble structure for time and frequency synchronization. Some other authors have proposed non-pilot-aided SNR estimation schemes [61], but they have not become popular and are out of the scope of this thesis.

The cost of adaptation in power control of communication systems, however, has not been fully investigated nor appreciated. In general, with papers concerned with estimating the channel or SNR using pilot sequences, they however go no further in applying the algorithm to an adaptive power control context, or quantifying the cost associated with the channel estimation scheme. Goldsmith [21] includes solutions to variable modulation and coding problems and power control based on SNR (or signal-

to-interference-noise ratio in the case of multiuser networks) but does not formalize the uninformative energy required to carry out the algorithms. Various studies [22, 23, 24] also deal with various types of adaptation problems such as rate, modulation, power and coding adaptations but none has taken into account the tradeoffs in terms of energy. Chi et. al. [25] also aims to design an optimal training sequence in OFDM system with minimum mean square error criterion and examines the tradeoffs that are inherited in OFDM such as peak-to-average power ratio and phase noise. However the paper considers a fixed amount of transmitted energy and is not concerned with finding the optimal amount.

Therefore, here in the thesis, we set out to formally state the power control problem and the algorithm we use in the adaptive scheme of power control. Then we shall formulate the total cost associated with the adaptation process in terms of the energy spent from the perspective of the MS transmitter. The aim is to improve the battery life of the MS terminals in communication networks.

## 2.2 Some definitions

To aid the readability of the thesis, we define the relevant concepts that will be used throughout the chapter.

**Definition 1 (Complex normal distribution [62])** *A complex random variable in  $\mathbb{C}^n$ ,  $Z = X + jY$ , where  $X, Y \in \mathbb{R}^n$  is distributed as complex normal distribution if its real and imaginary parts,  $X$  and  $Y$  respectively, are jointly normal. The complex normal random variable,  $Z$ , is characterized by three parameters: location parameter,  $\mu$ , covariance*

matrix,  $\Gamma$ , and relation matrix,  $C$ , defined as follows.

$$\begin{aligned}\mu &= E[Z], \\ \Gamma &= E[(Z - \mu)(\bar{Z} - \bar{\mu})^T], \\ C &= E[(Z - \mu)(Z - \mu)^T].\end{aligned}$$

The standard complex normal random variable is the univariate distribution with  $\mu = 0$ ,  $\Gamma = I_n$ , and  $C = 0$ .

The noise we shall consider in our setup will belong to a subclass of complex normal distribution, called the circularly symmetric complex normal. Its definition is as follows.

**Definition 2 (Circularly symmetric complex normal distribution [62])** *The circularly symmetric complex normal distribution is a complex normal distribution with zero mean and zero relation matrix, that is  $\mu = 0$  and  $C = 0$ . This distribution is denoted as  $C\mathcal{N}(0, \Gamma)$  where  $\Gamma$  is the covariance matrix.*

**Definition 3 (Central chi-square random variable [63])** *Let  $X_i \sim N(0, \sigma_i^2)$  for  $i = 1, \dots, k$  and  $\sigma_i^2 \neq 0$  for all  $i$ . Then the random variable*

$$\sum_{i=1}^k \left( \frac{X_i^2}{\sigma_i^2} \right)$$

*is a central chi-square random variable with  $k$  degrees of freedom, denoted as  $\chi_k^2$ .*

**Definition 4 (Non-central chi-square random variable [63])** *Let  $X_i \sim N(\mu_i, \sigma_i^2)$  for  $i = 1, \dots, k$  and  $\mu_i \neq 0, \sigma_i^2 \neq 0$  for all  $i$ . Then the random variable*

$$\sum_{i=1}^k \left( \frac{X_i^2}{\sigma_i^2} \right)$$

is a non-central chi-square random variable with  $k$  degrees of freedom and the non-centrality parameter

$$\lambda = \sum_{i=1}^k \left( \frac{\mu_i^2}{\sigma_i^2} \right).$$

The non-central chi-square random variable is denoted as  $\chi_k^2(\lambda)$ .

**Definition 5 ( $\mathcal{F}$  distribution [63])** Let  $X$  be a non-central chi-square random variable with  $\nu_1$  degrees of freedom and non-centrality parameter  $\lambda$ , and  $Y$  be a central chi-square random variable with  $\nu_2$  degrees of freedom that is statistically independent of  $X$ . The the following quantity

$$\frac{X/\nu_1}{Y/\nu_2}$$

is distributed as non-central  $\mathcal{F}$  distribution with  $\nu_1$  and  $\nu_2$  degrees of freedom and non-centrality parameter  $\lambda$ , denoted as  $\mathcal{F}(\nu_1, \nu_2; \lambda)$ .

## 2.3 SNR estimation in communication systems

In this section we shall develop an SNR estimator. First, the channel estimate will be obtained by means of LS estimation. This allows both the signal and noise power estimates to be computed. Then, the SNR estimate can be calculated with a full description of its statistical properties. The purpose is to use the statistics of this SNR estimation to select the transmitted power level for the MS to overcome the fading environment. The total energy cost association with power control of the system, including the cost of adaptation, will be ultimately calculated and analyzed.

### 2.3.1 System model

Consider a scalar, baseband communication channel with the uplink from the MS to the BS in Figure 2.1. We impose the following assumptions.

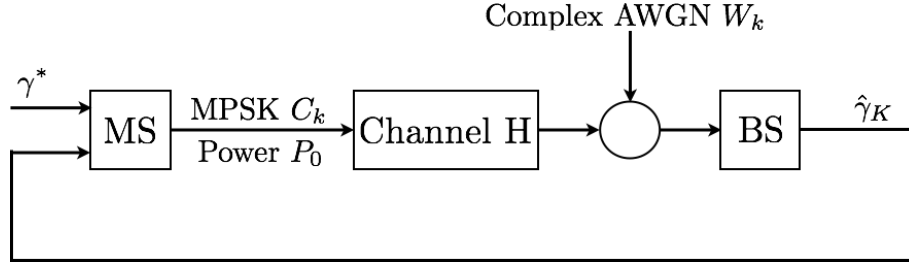


**Figure 2.1:** Communication system structure using pilot tones to estimate the link SNR

#### Assumption 1

- (1.A) The system is to follow a reference SNR,  $\gamma^*$  for data transmission, which is modulated as M-PSK signal.
- (1.B) The MS first transmits  $K$  pilot tones, also modulated as M-PSK and known to the BS, to aid channel estimation. The normalized constellation points of the M-PSK signal can be described as

$$C_k = e^{j\theta_m} = \cos \theta_m + j \sin \theta_m = C_{I_k} + jC_{Q_k}, k = 0, \dots, K - 1$$

where  $\theta_m$  is one of the  $M$  phases of the M-PSK signal constellation, and  $C_{I_k} = \cos \theta_m$  and  $C_{Q_k} = \sin \theta_m$  are the in-phase and quadrature components of the signal, respectively.

- (1.C) The pilot training signal power is  $P_0$ . The  $k^{\text{th}}$  transmitted pilot symbol therefore takes the form

$$X_k = \sqrt{P_0} C_k.$$

(1.D) Assume block fading in the channel. During the transmission, the channel is described by a single complex coefficient  $H = H_I + jH_Q$ , where  $H_I$  and  $H_Q$  are the in-phase and quadrature components of the channel, respectively.

(1.E) The signal is corrupted by scalar standard circularly symmetric complex (see Definition 2) AWGN, denoted by  $W_k$  and distributed as

$$W_k = W_{I_k} + jW_{Q_k} \sim C\mathcal{N}(0, 1).$$

where  $W_{I_k}$  and  $W_{Q_k}$  are independent AWGN noise samples, and  $C\mathcal{N}$  means complex normal. This means that the in-phase and quadrature components,  $W_{I_k}$  and  $W_{Q_k}$ , are independent, both normal with zero mean and variance  $1/2$ . This can be written as

$$\begin{pmatrix} W_{I_k} \\ W_{Q_k} \end{pmatrix} \sim \mathcal{N} \left( \begin{bmatrix} 0 \\ 0 \end{bmatrix}, \begin{bmatrix} \frac{1}{2} & 0 \\ 0 & \frac{1}{2} \end{bmatrix} \right). \quad (2.1)$$

Note that since the noise has been normalized, to take into account the noise power in the received signal, we shall use the noise power scaling factor  $N$ .

(1.F) The circularly symmetric complex AWGN noise is independent of the transmitted signal symbols.

(1.G) Based on the  $K$  pilot symbols, the BS will estimate the SNR as  $\hat{\gamma}_K$  and transmit the information back to the MS. Then, the MS will select an appropriate transmitted power level to send the actual message data to the BS.

(1.H) The complex received signal is

$$Y_k = HX_k + W_k = H\sqrt{P_0}C_k + \sqrt{N}W_k, \quad (2.2)$$

where  $N$  is the noise power scaling factor.

(1.I) The  $M$ -PSK signal strength is given by

$$\sqrt{S} = |H| \sqrt{P_0} = |H_I + jH_Q| \sqrt{P_0}. \quad (2.3)$$

Note that from (2.3), the signal power can be seen as the quantity  $S = |H|^2 P_0$  that includes the description of the complex channel gain  $H$  and the pilot power  $P_0$ .

(1.J) The SNR of the link is defined as

$$\gamma = \frac{S}{N}. \quad (2.4)$$

We pose the following problem.

**Cost of adaptation in power control:**

- Given the  $K$  pilot tones transmitted at power  $P_0$ , the channel estimate based on LS estimation will be computed. This allows the signal and noise power estimates, and ultimately, the SNR estimate to be calculated.
- After the  $K$  pilot tones, the BS receiver will know the SNR estimate of the channel and will inform the MS transmitter to transmit the next  $M$  data symbols at the appropriate power level  $P^*$  that results in a usable symbol error rate of  $10^{-3}$  [64]. For simplicity, assume the transmitted power is allowed to vary in 2dB step sizes.
- If the SNR estimate is lower than the true SNR by 2dB, retransmission is necessary for the data symbols that have been already transmitted at that too low an SNR. For the retransmission to complete, the SNR has to be estimated again. In other words, if this is the case, the whole process needs to restart from the beginning.

- *Our aim is to compute the total energy cost from the perspective of the transmitter including the above adaptation process. We shall then analyze this total energy cost.*

### 2.3.2 Channel estimation by least squares

In order to estimate the link SNR, first we shall derive the channel estimate by LS estimation technique. The LS estimation has been presented in many papers such as [36]. Its main advantage is low complexity that makes it easy to implement. We shall approach channel estimation by considering LS estimation for both the in-phase and quadrature components of the complex channel gain,  $H_I$  and  $H_Q$ , by using the assumption that the noise is circularly symmetric complex AWGN, hereafter referred simply as complex normal. A precise description of the complex normal noise  $W_k$  can be found in Assumption 1.

Consider the following form, given in (2.2), of the complex received signal

$$\begin{aligned}
 Y_k &= H \sqrt{P_0} C_k + \sqrt{N} W_k \\
 &= \sqrt{P_0} (H_I + jH_Q) (C_{I_k} + jC_{Q_k}) + \sqrt{N} (W_{I_k} + jW_{Q_k}) \\
 &= (\sqrt{P_0} H_I C_{I_k} - \sqrt{P_0} H_Q C_{Q_k} + \sqrt{N} W_{I_k}) \\
 &\quad + j(\sqrt{P_0} H_I C_{Q_k} + \sqrt{P_0} H_Q C_{I_k} + \sqrt{N} W_{Q_k})
 \end{aligned}$$

The in-phase and quadrature components of the measurement  $Y_k$  can therefore be written in the following matrix form

$$\begin{bmatrix} Y_{I_k} \\ Y_{Q_k} \end{bmatrix} = \begin{bmatrix} \sqrt{P_0} C_{I_k} & -\sqrt{P_0} C_{Q_k} \\ \sqrt{P_0} C_{Q_k} & \sqrt{P_0} C_{I_k} \end{bmatrix} \begin{bmatrix} H_I \\ H_Q \end{bmatrix} + \begin{bmatrix} \sqrt{N} W_{I_k} \\ \sqrt{N} W_{Q_k} \end{bmatrix}. \quad (2.5)$$



Multiplying both sides of (2.5) by

$$\begin{bmatrix} \sqrt{P_0}C_{I_k} & \sqrt{P_0}C_{Q_k} \\ -\sqrt{P_0}C_{Q_k} & \sqrt{P_0}C_{I_k} \end{bmatrix},$$

we have the following

$$\begin{bmatrix} \sqrt{P_0}C_{I_k} & \sqrt{P_0}C_{Q_k} \\ -\sqrt{P_0}C_{Q_k} & \sqrt{P_0}C_{I_k} \end{bmatrix} \begin{bmatrix} Y_{I_k} \\ Y_{Q_k} \end{bmatrix} = \begin{bmatrix} P_0 & 0 \\ 0 & P_0 \end{bmatrix} \begin{bmatrix} H_I \\ H_Q \end{bmatrix} + \begin{bmatrix} \sqrt{P_0}C_{I_k} & \sqrt{P_0}C_{Q_k} \\ -\sqrt{P_0}C_{Q_k} & \sqrt{P_0}C_{I_k} \end{bmatrix} \begin{bmatrix} \sqrt{N}W_{I_k} \\ \sqrt{N}W_{Q_k} \end{bmatrix}. \quad (2.6)$$

Now the in-phase and quadrature components of the channel  $H$  can be estimated from (2.6) by the LS estimator as follows

$$\begin{aligned} \begin{bmatrix} \hat{H}_I \\ \hat{H}_Q \end{bmatrix} &= \left( \sum_{k=0}^{K-1} \begin{bmatrix} P_0 & 0 \\ 0 & P_0 \end{bmatrix} \right)^{-1} \left( \sum_{k=0}^{K-1} \begin{bmatrix} \sqrt{P_0}C_{I_k} & \sqrt{P_0}C_{Q_k} \\ -\sqrt{P_0}C_{Q_k} & \sqrt{P_0}C_{I_k} \end{bmatrix} \begin{bmatrix} Y_{I_k} \\ Y_{Q_k} \end{bmatrix} \right) \\ &= \begin{bmatrix} KP_0 & 0 \\ 0 & KP_0 \end{bmatrix}^{-1} \left( \sum_{k=0}^{K-1} \begin{bmatrix} \sqrt{P_0}C_{I_k} & \sqrt{P_0}C_{Q_k} \\ -\sqrt{P_0}C_{Q_k} & \sqrt{P_0}C_{I_k} \end{bmatrix} \begin{bmatrix} Y_{I_k} \\ Y_{Q_k} \end{bmatrix} \right). \end{aligned}$$

Substituting equation (2.5) into the above equation yields the following

$$\begin{aligned} \begin{bmatrix} \hat{H}_I \\ \hat{H}_Q \end{bmatrix} &= \begin{bmatrix} KP_0 & 0 \\ 0 & KP_0 \end{bmatrix}^{-1} \sum_{k=0}^{K-1} \left( \begin{bmatrix} P_0 & 0 \\ 0 & P_0 \end{bmatrix} \begin{bmatrix} H_I \\ H_Q \end{bmatrix} + \sqrt{PN} \begin{bmatrix} W_{I_k}C_{I_k} + W_{Q_k}C_{Q_k} \\ -W_{I_k}C_{Q_k} + W_{Q_k}C_{I_k} \end{bmatrix} \right) \\ &= \begin{bmatrix} H_I \\ H_Q \end{bmatrix} + \frac{\sqrt{N}}{K\sqrt{P_0}} \sum_{k=0}^{K-1} \begin{bmatrix} W_{I_k}C_{I_k} + W_{Q_k}C_{Q_k} \\ -W_{I_k}C_{Q_k} + W_{Q_k}C_{I_k} \end{bmatrix} \end{aligned} \quad (2.7)$$

From (2.7), because  $W_{I_k}$  and  $W_{Q_k}$  are both gaussian and  $C_{I_k}$  and  $C_{Q_k}$  are both

deterministic, the LS estimates  $\hat{H}_I$  and  $\hat{H}_Q$  are also both gaussian. Their mean values can be calculated easily as

$$E \left( \begin{bmatrix} \hat{H}_I \\ \hat{H}_Q \end{bmatrix} \right) = \begin{bmatrix} H_I \\ H_Q \end{bmatrix}.$$

To find out their variances, consider first

$$\begin{aligned} \text{Var} \left( \sum_{k=0}^{K-1} (W_{I_k} C_{I_k} + W_{Q_k} C_{Q_k}) \right) &= \left( E \left[ \sum_{k=0}^{K-1} (W_{I_k} C_{I_k} + W_{Q_k} C_{Q_k}) \right]^2 \right) \\ &= \frac{1}{2} \sum_{k=0}^{K-1} (C_{I_k}^2 + C_{Q_k}^2) \\ &= \frac{K}{2}, \end{aligned}$$

using the independence of  $W_{I_k}$  and  $W_{Q_k}$ .

Similarly,

$$\text{Var} \left( \sum_{k=0}^{K-1} (-W_{I_k} C_{Q_k} + W_{Q_k} C_{I_k}) \right) = \frac{K}{2}.$$

Hence, the variance of both  $\hat{H}_I$  and  $\hat{H}_Q$  is

$$\text{Var} \hat{H}_I = \text{Var} \hat{H}_Q = \left( \frac{\sqrt{N}}{K\sqrt{P_0}} \right)^2 \frac{K}{2} = \frac{N}{2KP_0}.$$

Furthermore,  $\hat{H}_I$  and  $\hat{H}_Q$  are independent because

$$E \left[ \sum_{k=0}^{K-1} (W_{I_k} C_{I_k} + W_{Q_k} C_{Q_k}) (-W_{I_k} C_{Q_k} + W_{Q_k} C_{I_k}) \right] = 0.$$

Therefore, the distributions of  $\hat{H}_I$  and  $\hat{H}_Q$  are

$$\begin{bmatrix} \hat{H}_I \\ \hat{H}_Q \end{bmatrix} \sim \mathcal{N} \left( \begin{bmatrix} H_I \\ H_Q \end{bmatrix}, \begin{bmatrix} \frac{N}{2KP_0} & 0 \\ 0 & \frac{N}{2KP_0} \end{bmatrix} \right) \quad (2.8)$$

### 2.3.3 SNR estimation

Now we shall rely on the channel estimate from Section 2.3.2 to compute the SNR estimate for the communication link. With respect to the channel estimate,  $|\hat{H}|$ , the signal power estimate can be calculated as

$$\hat{S} = P_0 |\hat{H}|^2 = P_0 (\hat{H}_I^2 + \hat{H}_Q^2). \quad (2.9)$$

We state the following theorem regarding the pdf of  $\hat{S}$ .

**Theorem 1** *The signal power estimate,  $\hat{S} = P_0(\hat{H}_I^2 + \hat{H}_Q^2)$ , has pdf described as*

$$\frac{2K}{N} \hat{S} \sim \chi_2^2(\lambda), \quad (2.10)$$

*that is, a non-central chi-square distribution with 2 degrees of freedom and the non-centrality parameter given by*

$$\lambda = |H|^2 \frac{2KP_0}{N}. \quad (2.11)$$

*Proof:* Rewrite equation (2.9) as

$$\frac{\hat{S}}{P_0 \frac{N}{2KP_0}} = \frac{\hat{H}_I^2}{\frac{N}{2KP_0}} + \frac{\hat{H}_Q^2}{\frac{N}{2KP_0}},$$

so that

$$\frac{2K}{N}\hat{S} = \frac{\hat{H}_I^2}{\frac{N}{2KP_0}} + \frac{\hat{H}_Q^2}{\frac{N}{2KP_0}}. \quad (2.12)$$

Because  $\hat{H}_I$  and  $\hat{H}_Q$  are distributed as described in (2.8), we can conclude the following [63] about the distribution of  $\hat{H}_I^2$  and  $\hat{H}_Q^2$

$$\begin{aligned} \frac{\hat{H}_I^2}{\frac{N}{2KP_0}} &\sim \chi_1^2\left(H_I^2 \frac{2KP_0}{N}\right) \\ \frac{\hat{H}_Q^2}{\frac{N}{2KP_0}} &\sim \chi_1^2\left(H_Q^2 \frac{2KP_0}{N}\right), \end{aligned}$$

that is, the non-central chi-square distributions with one degree of freedom and non-centrality parameters  $H_I^2 \frac{2KP_0}{N}$  and  $H_Q^2 \frac{2KP_0}{N}$  respectively. Therefore, from (2.12) we have the following (see Definition 4) [65].

$$\frac{2K}{N}\hat{S} \sim \chi_2^2(\lambda), \quad (2.13)$$

that is, the non-central chi-square distribution with 2 degrees of freedom and the non-centrality  $\lambda$  which can be calculated as (see Definition 4)

$$\lambda = H_I^2 \frac{2KP_0}{N} + H_Q^2 \frac{2KP_0}{N} = |H|^2 \frac{2KP_0}{N}.$$

□

According to Theorem 1, if the noise power  $N$  is known, the variance of  $\hat{S}$  can be calculated. The variance of  $\chi_2^2(\lambda)$  is given by [63]

$$2(2 + 2\lambda) = 2\left(2 + 2|H|^2 \frac{2KP_0}{N}\right),$$

and because  $\frac{2K}{N}\hat{S} \sim \chi_2^2(\lambda)$ ,

$$\begin{aligned}\text{Var}\left(\frac{2K}{N}\hat{S}\right) &= 2\left(2 + 2|H|^2\frac{2KP_0}{N}\right), \\ \text{Var}(\hat{S}) &= \frac{N^2}{K^2}\left(1 + |H|^2\frac{2KP_0}{N}\right).\end{aligned}$$

We make the following remark about the above equation.

**Remark 1** *If  $N$  is constant, for fixed  $K$ , the variance of  $\hat{S}$  decreases with  $P_0$ . Whereas, for fixed  $P_0$ , the variance of  $\hat{S}$  decreases when  $K$  increases.*

Remark 1 is interesting because it is saying that in an environment where the noise does not change, while increasing the number of pilot tones helps refine the estimate of the signal power, which is intuitive, increasing the pilot transmitted power has a negative effect on the signal power estimate.

The noise power estimate can be found by first finding the second moment of the received signal (2.2)

$$M_{\mathbf{Y}}^2 = \frac{1}{K} \sum_{k=0}^{K-1} |Y_k|^2,$$

and then the noise power estimate is given by

$$\hat{N} = M_{\mathbf{Y}}^2 - \hat{S} = \frac{1}{K} \sum_{k=0}^{K-1} |Y_k|^2 - \hat{S}. \quad (2.14)$$

We state the following theorem regarding the pdf of  $\hat{N}$ .

**Theorem 2** *The noise power estimate,  $\hat{N}$  (2.14), has pdf described as*

$$\frac{2K}{N}\hat{N} \sim \chi_{2K-2}^2, \quad (2.15)$$

*that is, a central chi-square distribution with  $(2K - 2)$  degrees of freedom.*

*Proof:* From (2.5), we have the following regarding the distribution of the in-phase and quadrature components of  $Y_k$ , that are independent,

$$\begin{bmatrix} Y_{I_k} \\ Y_{Q_k} \end{bmatrix} \sim \mathcal{N} \left( \begin{bmatrix} \sqrt{P_0}C_{I_k} & -\sqrt{P_0}C_{Q_k} \\ \sqrt{P_0}C_{Q_k} & \sqrt{P_0}C_{I_k} \end{bmatrix} \begin{bmatrix} H_I \\ H_Q \end{bmatrix}, \begin{bmatrix} N/2 & 0 \\ 0 & N/2 \end{bmatrix} \right)$$

Further, for each  $k$ , the  $Y_{I_k}$  and  $Y_{Q_k}$  sequences are white and  $Y_{I_k}$  is independent of  $Y_{Q_k}$ . Therefore,

$$\frac{2}{N} \sum_{k=0}^{K-1} |Y_k|^2 = \sum_{k=0}^{K-1} \left( \frac{Y_{I_k}^2}{N/2} + \frac{Y_{Q_k}^2}{N/2} \right) \sim \chi_{2K}^2(\bar{\lambda}),$$

that is, a non-central chi-square distributed quantity with  $2K$  degrees of freedom and the non-centrality parameter  $\bar{\lambda}$  which can be calculated as

$$\begin{aligned} \bar{\lambda} &= \sum_{k=0}^{K-1} \frac{(\sqrt{P_0}C_{I_k}H_I - \sqrt{P_0}C_{Q_k}H_Q)^2}{N/2} + \frac{(\sqrt{P_0}C_{Q_k}H_I + \sqrt{P_0}C_{I_k}H_Q)^2}{N/2} \\ &= \frac{2P_0}{N} (H_I^2 + H_Q^2) \sum_{k=0}^{K-1} (C_{I_k}^2 + C_{Q_k}^2) \\ &= |H|^2 \frac{2KP_0}{N}, \end{aligned}$$

and so,  $\bar{\lambda} = \lambda$  from (2.11). Therefore,

$$\frac{2}{N} \sum_{k=0}^{K-1} |Y_k|^2 \sim \chi_{2K}^2(\lambda). \quad (2.16)$$

Now, multiply both sides of (2.14) by

$$\frac{2K}{N}$$

and we have the following

$$\frac{2K}{N}\hat{N} = \frac{2}{N} \sum_{k=0}^{K-1} |Y_k|^2 - \frac{2K}{N}\hat{S} \quad (2.17)$$

The first term on the right hand side of (2.17) is distributed as  $\chi_{2K}^2(\lambda)$  as pointed out in (2.16). Furthermore, the second term on the right hand side of (2.17) is distributed as  $\chi_2^2(\lambda)$  as concluded in Theorem 1. Therefore, by the decomposition of chi-square random variables, which is the direct result of Cochran's Theorem [66, 67], we have the following conclusion regarding the distribution of  $\hat{N}$ .

$$\frac{2K}{N}\hat{N} \sim \chi_{2K-2}^2,$$

that is, a central chi-square distribution with  $(2K - 2)$  degrees of freedom.  $\square$

According to Theorem 2, the variance of  $\hat{N}$  is given by

$$\text{Var}(\hat{N}) = N^2 \frac{K-1}{K^2}.$$

We make the following remark about the above equation.

**Remark 2** *The variance of the noise estimate does not depend on the pilot transmitted power  $P_0$ , and it decreases as  $K$  increases.*

Now that we have the noise and signal power estimates, the SNR estimate,  $\hat{\gamma}_K$ , can be calculated via

$$\hat{\gamma}_K = \frac{\hat{S}}{\hat{N}}. \quad (2.18)$$

We state the following theorem regarding the pdf of  $\hat{\gamma}_K$ .

**Theorem 3** *The SNR estimate based on  $K$  pilot tones,  $\hat{\gamma}_K$ , has pdf given by*

$$(K-1)\hat{\gamma}_K \sim \mathcal{F}(2, 2K-2; \lambda), \quad (2.19)$$

that is an  $\mathcal{F}$  distribution with 2 and  $(2K-2)$  degrees of freedom and the non-centrality parameter

$$\lambda = |H|^2 \frac{2KP_0}{N}.$$

*Proof:* With  $\hat{H}_I$  and  $\hat{H}_Q$  estimated using LS and our formulation of  $\hat{S}$  and  $\hat{N}$  from (2.9) and (2.14) respectively, according to [65],  $\hat{S}$  and  $\hat{N}$  are independent. Hence, based on Theorems 1 and 2, the following conclusion can be drawn according to Definition 5.

$$\frac{(\hat{S} \frac{2K}{N})/2}{(\hat{N} \frac{2K}{N})/(2K-2)} \sim \mathcal{F}(2, 2K-2; \lambda), \quad (2.20)$$

where  $\mathcal{F}(2, 2K-2; \lambda)$  is used to denote a  $\mathcal{F}$  distribution with 2 degrees of freedom on the numerator and  $(2K-2)$  degrees of freedom on the denominator, and the non-centrality parameter  $\lambda$  (2.11).

Since the SNR estimate based on  $K$  transmitted pilot tones can be expressed as (2.18), we rewrite (2.20) as

$$(K-1) \frac{\hat{S}}{\hat{N}} \sim \mathcal{F}(2, 2K-2; \lambda).$$

Therefore,

$$(K-1)\hat{\gamma}_K \sim \mathcal{F}(2, 2K-2; \lambda),$$

that is an  $\mathcal{F}$  distribution with 2 and  $(2K-2)$  degrees of freedom and the non-centrality parameter  $\lambda$  (2.11).  $\square$



To get the distribution of  $\hat{\gamma}_K$ , the pdf transformation [68] yields

$$p(\hat{\gamma}_K) = (K - 1)p(f)$$

where  $p$  is used to denote probability density functions and  $f$  is the random variable distributed as  $\mathcal{F}(2, 2K - 2; \lambda)$ . Note that  $p(\hat{\gamma}_K)$  is a function of  $\hat{\gamma}_K$  while  $p(f)$  is a function of  $f$  and that  $\hat{\gamma}_K$  is related to  $f$  via

$$\partial \hat{\gamma}_K = \frac{\partial f}{K - 1}.$$

Figure 2.2 is the plot of an example density of the SNR estimate,  $\hat{\gamma}_K$ , following (2.19). Notice that with increasing number of pilot tones  $K$ , the mean value comes closer to the actual link SNR. Here, it is useful to note that for a sufficiently large number of pilot tones, the density of  $\hat{\gamma}_K$  is concentrated mostly  $\pm 2$ dB around the actual link SNR. We shall make use of this observation later on when it comes to assessing the link quality of the system in subsequent sections.

## 2.4 Examination of the SNR estimate

To examine the statistics of the SNR estimate in Theorem 3, we first look at the distribution  $\mathcal{F}(2, 2K - 2; \lambda)$ . For convenience, let  $f$  denote the random variable distributed as  $\mathcal{F}(2, 2K - 2; \lambda)$ . The mean value of this random variable is given by [63]

$$E[f] = \frac{\nu_2(\nu_1 + \lambda)}{\nu_1(\nu_2 - 2)} \text{ for } \nu_2 > 2,$$

where  $\nu_1$  is the first number of degrees of freedom of  $f$ , i.e.  $\nu_1 = 2$ , and  $\nu_2$  the second number of degrees of freedom of  $f$ , i.e.  $\nu_2 = 2K - 2$ . We assume that the condition

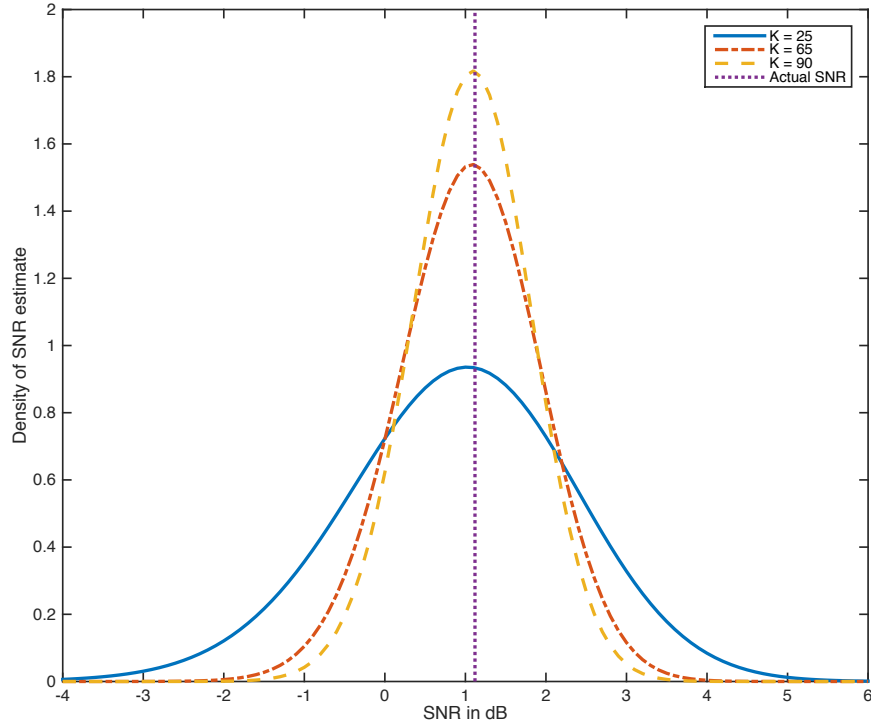


**Figure 2.2:** An example of pdf of the SNR estimate,  $\hat{\gamma}_K$ , as  $\mathcal{F}$  distribution (2.19). In the plot,  $K$  is the number of pilot tones.

$v_2 > 2$  is satisfied, that is  $K > 2$ , meaning we have more than 2 pilot symbols. This is a reasonable assumption. Since, from Theorem 3,

$$E[\hat{\gamma}_K] = \frac{1}{K-1} E[f],$$

the mean value of  $\hat{\gamma}_K$  is then calculated as

$$E[\hat{\gamma}_K] = \frac{2 + \lambda}{2K - 4} = \frac{1 + |H|^2 \frac{KP_0}{N}}{K - 2} \text{ for } K > 2. \quad (2.21)$$

Regarding the variance of the SNR estimate, we propose the following Lemma.

**Lemma 1** *For a fixed value of  $H$  and  $N$ , to minimize the variance of the SNR estimate,  $\hat{\gamma}_K$ , the strategy is  $P_0 \downarrow 0$  and  $K \rightarrow \infty$ .*

*Proof:* The variance of the random variable  $f \sim \mathcal{F}(2, 2K - 2; \lambda)$  is given by [63]

$$\text{Var}(f) = 2 \frac{(v_1 + \lambda)^2 + (v_1 + 2\lambda)(v_2 - 2)}{(v_2 - 2)^2(v_2 - 4)} \left( \frac{v_2}{v_1} \right)^2 \text{ for } v_2 > 4.$$

Again, we assume  $v_2 > 4$ , that is  $K > 6$ .

Since, from Theorem 3,

$$\text{Var}(\hat{\gamma}_K) = \frac{1}{(K - 1)^2} \text{Var}(f),$$

the variance of  $\hat{\gamma}_K$  is then calculated as

$$\text{Var}(\hat{\gamma}_K) = \frac{\lambda^2 + 4(K - 1)\lambda + 4(K - 1)}{4(K - 2)^2(K - 1)^2(K - 3)} \text{ for } K > 3.$$

Substituting  $\lambda = |H|^2 \frac{2KP_0}{N}$ , we have

$$\text{Var}(\hat{\gamma}_K) = \frac{|H|^4 \left( \frac{2KP_0}{N} \right)^2 + 4(K - 1)|H|^2 \frac{2KP_0}{N} + 4(K - 1)}{4(K - 2)^2(K - 1)^2(K - 3)} \text{ for } K > 3. \quad (2.22)$$

With  $H$  and  $N$  fixed, for a fixed value of  $P_0$ , the denominator of  $\hat{\gamma}_K$  (2.22) is a function of  $K^5$  while the numerator is a function of  $K^2$ . Therefore, for  $K \rightarrow \infty$ ,  $\text{Var}(\hat{\gamma}_K) \rightarrow 0$ .

On the other hand, with  $H$  and  $N$  fixed, for a fixed value of  $K$ , the SNR estimate  $\hat{\gamma}_K$  (2.22) apparently increases with increasing  $P_0$ .

Therefore, the optimal strategy to minimize  $\hat{\gamma}_K$  is  $P_0 \downarrow 0$  and  $K \rightarrow \infty$ .  $\square$

Notice that Lemma 1 is not a surprise when considering Remarks 1 and 2 altogether. Lemma 1 poses a conundrum in the problem of minimizing the total energy cost of power control of communication systems. The conundrum is that to minimize the total energy cost, one should use an infinite number of pilot tones transmitted at zero power.

## 2.5 Results in the real-channel case

In the real-channel case with real AWGN noise, real channel coefficient and real signal (e.g. BPSK signal), the result is a special case of what we have derived so far. The formulae can easily be found by replacing complex parameters with real ones. Since the derivation is straightforward in the real-channel given the results in the complex-channel case, we only summarize the results in the real-channel case in a theorem without proof.

**Theorem 4** *Consider the power control problem formulated in Section 2.3.1, but with a real channel gain  $h$ , real standard AWGN,  $w_k \sim N(0, 1)$ , and real BPSK signal  $c_k \in \{-1, 1\}$ . The received signal is therefore real, denoted by*

$$y_k = h\sqrt{P_0}c_k + \sqrt{N}w_k.$$

*We have the following results.*

*The LS channel estimate based on  $K$  pilot symbols is given by*

$$\hat{h} = h + \frac{\sqrt{N}}{K\sqrt{P_0}} \sum_{k=0}^{K-1} c_k w_k,$$

*which is distributed as  $\hat{h} \sim N\left(h, \frac{N}{KP_0}\right)$ . The signal power estimate in the real-channel case,  $\hat{S}_r = \hat{h}^2 P_0$ , has a distribution given by*

$$\frac{K}{N} \hat{S}_r = \frac{\hat{h}^2}{\frac{N}{KP_0}} \sim \chi_1^2(\lambda_r),$$

*where  $\lambda_r$  is the non-centrality parameter for the real-channel case which is calculated as*

$$\lambda_r = h^2 \frac{KP_0}{N}.$$

The noise power estimate is given by

$$\hat{N}_r = \frac{1}{K} \sum_{k=0}^{K-1} y_k^2 - \hat{S}_r,$$

that has a distribution given by

$$\frac{K}{N} \hat{N}_r = \frac{1}{N} \sum_{k=0}^{K-1} y_k^2 - \frac{K}{N} \hat{S}_r \sim \chi_{K-1}^2$$

Therefore, the SNR estimate,  $\hat{\gamma}_{K,r} = \frac{\hat{S}_r}{\hat{N}_r}$ , has the following distribution

$$(K-1)\hat{\gamma}_{K,r} \sim \mathcal{F}(1, K-1; \lambda_r),$$

with variance given by

$$\text{Var}(\hat{\gamma}_{K,r}) = \frac{1}{(K-3)^2(K-5)} \left[ \left( \frac{h^2}{N} K P_0 \right)^2 + 2(K-2) \frac{h^2}{N} K P_0 + (K-2) \right] \text{ for } K > 5.$$

Figure 2.3 is the plot of the pdf of the SNR estimate in both complex-channel and real-channel cases, as computed in Theorems 3 and 4 respectively, for a fixed  $P_0$ ,  $H$ , and  $N$  that are the same for each case, and  $K = 50$  pilot symbols for the real-channel case and  $K = 25$  for the complex-case. From the graph, it can be seen that the two pdfs are almost the same as each other. This is because, while the number of pilot tones in the complex-channel case is only a half of that in the real-channel case, the former has two components, namely in-phase and quadrature, that are used at the same time to estimate the channel. This implies that in the complex channels, the same estimation quality as in the real channels can be achieved with only half the pilot length compared to real channels.

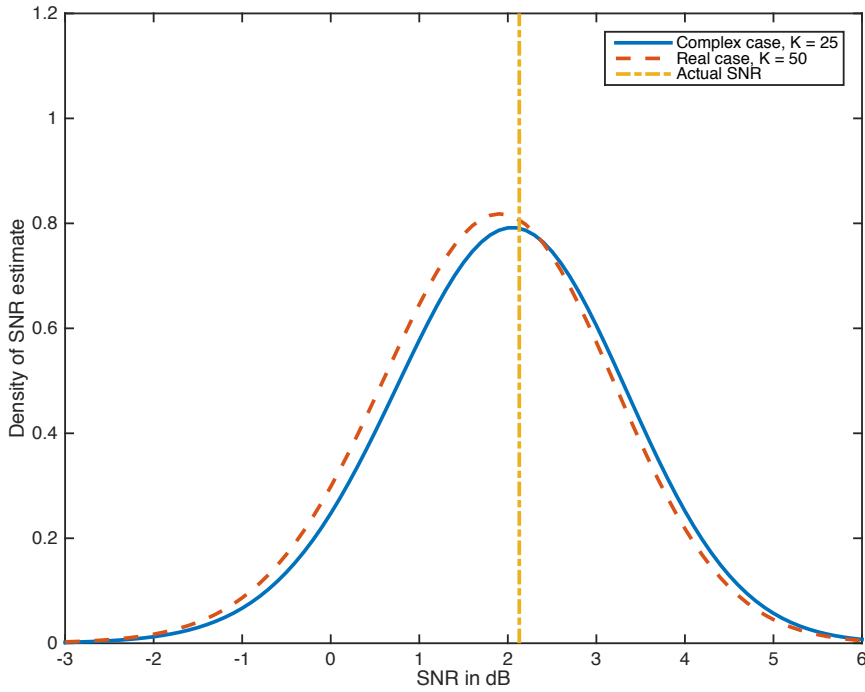


**Figure 2.3:** Pdf of the SNR estimate in the complex-channel case,  $\hat{\gamma}_K$ , and in the real-channel case,  $\hat{\gamma}_{K,r}$ , as computed in Theorems 3 and 4 respectively. In the plot,  $P_0$ ,  $N$  and  $H$  are fixed and the same for both cases, and  $K = 25$  for the complex-channel case and  $K = 50$  for the real-channel case.

The results from Theorem 4 are similar to what has been found by the authors in [26], using the ML estimator. As can be seen from the variance of the SNR estimate in Theorem 4, the optimal strategy to minimize it is similar to the complex case that is stated in Lemma 1, which is to let  $P_0 \downarrow 0$  and  $K \rightarrow \infty$ .

Evidence of this result is present but unremarked in [26]. Figure 5 from [26], associated with the SNR estimation with unknown noise power, is reproduced here as Figure 2.4 with annotation of 2 circles and 2 squares. The notation of [26] has  $\rho \equiv \gamma$ ,  $2BT \equiv K$ , and  $\hat{\rho} \equiv \hat{\gamma}_K$ . The curves in this figure represent the 90% confidence intervals for  $\hat{\gamma}_K$  versus true SNR,  $\gamma$ , for different values of  $K$ . Thus the two pairs of indicated points have the same value of  $KP_0$ . It is evident, even on the logarithmic scale of this figure, that the circled points with the larger value of  $K$  have the better confidence values.

This illustrates the result in Lemma 1.

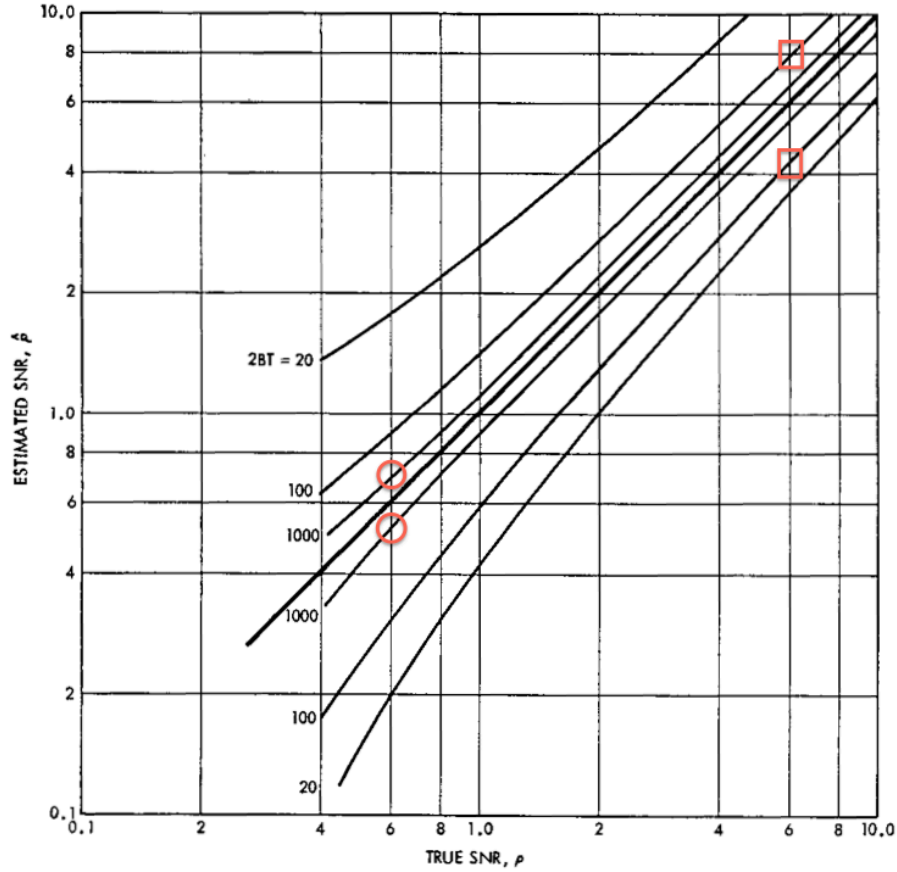


**Figure 2.4:** 90% confidence interval curves for SNR estimate as  $F$ -distribution (reproduced from [26] with annotation of 2 circles and squares). Here  $\rho \equiv \gamma$ ,  $\hat{\rho} \equiv \hat{\gamma}_K$  and  $2BT \equiv K$ . The circled and squared points all have the same value  $KP_0$ . The circled points, with higher  $K$ , yield tighter confidence intervals than do the squared points, even on this logarithmic scale.

## 2.6 Link quality and formulation of energy cost

In Section 2.3.1, we have stated that the purpose of the power control algorithm is to follow a reference SER value of  $P_s = 10^{-3}$ . To formulate the energy cost precisely, we assume the signal is modulated as QPSK and Gray coding in the system. The approximated relation between SER,  $P_s$ , and SNR per symbol,  $\gamma$ , for QPSK signal can be

expressed as follows [21].

$$P_s = 2Q(\sqrt{\gamma}),$$

where  $Q$  signifies the  $Q$  function.

And so, to track a reference SER value of  $10^{-3}$  is equivalent to tracking a reference SNR-per-symbol value of

$$\gamma^* = \left[ Q^{-1} \left( \frac{10^{-3}}{2} \right) \right]^2 = 10.8. \quad (2.23)$$

Converted to dB scale, this value is

$$\gamma^* = 10.3\text{dB}.$$

Our criterion for the link quality is to choose a transmitted power level that results in a value of SNR that is at most 2dB less than the reference SNR,  $\gamma^*$  (2.23). That is, during the transmission of  $M$  OFDM data symbols, the actual link SNR,  $\gamma$ , must satisfy

$$\gamma \geq \gamma^* - 2\text{dB}, \quad (2.24)$$

at all times. If the criterion (2.24) is not met, the retransmission of the first part of data symbols that has been sent with the unsatisfactory SNR is necessary to maintain the quality of the communication link. However, in order to retransmit, the SNR has to be estimated and the transmitted power for the data symbols computed again. In other words, the whole power control process needs to restart from the beginning. We assume that the decoding process and error detection schemes detect that the SER is too high after  $L < M$  data symbols have been sent, after which the power control algorithm restarts from the



beginning with estimating the SNR by  $K$  pilot tones. Assume further that  $L$  is known to both the MS transmitter and BS receiver.

When the power is chosen that results in an actual link SNR more than  $\gamma^*$ , the energy overhead however will be wasted. We shall consider this overhead to be the case when the actual SNR is 2dB more than  $\gamma^*$ . This, in addition to criterion (2.24), means that after the pilot phase where the SNR is estimated, the chosen transmitted power for the data symbols is considered correct when the actual SNR,  $\gamma$ , is within 2dB of the reference  $\gamma^*$ .

By certainty equivalent principle, we shall assume that the MS transmitter, in determining its transmitted power for message data symbols, considers the SNR estimate  $\hat{\gamma}_K$  the actual link SNR. Based on this assumption, we shall define a cost in terms of the energy spent to adapt to the link quality criterion we have built up so far. This energy cost includes the following.

- The energy spent of the  $K$  pilot symbols used to estimate the link SNR.
- The energy of the  $M$  data symbols transmitted successfully at an SNR within 2dB of  $\gamma^*$  that can be achieved by following the SNR estimate,  $\hat{\gamma}_K$ , and choosing the appropriate power level. Because the chosen transmitted power of data symbols is based on the SNR estimate, this is the case when the SNR estimate,  $\hat{\gamma}_K$ , is within 2dB of the real SNR value. Recall that the transmitted power is allowed to vary in 2dBm step sizes.
- The wasted energy overhead if the transmitted power of data symbols results in an actual link SNR of 2dB more than  $\gamma^*$ . This is the case when the SNR estimate is 2dB *below* the real SNR value, that leads the MS transmitter to make a wrong decision and choose a transmitted power level that is higher than necessary.
- The energy associated with the retransmission when, after the estimation phase,

the transmitter power is 2dBm lower than the desired value and criterion (2.24) is not met. This is the case when the SNR estimate is wrong by 2dB *above* the real SNR value. As mentioned earlier, after  $L < M$  data symbols have been sent, both the MS and BS will know whether or not retransmission is necessary.

The probabilities of the MS transmitter choosing the appropriate power level, or the incorrect power level that results in a value of link SNR 2dB less or more than the reference SNR,  $\gamma^*$ , can be computed by following the statistical properties of  $\hat{\gamma}_K$  as described in (2.19).

Next, we need to define the some probabilities regarding the quality of the power control algorithm.

**Definition 6** *Define the following probabilities to characterize the power control quality in the communication link.*

$\epsilon_K$  *the probability of  $\hat{\gamma}_K$  being 2dB less than the true SNR,  $\gamma$ . This means that  $\epsilon_K$  is the probability of the MS transmitter, after the pilot phase, choosing higher power than necessary, that results in wasted energy overhead. This probability can be computed as*

$$\epsilon_K = P(\hat{\gamma}_K \leq \gamma/1.26) = P\left((K-1)\hat{\gamma}_K \leq (K-1)\gamma/1.26\right), \quad (2.25)$$

*where 2dB has been converted into a factor of 1.26 in linear scale, and the factor  $(K-1)$  added to the calculation of the probabilities to be able to utilize the distribution (2.19).*

$\delta_K$  *the probability of  $\hat{\gamma}_K$  being 2dB more than the true SNR,  $\gamma$ . This means that  $\delta_K$  is the probability of the MS transmitter, after the pilot phase, choosing insufficient power. This results in restarting the power control process after  $L < M$  data symbols have*

been sent. This probability can be computed as

$$\delta_K = P(\hat{\gamma}_K \geq 1.26\gamma) = P\left((K-1)\hat{\gamma}_K \geq (K-1)1.26\gamma\right). \quad (2.26)$$

$1 - \epsilon_K - \delta_K$  the probability of of the transmitter, after the pilot phase, choosing just enough transmitted power to complete the transmission of the  $M$  data symbols. This is the probability that  $\hat{\gamma}_K$  is within 2dB of the actual SNR,  $\gamma$ .

The total energy cost of the power control process in the communication network can be formulated as follows.

$$J_K = J_K^p + J_K^d + J_K^{high} + J_K^{low}, \quad (2.27)$$

where  $J_K^p$  is the energy spent on  $K$  pilot tones,  $J_K^d$  the energy spent on  $M$  message data tones,  $J_K^{high}$  and  $J_K^{low}$  the energy spent when the chosen transmitted power after the adaptation phase is higher or lower than the optimal amount, respectively. The calculations for the components of the total cost  $J_K$  (2.27) are as follows.

**Energy cost of pilot symbols:** Since the pilot tones are transmitted at power  $P_0$ , the energy of the MS transmitter spent on  $K$  pilot tones is

$$J_K^p = KP_0.$$

**Energy cost of data symbols:** As mentioned before, when the SNR estimate is in the interval  $[\gamma - 2\text{dB}; \gamma + 2\text{dB}]$ , or  $[\gamma/1.26; \gamma \times 1.26]$  in linear scale, where  $\gamma$  is the actual link SNR, the estimate is considered correct to enable the MS transmitter to choose just enough power to maintain the link quality. This happens with probability  $Pr_K$  as defined in Definition 6. When this is the case, the  $M$  data symbols will be

transmitted without wasted energy or retransmission. The associated energy cost is given by

$$J_K^d = MP^* Pr_K,$$

where  $P^*$  is the optimal transmitted power for data symbols.

**Energy cost when power is too high:** Transmitted power that is too high leads to a higher achieved value of SNR than is needed. The transmission is still successful but at a wasted energy cost overhead. For simplicity, we assume that if the transmitted power is chosen too high, it is chosen as  $(P^* + 2)$ dBm, or  $1.26P^*$  in linear scale. This happens with probability  $\varepsilon_K$  as explained in Definition 6, where  $\hat{\gamma}_K \leq \gamma/1.26$ . Note that we do not consider the unlikely case where the chosen power is more than 2dBm wrong. This is based on the assumption that we only allow the transmitted power to vary in 2dBm step sizes, and on the density of the SNR estimate (2.19) in Figure 2.2, where most of the density is concentrated around  $\pm 2$ dB of the mean value for a sufficiently large number of pilot tones. The energy associated with this case is given by

$$J_K^{high} = \varepsilon_K M(1.26P^*).$$

**Energy cost when BER is too low:** In the case of the MS transmitter choosing too low a power to transmit the data symbols, after  $L < M$  data symbols have been transmitted, both the MS transmitter and BS receiver acknowledge that retransmission is necessary. Thus the power control algorithm needs to restart from the beginning with SNR estimation. This happens with probability  $\delta_K$ . Similar to the preceding case, we consider only the most likely case that if the power is chosen too low, it is

chosen as  $(P^* - 2)$ dBm, or  $P^*/1.26$  in linear scale.

First, realize that if the transmission of  $L$  data symbols is unsuccessful, the energy spent on them goes to waste. This energy is simply  $LP^*/1.26$ . After this the SNR estimation has to be carried out again and the power control process restarted. Therefore, the energy cost associated with this case is

$$J_K^{low} = \delta_K \{ LP^*/1.26 + J_K^p + J_K^d + J_K^{high} + \delta_K [ LP^*/1.26 + J_K^p + J_K^d + J_K^{high} + \dots ] \},$$

where the infinite series signifies the restart of the whole power control process. Expanding the above equation yields

$$\begin{aligned} J_K^{low} &= \delta_K (LP^*/1.26 + J_K^p + J_K^d + J_K^{high}) (1 + \delta_K + \delta_K^2 + \dots) \\ &= \delta_K (LP^*/1.26 + J_K^p + J_K^d + J_K^{high}) \sum_{n=0}^{\infty} (\delta_K)^n, \end{aligned}$$

where the geometric series  $\sum_{n=0}^{\infty} (\delta_K)^n$  converges with the assumption that  $\delta_K < 1$ , meaning choosing a transmitted power 2dBm below the desired value cannot happen with probability 1. Completing the geometric series yields

$$J_K^{low} = (LP^*/1.26 + J_K^p + J_K^d + J_K^{high}) \frac{\delta_K}{1 - \delta_K}$$

**Total energy cost:** Now the total energy cost  $J_K$  (2.27) can be computed as

$$\begin{aligned} J_K &= J_K^p + J_K^d + J_K^{high} + J_K^{low} \\ &= (J_K^p + J_K^d + J_K^{high}) + (LP^*/1.26 + J_K^p + J_K^d + J_K^{high}) \frac{\delta_K}{1 - \delta_K}. \end{aligned} \quad (2.28)$$

## 2.7 Examination of the total energy cost

In the formulation for the total energy cost of adaptation (2.28), the cost components are all functions of the SNR estimate,  $\hat{\gamma}_K$ , whose statistical properties are described by (2.19), (2.21), (2.22). Since  $\hat{\gamma}_K$  exhibits a pathological behavior as stated in Lemma 1, one might expect this behavior to manifest when examining the total energy cost (2.28). This means that the least total energy cost occurs when  $P_0 \downarrow 0$  and  $K \rightarrow \infty$ , that is the same as the strategy for minimizing the variance of  $\hat{\gamma}_K$  (2.22) as described in Lemma 1. We make this observation a remark.

**Remark 3** *The strategy to minimize the total energy cost, including the cost of adaptation, of the power control process is  $P_0 \downarrow 0$  and  $K \rightarrow \infty$ .*

We shall demonstrate Remark 3 by simulations through `matlab`. The following parameters are used throughout the simulations.

**Complex Channel Gain:**  $H = 0.7 + j0.4$ .

**Noise Power:**  $N = 0.001W$ , or 0dBm.

**Reference BER:**  $10^{-3}$  that results in a reference SNR of  $\gamma^* = 10.3\text{dB}$  for QPSK signal.

**Number of Data Symbols:**  $M = 1024$ .

**Number of Data Symbols Transmitted Before Retransmission:**  $L = 24$ .

**Pilot Transmitted Power,  $P_0$ :** This will vary to demonstrate Remark 3.

**Number of Pilot Symbols,  $K$ :** This will vary to demonstrate Remark 3.

First in Figure 2.5, the transmitted power for the pilot symbols takes the value in the set  $\{6, 8, 10, 12\}$ dBm. In this figure, we have the plot of the cost (2.28) as a function of the number of pilot symbols for different values of pilot transmitted power.

Note that because we have not specified a bit rate, the energy cost  $J_k$  (2.28) plotted in Figure 2.5 is in a nominal scale. The minima of the cost arrive in the reverse order of pilot power levels  $P_0$ , with the smallest minimum belonging to the smallest pilot transmitted power of 6dBm. For each curve, the informative message energy cost  $MP^* = 17.06\text{J}$  dominates the energy cost of pilot symbols. The optimal pilot-to-total-energy ratio, that is the ratio of the optimal pilot energy to the total energy cost, is at 6dBm and equals to

$$\frac{K^* P_0}{J_K^*} = \frac{95 \times 0.004}{17.6502} = 2.14\%,$$

where  $K^*$  is the number of pilot tones at which the cost is minimal,  $P_0 = 6\text{dBm} = 0.004\text{W}$ , and  $J_K^*$  is the minimal cost.

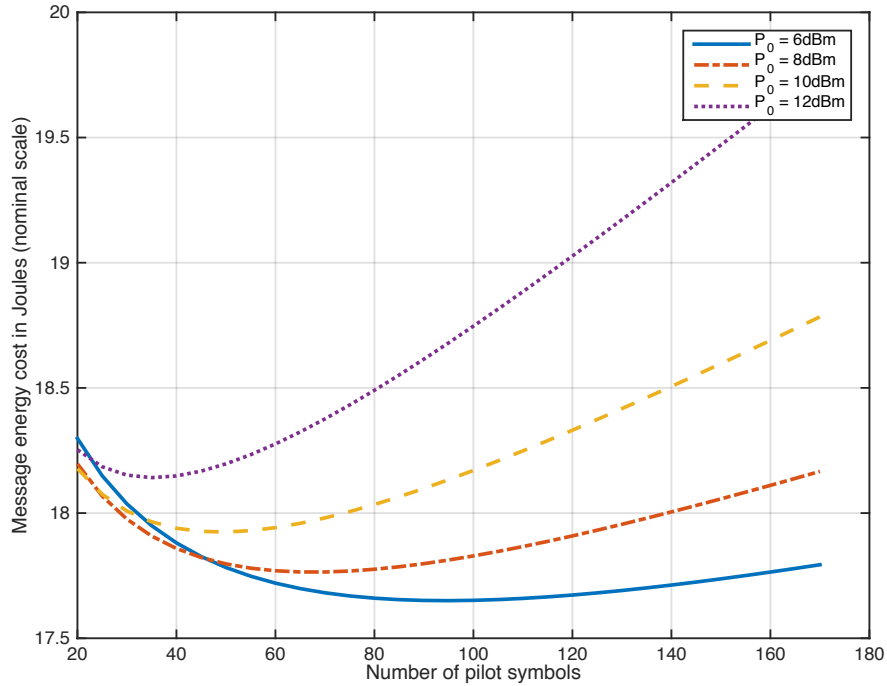


**Figure 2.5:** The total message energy: Simulation 1. The minimal energy values decrease with diminishing  $P_0$

Next, in Figure 2.6 and Figure 2.7, the pilot power is reduced further and, again, the total energy cost  $J_k$  (2.28) is plotted against the pilot length  $K$ . Similar to the results in Figure 2.5, the minima of the cost arrive in the reverse order of pilot power levels  $P_0$ , with the smallest minimum occurring at the smallest pilot transmitted power.

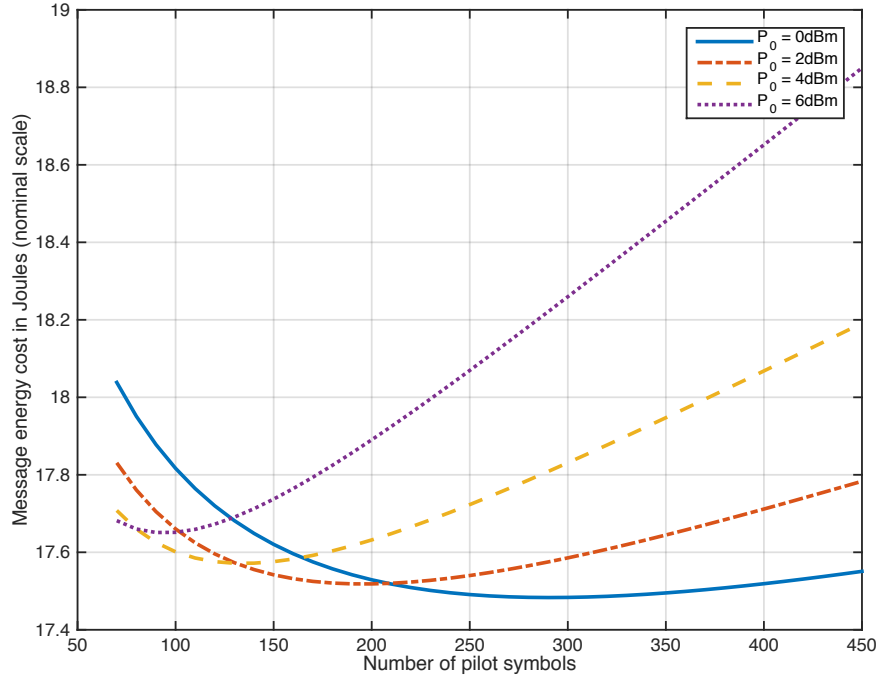


**Figure 2.6:** The total message energy: Simulation 2. The minimal energy values decrease with diminishing  $P_0$

We summarize the simulation results from Figures 2.5, 2.6 and 2.7 in Table 2.1. The simulations demonstrate the result of Lemma 1, where we have found the optimal strategy to minimize the total energy cost of adaptation in power control is  $P_0 \downarrow 0$  and  $K \rightarrow \infty$ . In Table 2.1,  $K^*$  is the optimal number of pilot tones at which the total energy cost is minimal for its respective  $P_0$ , and the corresponding minimal cost is  $J_K^*$ . The optimal pilot-to-total-energy ratio is denoted as  $R^*$ . This ratio can be computed by

$$R^* = \frac{K^* P_0}{J_K^*}.$$



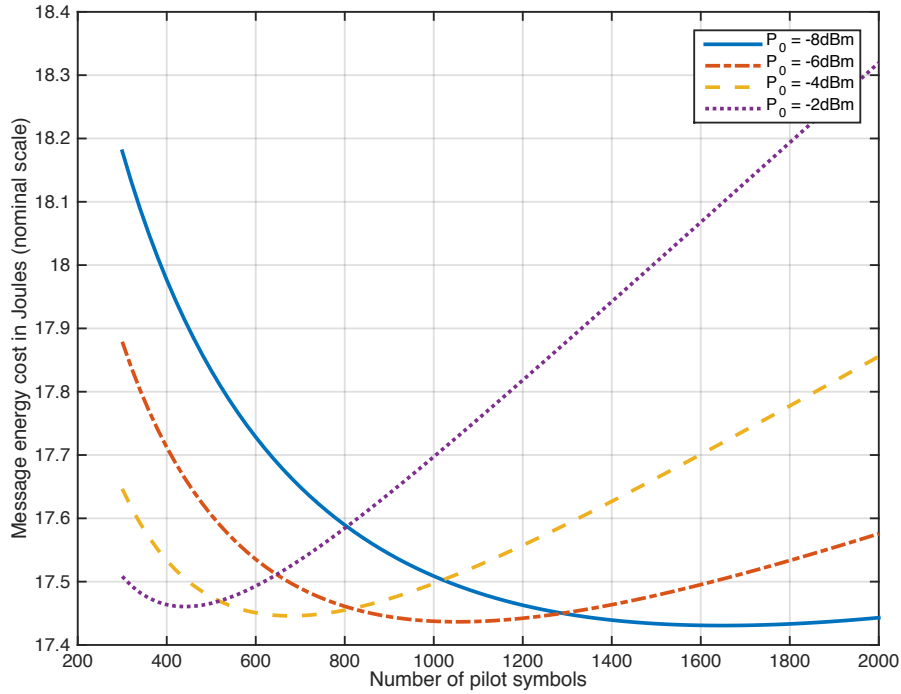


**Figure 2.7:** The total message energy: Simulation 3. The minimal energy values decrease with diminishing  $P_0$

Note that in the real-channel case, whose results are summarized in Theorem 4, the cost  $J_K$  exhibits the same behavior as in the complex-channel case stated in Remark 3. That is, to minimize the total energy cost spent on power control, one should use zero power to transmit an infinite number of pilot tones.

## 2.8 Total energy cost with MS mobility

In the previous sections, we have assumed that the channel is static. Now we quantify the case where the MS is moving with a certain velocity. The Rayleigh fading channel model includes a mobility description, whereby the channel response, now a complex random variable with the independent in-phase and quadrature components both being gaussian with zero mean and variance  $\sigma^2$ , possesses a normalized autocorrelation

**Table 2.1:** Summary of simulation results.

$P_0$	-8	-6	-4	-2	0
$K^*$	1640	1060	680	440	290
$J_K^*$	17.43	17.44	17.45	17.46	17.48
$R^*(\%)$	1.49	1.53	1.55	1.59	1.66

$P_0$	2	4	6	8	10	12
$K^*$	200	130	95	70	50	35
$J_K^*$	17.52	17.57	17.65	17.76	17.92	18.14
$R^*(\%)$	1.81	1.86	2.14	2.49	2.79	3.06

function. This function describes how the values of the channel gain  $H$  before and after the MS has moved a certain distance during a time interval  $\tau$  are spatially correlated to each other. It is a function of the constant speed of the MS expressed as a so-called Doppler frequency shift,  $f_d$  [69]

$$R_{HH}(\tau) = \sigma_{|H|}^2 J_0(2\pi f_d \tau), \quad (2.29)$$

where  $\sigma_{|H|}^2$  is the variance of  $|H|$  and  $J_0(\cdot)$  is the zeroth-order Bessel function of the first kind. The absolute value of the channel gain,  $|H|$ , is Rayleigh distributed and has a pdf described as [70]

$$p_{|H|}(x) = \frac{x}{\sigma^2} e^{-x^2/2\sigma^2},$$

where, again,  $\sigma^2$  is the variance of both the in-phase and quadrature components of  $H$ .

We have the following properties of  $|H|$  [71]:

$$E[|H|] = \sigma \sqrt{\frac{\pi}{2}} \approx 1.253\sigma, \quad \sigma_{|H|}^2 = \frac{4-\pi}{2}\sigma^2 \approx 0.43\sigma^2, \quad (2.30)$$

where, again,  $\sigma_{|H|}^2$  is the variance of  $|H|$  that is different from the variance of its in-phase and quadrature components,  $\sigma^2$ . From (2.30),  $E[|H|^2] = 2\sigma^2$ .

To accommodate the change of the channel due to mobility of the MS, we propose a modified total energy cost function based on the original total energy cost function  $J_K$  (2.28), computed as follows.

$$J_K^{mod} = (1 + P_M)J_K, \quad (2.31)$$

where  $P_M$  is the probability that, after a pilot sequence of length  $K$  has been used and an informative data sequence of length  $M$  transmitted, the channel gain has changed more than 2dB as a result of the MS mobility, making the SNR estimate no longer usable. The following theorem states the upper bound on this new, modified total energy cost function.

**Theorem 5** *The modified total energy cost function (2.31) accounting for the mobility of the MS is bounded by*

$$J_K^{mod} \leq [10.75 - 9.75J_0(2\pi f_m \tau)]J_K,$$

where  $\tau = K + M$ ,  $f_m = f_d T$  is the maximum Doppler shift normalized by sampling time  $T$ , and  $J_K$  is the total energy cost in the case of immobile MS transmitter (2.28).

*Proof:* Since the adaptive power control algorithm we are employing adjusts the transmitted power by steps of 2dBm, retraining will be required if, because of a change in the SNR after a time interval corresponding to  $\tau = K + M$  symbols, the optimal transmitted power level deviates by 2dBm from the previous optimal transmitted power level. Let the superscripts  $(0)$  and  $(\tau)$  signify the beginning and the end of the transmission of  $(K + M)$  symbols, respectively. The probability that training is required again after

$(K + M)$  symbols due to mobility is given by

$$P_M = Pr(|P^{*(\tau)} - P^{*(0)}| \geq 2dBm).$$

where  $P^*$  denotes the optimal transmitted power level and  $Pr$  probability.

To find  $P_M$ , notice that  $P^* = \frac{N\gamma^*}{|H|^2}$ , where  $\gamma^*$  is the constant optimal value of SNR.

Here, to assess the effect of mobility, we keep the noise power,  $N$ , constant. Thus,

$$\begin{aligned} P_M &= Pr\left(\left|10\log\frac{|H^{(\tau)}|^2\gamma^*}{N} - 10\log\frac{|H^{(0)}|^2\gamma^*}{N}\right| \geq 2dBm\right) \\ &= Pr\left(\left|\log\frac{|H^{(\tau)}|}{|H^{(0)}|}\right| \geq 0.1dBm\right) \\ &= Pr\left(\frac{|H^{(\tau)}|}{|H^{(0)}|} \geq 10^{0.1}\right) + Pr\left(\frac{|H^{(\tau)}|}{|H^{(0)}|} \leq 10^{-0.1}\right) \\ &= Pr\left(|H^{(\tau)}| - |H^{(0)}| \geq 0.26|H^{(0)}|\right) + Pr\left(|H^{(\tau)}| - |H^{(0)}| \leq -0.21|H^{(0)}|\right). \end{aligned}$$

Additionally, notice the following:

$$Pr\left(|H^{(\tau)}| - |H^{(0)}| \geq 0.26|H^{(0)}|\right) \leq Pr\left(|H^{(\tau)}| - |H^{(0)}| \geq 0.21|H^{(0)}|\right),$$

and

$$Pr\left(|H^{(\tau)}| - |H^{(0)}| \leq -0.21|H^{(0)}|\right) \geq Pr\left(|H^{(\tau)}| - |H^{(0)}| \leq -0.26|H^{(0)}|\right).$$

Hence the bounds on  $P_M$  are

$$Pr\left(\left||H^{(\tau)}| - |H^{(0)}|\right| \geq 0.26|H^{(0)}|\right) \leq P_M \leq Pr\left(\left||H^{(\tau)}| - |H^{(0)}|\right| \geq 0.21|H^{(0)}|\right). \quad (2.32)$$

Now define a new random variable  $\Delta = |H^{(\tau)}| - |H^{(0)}|$ . Since  $H$  is composed of the in-phase and quadrature components that are both gaussian with zero mean and variance  $\sigma^2$ , according to (2.30), it follows that  $E[\Delta] = 0$  which makes  $\text{Var}(\Delta) = E[\Delta^2]$ . Now for any real number  $\epsilon > 0$ , Chebyshev's Inequality states that [63]

$$Pr(|\Delta - E[\Delta]| \geq \epsilon) \leq \frac{\text{Var}(\Delta)}{\epsilon^2},$$

so that

$$Pr\left(\left||H^{(\tau)}| - |H^{(0)}|\right| \geq \epsilon\right) \leq \frac{E\left[\left||H^{(\tau)}| - |H^{(0)}|\right|^2\right]}{\epsilon^2}$$

Note also

$$\begin{aligned} E\left[\left||H^{(\tau)}| - |H^{(0)}|\right|^2\right] &= E\left[\left(|H^{(\tau)}| - |H^{(0)}|\right)^2\right] \\ &= 2E[|H|^2] - 2E[|H^{(0)}||H^{(\tau)}|] \\ &= 4\sigma^2 - 2E[|H^{(0)}||H^{(\tau)}|], \end{aligned}$$

that leads to

$$Pr\left(\left||H^{(\tau)}| - |H^{(0)}|\right| \geq \epsilon\right) \leq \frac{4\sigma^2 - 2E[|H^{(0)}||H^{(\tau)}|]}{\epsilon^2}. \quad (2.33)$$

Now the autocorrelation function of  $|H|$  as stated earlier (2.29) is

$$R_{HH}(\tau) = E\left[\left(|H^{(0)}| - E[|H|]\right)\left(|H^{(\tau)}| - E[|H|]\right)\right] = \sigma_{|H|}^2 J_0(2\pi f_m \tau),$$

which is equivalent to

$$E \left[ |H^{(0)}| |H^{(\tau)}| - (E[|H|])^2 \right] = \sigma_{|H|}^2 J_0(2\pi f_m \tau),$$

and so,

$$\begin{aligned} E \left[ |H^{(0)}| |H^{(\tau)}| \right] &= \sigma_{|H|}^2 J_0(2\pi f_m \tau) + (E[|H|])^2 \\ &= 0.43\sigma^2 J_0(2\pi f_m \tau) + 1.57\sigma^2. \end{aligned}$$

Combining the above with (2.33) yields

$$Pr \left( \left| |H^{(\tau)}| - |H^{(0)}| \right| \geq \varepsilon \right) \leq \frac{4\sigma^2 - 2\sigma^2[0.43J_0(2\pi f_m \tau) + 1.57]}{\varepsilon^2}. \quad (2.34)$$

In addition to (2.32) and (2.34), let  $\varepsilon = 0.21|H^{(0)}| > 0$ . Then we have the following bound on  $P_M$

$$P_M \leq \frac{4\sigma^2 - 2\sigma^2[0.43J_0(2\pi f_m \tau) + 1.57]}{0.21^2 |H^{(0)}|^2}.$$

Averaging the above over the channel gain  $H$  we have

$$P_M \leq \frac{4\sigma^2 - 2\sigma^2[0.43J_0(2\pi f_m \tau) + 1.57]}{0.0441 \times 2\sigma^2},$$

or

$$P_M \leq 9.75[1 - J_0(2\pi f_m \tau)].$$

Substituting the above equation into the modified total energy cost function (2.31)

yields the following bound for the modified total energy cost function

$$J_K^{mod} \leq [10.75 - 9.75J_0(2\pi f_m \tau)]J_K.$$

□

Since we are concerned with the minimum of the total energy cost, we take

$$J_K^{mod} = [10.75 - 9.75J_0(2\pi f_m \tau)]J_K. \quad (2.35)$$

Note that in the case of stationary MS, we have no Doppler shift, i.e.  $f_d = 0$  and  $J_0(2\pi f_m \tau) = 1$ . The modified total energy cost  $J_K^{mod}$  then becomes the original total energy cost  $J_K$ .

We now can plot the modified total energy cost to see the effect of mobility. In addition to the parameters used in Section 2.7, the following parameters are employed.

**Communication network:** We take as GSM 1900GHz, also known as PCS-1900.

**MS velocity:** Take a MS transmitter moving at a speed of  $v = 40\text{km/h}$ , which corresponds to a maximum Doppler frequency shift of

$$f_d = \frac{vf_{GSM}}{c} = 70.37\text{Hz},$$

where  $f_{GSM} = 1900\text{GHz}$  is the frequency of PCS-1900 and  $c$  is the speed of light.

**Sampling time:**  $T = 1/22800\text{s}$ , where 22800bps is the full-rate speech traffic channel (TCH/FS) bit rate in GSM [72]. This results in a maximum normalized Doppler shift of  $f_m = f_d T = 0.003$ .

In Figure 2.8, unlike the stationary MS case summarized in Table 2.1, notice that there is now an optimal pilot transmitted power, 10dBm to be exact, and a corresponding

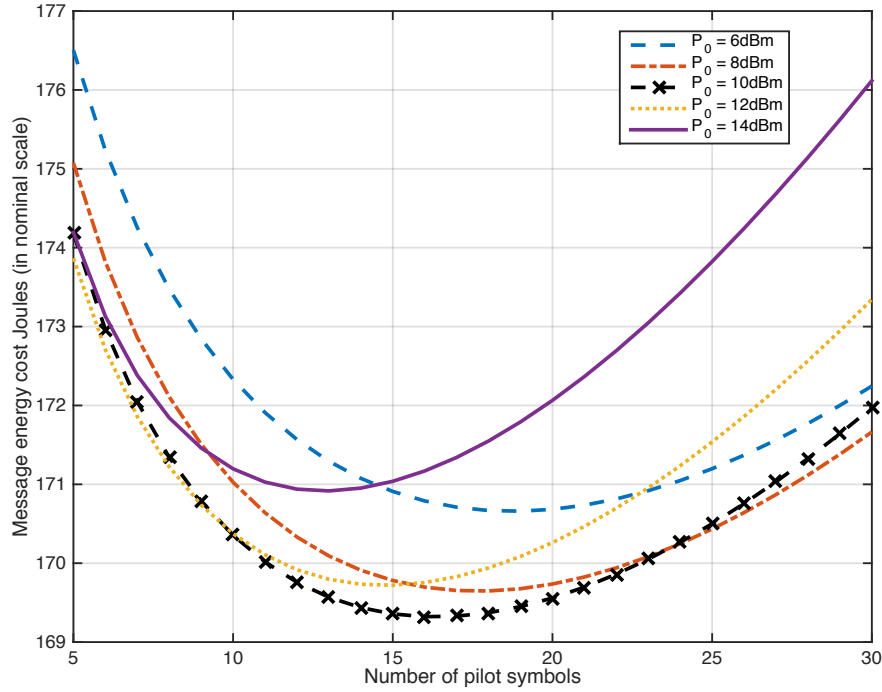


**Figure 2.8:** Modified total energy cost of power control with MS mobility illustrating the absence of pathological behavior noted in Remark 3; a minimal energy exists over  $K$  and  $P_0$ .

optimal pilot length of  $K = 12$  pilot symbols that result in an optimal total energy cost, i.e. energy cost that has the smallest minimum value, across the range of transmitted power levels considered. Clearly, the introduction of MS mobility into the total energy cost resolves its pathological behavior stated in Remark 3 where the MS is assumed stationary. When comparing Figure 2.8 to Table 2.1, the energy cost in the moving-transmitter case is much bigger than that in the stationary-transmitter case. This is due to the effect of mobility.

## 2.9 Blind adaptation via hypothesis testing

We now consider avoiding the use of the information-free pilot sequence altogether, thus effectively sidestepping the pathological behavior of the cost function as



noted in the previous sections. We shall employ statistical hypothesis testing to detect whether the current SER in the link is lower or higher than a certain usable threshold (for example,  $10^{-3}$ .)

Assume that  $m$  message symbols are sent over the link and the number of errors,  $b$ , is reported. Random variable  $b$  is binomial distributed with parameters  $(m, p)$  where  $m$  is the sample size and  $p$  is the actual SER. The test statistic is the quantity  $b/m$ , i.e. the  $m$ -sample SER estimate.

The first hypothesis test is to detect whether the SER is higher than  $10^{-3}$  and thus to determine whether or not the transmitted power should be increased.

$$\begin{cases} \text{Null hypothesis} & H_{01} : SER = p_0 = 10^{-3} \\ \text{Alternative hypothesis} & H_{11} : SER = p_1 = 10^{-2} \end{cases} \quad (2.36)$$

The second hypothesis test involves determining whether the SER is lower than  $10^{-3}$  and thus whether or not the transmitted power should be decreased.

$$\begin{cases} \text{Null hypothesis} & H_{02} : SER = p_0 = 10^{-3} \\ \text{Alternative hypothesis} & H_{12} : SER = p_2 = 10^{-4} \end{cases} \quad (2.37)$$

Following convention, denote by  $\alpha$  the probability of Type-I error, rejection of the null hypothesis when it is true; we use a common value of 5% here. Figure 2.9 depicts these 95% confidence values for the two hypothesis tests. In the figure, if  $b$  exceeds the “x” values for  $m$  samples, we reject the null hypothesis and declare the SER too high. Likewise, if  $b$  falls below the “o” values for a given  $m$ , we declare the SER too low.

To moderate this decision, the power,  $1 - \beta$ , of these tests is evaluated by computing the corresponding probability,  $\beta$ , of a Type-II error, i.e. accepting the null hypothesis when it is false. Figures 2.10 and 2.11 display the power of each test as a function of

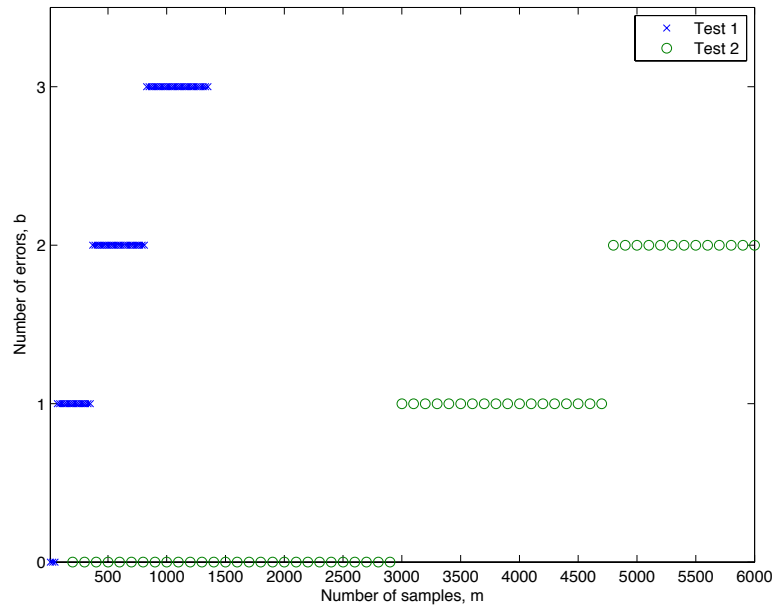


**Figure 2.9:** Number of errors  $b$  in  $m$  samples to reject the null hypothesis with 95% confidence, above the “x” values (SER too high) or below “o” values (SER too low).

sample size,  $m$ . Traditionally a power value of 80% is chosen [73]. Figures 2.9 (“x” values) and 2.10 show that for the decision to be made that the SER is too high with confidence 95% and power 80% one would require seeing more than one error in a sample of 350 bits, or, more than two errors in 360 to 810 samples. Similarly, Figures 2.9 (“o” values) and 2.11 indicate that we would need to see less than one error in 3000 samples to decide confidently that the SER was too low.

From the perspective of mobile Rayleigh fading channels, it is apparent that these sample lengths, 350 and 3000, are too large to accommodate reasonable mobilities. That is, pilot tones are necessary with realistic mobilities.

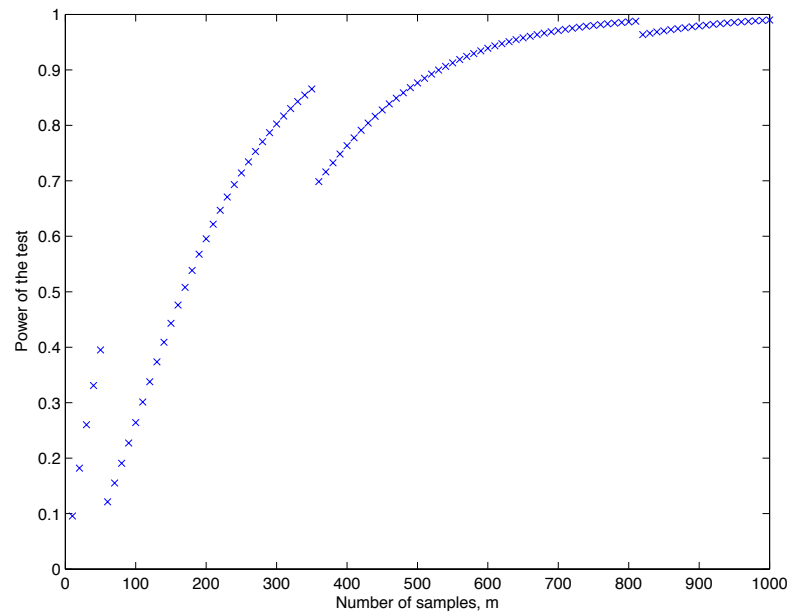


**Figure 2.10:** Power-of-test values for the first hypothesis test: SER too high.

## 2.10 Conclusion

In this chapter, an SNR estimation technique for complex channels has been proposed in communication networks with the use of pilot symbols. This is based on the LS estimate of the channel gain by the pilot symbols, followed by estimates of the signal power and noise power, and ultimately of the link SNR. Based on the SNR estimate, the MS transmitter completes the power control algorithm by choosing an appropriate transmitted power level to meet a certain BER requirement of the communication link. Our results here are applicable to OFDM systems because of their structure in the frequency domain. The results in the real-channel case are also found.

The SNR estimate is analyzed and found to exhibit a conundrum in which, to minimize the variance of the SNR estimate, the MS transmitter should employ an infinite number of pilot tones at zero transmitted power. The SNR estimate in the real-channel case also exhibits the same behavior as its complex-channel counterpart.

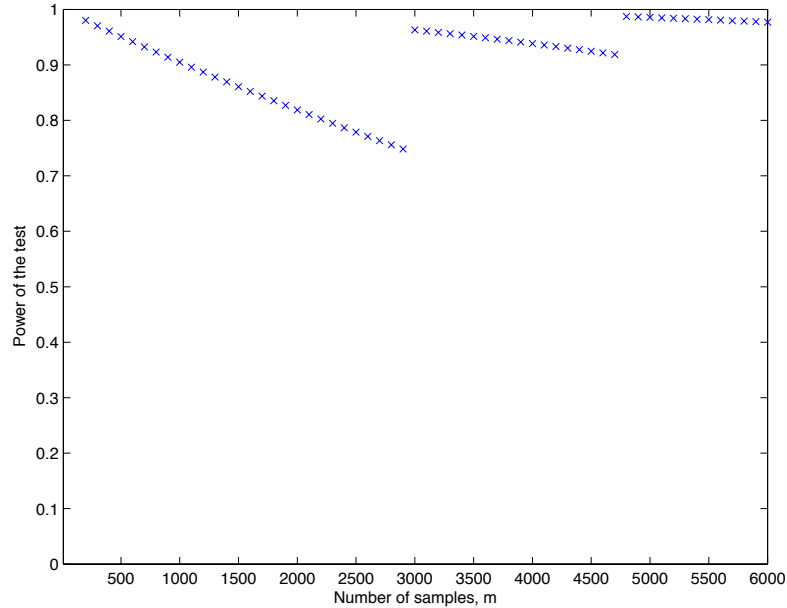


**Figure 2.11:** Power-of-test values for the second hypothesis test: SER too low.

Next, the total energy cost of power control, including the energy cost of adaptation, is formulated based on the statistics of the SNR estimate. The total energy cost takes into account the case when the SNR estimate is wrong by 2dB, both lower and higher, compared to the actual SNR, that results in either too high or too low transmitted power for the actual message data symbols. When the transmitted power is higher than necessary, the MS wastes energy. When the transmitted power is lower than necessary, a retransmission of data is required to satisfy the quality of the link. The retransmission includes the restart of the power control algorithm. As a function of the SNR estimate, the total energy cost also exhibits the same behavior as the SNR estimate, in which, to minimize the total energy cost, the MS should send an infinite number of pilot tones at zero transmitted power, as noted in Remark 3.

When the MS transmitter is assumed to have a velocity, the total energy cost is modified to take into account the change in the channel condition due to the MS mobility. The above pathological behavior of the total energy cost disappears when the

MS mobility is introduced. In this case, there exists an optimal pilot length  $K$  and pilot transmitted power  $P_0$  that results in the smallest minimum of the total energy cost across the range of the pilot transmitted power.

Finally, we propose a non-data-aided, known as blind adaptation, technique to apply to the power control problem. It is, however, found that in the setting of mobile wireless communication, the blind adaptation algorithm takes too long to compute the BER of the link, making it unimplementable.

Chapter 2, in full, is currently being prepared for submission for publication of the material, by M. H. Ha and R. R. Bitmead. The dissertation author was the primary investigator and author of this material.

# Chapter 3

## Optimal Mobile Wireless Power

## Control as a Dual Adaptive Control

## Problem

In this chapter, the power control problem in mobile wireless communications will be considered at a fundamental level where it is recognized to exhibit features that exist in optimal dual adaptive control. The problem of ODAC is first formulated by Fel'dbaum in his seminar work in the 1960's [74, 75, 76] and remains unsolved due to the *curse of dimensionality* of the Bellman's equation present in the SDP algorithm that is employed to solve the problem. Here our aim is to solve the power control problem formulated as a ODAC problem in a finite horizon and finite state space setting.

### 3.1 Introduction

Consider the power control problem in mobile wireless communication networks, where an appropriate power level must be chosen, based on the condition of the link,

to transmit information between the MS transmitter and the BS receiver. From the perspective of this chapter, we are only concerned with the battery life problem. The current power control routine is carried out billions of billions of times everyday without human monitoring. It is costly in energy; MS spends approximately 19% of the total transmitted power in the form of training sequences, known to both MS and BS, to study the communication link. The benefits of improving the power control algorithm are therefore clear. In this thesis, we set out to find a better power control routine.

This process is an adaptive control problem where MS adapts to the channel by means of studying it and selecting an appropriate transmitted power level. The transmitted power from MS should just be enough, but no more than, to overcome the fading and noise in the air interface to achieve a pre-specified target BER. Too high transmitted power levels results in wasted energy and consequently, reduced battery life, while too low a transmitted power level causes excessive errors necessitating retransmission, which conclusively is a waste of energy. However, to determine the necessary transmission power itself consumes energy. Since communications channels are subject to random noise and the attenuation is described by a probability distribution, the energy consumption is expressed in terms of expected values. We shall see that the energy-optimal power assignment depends on the initial probability distribution of the channel attenuation.

In mobile communications, the channels and their attenuation change with position and orientation, leading to a requirement of frequent updating of the transmission power to accommodate these variations. In practice, this is accomplished using channel impulse response estimation in every transmitted packet, through the inclusion of a known information-free pseudo-random *mid-amble* training sequence in every packet. This sequence is then used at the receiver to determine an estimate of the channel impulse response (usually a 6-tap finite impulse response model) and corresponding channel fade value. On the basis of this fade estimate, the receiver communicates to the transmitter

and instructs it to increase or decrease its transmission power by, for example, a quantum of 2dBm in GSM 1900GHz, also known as PCS-1900, network [11]. This is an adaptive control system aimed at minimizing the power consumption of communication and adjusting to the current channel fade. Within the context of adaptive control, this application is of interest because of its ubiquity and routine performance without human monitoring or intervention. However, we suspect it might be far from optimal.

Our aim in this thesis is to explore the nature of the power control problem from an adaptive control perspective with a focus on the aspects of ODAC first introduced by Fel'dbaum [74, 75]. For a detailed comparison of dual adaptive control to non-dual adaptive control, see [77, 76]. The dual adaptive control problem considered here combines the following features:

- (i) The control problem is specified as an optimal feedback control problem over a finite horizon.
- (ii) There is an uncertain parameter which must be estimated to achieve performance.
- (iii) The control input serves two competing purposes: probing the system to improve estimation of the critical parameter and regulating the system to achieve performance.

The nature of the dual adaptive control solution is that it depends critically on the initial probability distribution function of the parameter to be estimated. Indeed, dual adaptive solutions can bifurcate between vigorous probing and quiescence depending on this distribution. The other central feature of dual adaptive control is that its solution is computationally intractable because of the need to incorporate the future effects of the control signal on the resolution of the parameter estimate and its subsequent effect on achievable control performance. We shall rely on the (slightly) more recent formulation



of dual adaptive control due to [78] which includes the concept of *information state*, or *hyperstate*, and its evolution.

We proceed by firstly considering an archetypal dual adaptive control problem in which the transmitter and receiver share the channel fade estimate. This helps to fix ideas about the nature of power control in a simplified framework and to develop an approach to the use of the information state which is denumerable. For this case, we can compute the explicit dual adaptive control solution using a sufficiently muscular computer. This illustrates the dual adaptive nature of the problem and demonstrates the dependence of the solution on the information state. The heuristics obtained from simulation results will be presented that greatly benefit the mobile wireless power control problem. We then move to the more realistic situation where BS and MS may only communicate through a low-capacity side-channel and demonstrate how the dual adaptive formulation still holds but now acquires a level of difficulty beyond computationally intractable.

## 3.2 Literature review

Adaptive control problem is not a well defined one in control theory. Intuitively, an adaptive controller can modify its behavior to response to changes in the dynamics of the systems and the disturbances. This is often confused with feedback control that performs the same job. A long discussion at an symposium in 1961 ended with the following definition: “An adaptive system is any physical system that has been designed with an adaptive viewpoint” [79]. In their book [79], Astrom and Wittenmark suggest that “an adaptive controller is a controller with adjustable parameters and a mechanism for adjusting the parameters”, and that because of the adjustment mechanism, the controller is nonlinear. Following their suggestion, we treat adaptive control as a arbitrary subset of optimal stochastic control. It is well established that an optimal stochastic control

problem can be solved by SDP developed by Bellman [80]. It is followed that an adaptive control problem can also be solved using SDP.

As a class of adaptive control, the problem of DAC was first formulated by Fel'dbaum in his seminal work [74, 75, 76]. He established that in order to control a system with unknown parameters, it is necessary for the controller to have two purposes, namely identification and regulation. The controller, on the one hand, must provide the system with adequate amount of control in a timely manner. On the other hand, it also has to continually probe the system to get better estimates of the unknown parameters, effectively controlling the system all the more better in future steps. Such a controller is called a dual controller. The two purposes, however, are in conflict in the sense that by injecting disturbances to better estimate the unknown parameters, the regulation process has to suffer. The idea of DAC deals with this compromise in an optimal way, where the controller is neither too "cautious" (i.e. waiting for an unnecessarily long time to gather information thus not being able to direct the system in time) nor too "hurried" (i.e. performing unjustified control actions which will not be substantiated properly by the gathered information. The information obtained as the result of studying the system is contained in the conditional probability distributions of its characteristics. Unlike certainty equivalence principle, in DAC the learning process is active and the parameter uncertainty is taken into account. This characterizes DAC as closed-loop control [81] [82], to be distinguished from feedback control where parameter uncertainty is taken into account but the knowledge of future measurements via statistical description is completely ignored. A DAC problem, as a class of the general optimal stochastic control problem, can be solved by the Bellman equation and dynamic programming, but even very simple problems require enormous computation power due to the rapid growth of the dimensionality (the curse of dimensionality) of the conditional probabilities. The optimal DAC (ODAC) problem is therefore deemed unsolvable, although recent improvements in

computational power of modern computers allow some very simple problems with finite horizon to be solved numerically. Well known solved examples of ODAC are reviewed below.

One of the first ODAC problems is formulated in [82]. The system is described as a partially observable Markov process with finite state space and finite horizon. The model is then converted to a complete state information problem in addition to the problem of calculating the conditional probability distributions of the states of the associated Markov process from the measurements. The ability to solve the first part of the problem off-line means a significant reduction of the real-time computational effort. The functional Bellman loss function is found to be bounded lower by the minimal cost of the case of perfect measurements and upper by the minimal cost of the case of no measurements at all.

A similar ODAC problem where the system is described as a four-state Markov chain with finite horizon is posed in [83]. The paper considers 2 problems: open-loop and closed-loop. The simple setup allows the Bellman equation to be solved analytically and comparison to be made for various controllers including suboptimal controllers and the optimal dual controller in terms of loss functions, with differing time horizons. It is found that the open-loop regulators give the biggest loss. The open-loop control and one-step regulator (cautious control, as pointed out in [77]) do not use identification, thus called passively adaptive. The rest of the strategies, the two-step and approximate multistep controllers and the optimal dual controller use identification and give less loss than the other regulators. These are called actively adaptive, another term coined to describe a DAC problem. For the particular problem considered in the paper, it seems that a good way to derive a suboptimal controller is to include some approximation of the future loss when taking expectation and minimizing the loss function.

In [84], Astrom & Helmersson take on a similar problem to that of Bohlin [85]

and numerically solve a ODAC problem of an integrator with a constant unknown gain. It is shown that for a time horizon greater than 1, the optimization can no longer be done analytically but a longer time horizon improves the estimates. The optimal control can be discontinuous when a probing signal is introduced to improve the estimates. The DAC controller is then compared to the CE and cautious controllers. It is found for poor estimation and large control errors, the dual control gives larger control actions than the other laws. A note to the cautious control is that “The cautious control is too cautious which results in long learning periods when gain estimate is close to zero because of turn-off”.

An example that is closest to our specific problem can be found in [86]. In this simple example, the parameter takes on only two possible values that allows the resulted Bellman equation to be solved numerically. The control law is then found for different time horizons,  $T$ . When the time horizon is  $T = 1$ , the controller is cautious. When  $T \geq 3$ , the exact closed form for the Bellman equation cannot be obtained and has to be solved numerically by interpolation. When  $T \geq 4$ , the control law for the problem converges and there is hardly a difference between the control laws from that point onwards. It is also found that probing, arising as the controller tries to compromise between identification and regulation, increases as the system becomes more unstable.

It is worth being mentioned that all the ODAC problems above are formulated at a fundamental and academic level and has no real-life applications. Due to the computational complexity and the lack of a closed-form solution, the literature is motivated to develop methods of suboptimal solutions while trying to retain the dual feature. Most of other works on DAC are therefore suboptimal (SDAC). For a thorough survey on history of DAC and methods of suboptimal DAC, the reader is referred to [87] and [77]. According to [77], if the loss function is minimized only one-step ahead, the controller is called a cautious controller. The author presents ways to derive suboptimal controllers,

such as adding perturbation signals to the one-step ahead (cautious) controller, constraining the variance of the parameter estimates and using finite parameter sets. The author recommends dual control when the time horizon is short and initial estimates are poor, or when the process is changing rapidly. In [88] adds to the loss function new information, an innovations sequence, about the unknown system parameters contained in the outputs. In [89], active suboptimal dual adaptive control is developed where the suboptimal controller takes into account the future changes of unknown system parameters by including the conditional variance of the estimate in the loss function. In [90], the authors analyze approximations to DAC, where two step time horizon and reformulation of the loss function are considered, and various suboptimal controllers compared. In [91], for a nonlinear stochastic system, approximation is introduced to the cost function while preserving its closed-loop feature. The authors call this actively adaptive, their term for DAC. The control tries to track a specific target of the state. It is found that the dual controller spends a significant amount of energy at initial time to actively learn the system, resulting in a substantially smaller terminal miss distance to the reference point compared to the CE that only has “accidental” learning due to the noise acting as perturbation to the system. However the computational burden is still there as it is to be carried out on-line.

An approximation to the ODAC problem is posed in [81] by using a wide-sense information state (or hyper-state) and linearization of the cost function. Here the dual aspect is realized in stochastic nonlinear systems where the uncertainty consists of the inaccuracy of state estimation. Weighting of the future parameter covariance is introduced to the cost function to signify the “value of future information”. The CE controller is found to be optimal solution of the linear quadratic gaussian control problem. The result of simulation study provides some practical applications of dual control in soft landing, interception and stochastic resource allocation. Pre-posterior analysis is when a

non-anticipative controller uses the probabilistic description of the future observations, before they are actually taken, to benefit the control performance. This is closed-loop as opposed to feedback control. The latter utilizes the past measurements but does not use the probabilistic description of the future measurements to anticipate them.

Astrom & Wittenmark [92] analyze the problems of identification and control, both separately and combined altogether, in a simple regression model. When identification and control are separate, the data obtained from observations during control phase cannot be used to improve the estimates. A sufficient statistic for the conditional distributions is derived. It is found the complexity of the problem remains unchanged whether the parameters are assumed constants or stochastic processes. The control policies of the one-stage and N-stage control problems that take different forms of the cost function are found to be very different. For the former, the control signal in the combined problem exhibits a “falling asleep” effect where it is close to zero over long periods.

Next, we shall look at some real life industrial applications of suboptimal DAC. Note that as far as we know, there is no application that employs the optimal solution of the DAC problem

Considered the first real life industrial application of DAC, [93] deals with the nonlinear system of a thermomechanical pulping refiner motor and draws heuristics. A suboptimal controller is derived by a constrained certainty equivalent approach coupled with an extended output horizon and a modification (adding future uncertainty of the unknown parameter) to the cost function to get probing effects. This suboptimal DAC algorithm is originally derived in [89]. A sign change of the gain however can cause discontinuity in the control signal that leads to failure.

Another application of DAC on paper coating industry is developed in [94]. The controller is an active suboptimal dual controller that minimizes a nonlinear performance index that reflects the nonlinearity of the paper coating process and Kalman filter is used

to track gain variations. The controller is derived by including the future covariance of the parameters in the loss function as a suboptimal way to introduce probing effect to the controller. The controller has some constraints which, if violated, make the minimization of the cost function become a quadratic programming problem that can also be solved.

Dual control of nonholonomic mobile robots is analyzed in [95]. The loss function is explicit, suboptimal, innovation-based following the method of [88]. Using Monte Carlo simulation and hypothesis test, DAC is proved to exhibit improvements over non-adaptive and non-dual adaptive control methods.

Some other industrial applications include the dual control solution to a lab-scale vertical take-off aircraft [96], a solar collector field [97] and a Hammerstein neural system [98].

Our approach is similar to the representation of the ODAC problem in [78]. We choose to study an existing practical ODAC problem, the mobile wireless power control problem, which is actually an optimal stochastic control problem with an unknown parameter, namely the channel fading coefficient, in order to look for heuristics and to compare the optimality of ODAC to the CE approach. As far as we know, this is the first time ODAC is used on a real-life industrial application. Here, unlike previous real-life examples, we look for an approximation of ODAC solution and not an approximation of the optimization problem, that is SDAC.

### **3.3 Solution to optimal dual adaptive control**

The SDP algorithm and Bellman's equation have been well known to offer the solution to the DAC problem. In his 1965 book [76], Fel'dbaum employed the SDP algorithm to pose and analyze, but not fully solve, some very simple examples categorized as ODAC. However he was not able to obtain the solutions to the problems, deliberately

selected to be of minimal complexity. Even though he employed an approximation to deal with integration, he was unable to yield computational answers, because of the limited availability of computing power at the time. Essentially the formulation of Fel'dbaum was translated and updated by Kumar and Varaiya [78, 99] with the adoption of the information state, also known as the hyperstate, to be discussed shortly. Here we shall follow them closely, with clarification to the original source, to develop the general solution to ODAC using SDP.

### 3.3.1 Problem formulation and information state

The dynamics of the problem take the form

$$\begin{aligned} x_{k+1} &= f_k(x_k, u_k, v_k), \\ y_k &= h_k(x_k, w_k), \quad k = 0, 1 \dots \end{aligned} \tag{3.1}$$

where  $w_k$  and  $v_k$  are process noises. The state is not observable because of the measurement noise  $w_k$ . For each  $k$ , the control value  $u_k$  is selected from a pre-specified control set  $\mathbf{U} \subset \mathbb{R}^m$ . A feasible control law is any sequence  $g = \{g_0, g_1, \dots\}$  such that  $u_k = g_k(Y^k) \in \mathbf{U}$ , where  $Y^k = \{y_0, y_1, \dots, y_k\}$ . Denote by  $\mathbf{G}$  the set of all feasible control laws. We are to find the best control law in  $\mathbf{G}$  that minimizes the following performance index

$$J^g = E^g \left[ \sum_{k=0}^{N-1} c_k(x_k, u_k) + c_N(\pi_N) \right], \tag{3.2}$$

where  $c_k$  are the cost functions whose formulation depends upon the purposes of the control process. The cost functions  $c_k$  are defined for  $k = 0, \dots, N-1$ , where  $N$  is the finite time horizon, and  $c_N$  being the terminal cost.

Consider a finite state space of dimension  $I$ , that is  $x_k \in \{1, 2, \dots, I\}$ . The system



is described by the state transition matrix

$$\begin{aligned} P(u) &= \{P_{ij}(u), 1 \leq i, j \leq I\} \\ &= P(x_{k+1} = j | x_k = i, u_k = u), \end{aligned}$$

where capital  $P$  signifies probabilities, and the output transition probability density

$$p(y_k | i) = p(y_k | x_k = i) \quad (3.3)$$

where the lower case  $p$  denotes probability density functions (pdf).

Because the state is not measured, we need a new quantity, a sufficient statistic, that allows the state estimate to be computable based only upon the available information

$$Z^k = (Y^k, U^{k-1}) = (u_0, y_1, u_1, y_2, \dots, u_{k-1}, y_k), \quad (3.4)$$

where  $U^{k-1} = \{u_0, u_1, \dots, u_{k-1}\}$ . As the next control and measurement are obtained, the information state can also be updated based on its previous value and the new information.

The definition of the information state can be expressed as follows.

**Definition 7 (Information State: Kumar & Varaiya [78] Definition (4.2))** *The quantity  $\pi_k$  is an information state for the stochastic system (3.1) if*

- $\pi_k$  is a function of  $Z^k$  (3.4), and
- $\pi_{k+1}$  can be determined from  $\pi_k$ ,  $y_{k+1}$  and  $u_k$ .

For our purposes, the information state is formulated as the conditional probability vector of the state  $x_k$  given the available history (3.4)

$$\pi_k(Z^k) = [P(x_k = 1 | Z^k), \dots, P(x_k = I | Z^k)]. \quad (3.5)$$

An important note is that the information state does not depend on the policy  $g$  as proved in [78], and it can be finite-dimensional when the state  $x_k$  takes its values in a finite set.

### 3.3.2 Information state update

With new information obtained to add to the history  $Z^k$  (3.4), the information state can be updated to take into account the effect of the controls on the evolution of the state's statistics. This is a crucial feature that sets DAC apart from non-dual adaptive control.

Define, for each measurement  $y_k$ , the  $I \times I$  diagonal matrix

$$D(y_k) = \text{diag}[p(y_k|x_k = i), i = 1, \dots, I]. \quad (3.6)$$

Then the information state  $\pi_{k+1}(Z^{k+1})$  update equation based on the current measurement,  $y_{k+1}$ , the current control,  $u_k$ , and the previous information state,  $\pi_k(Z^k)$ , can be obtained by Bayes' rule as [78, 100]

$$\begin{aligned} \pi_{k+1}(Z^{k+1}) &= \frac{\pi_k(Z^k)P(u_k)D(y_{k+1})}{\pi_k(Z^k)P(u_k)D(y_{k+1})\underline{1}} \\ &:= T_k(\pi_k(Z^k), y_{k+1}, u_k), \end{aligned} \quad (3.7)$$

where  $\underline{1}$  is the unit column vector of length  $I$ . Note that the denominator of the above equation is just a normalization factor to ensure that we have a probability.

The information state update equation (3.7) shows the duality of the control problem. Here the effect of the control is to alter the evolution of the information state in two ways:

- the control can alter the future values of the actual state  $x_k$ , and
- the control can alter future values of the history  $Z^k$  and hence the knowledge that

one has of  $x_k$  through the information state.

The first feature can be viewed as regulating the system, while the second feature actively learning the system. The two aspects are in conflict, where the policy in attempts to minimize the cost function favors smaller controls, but to effectively learn the system to regulate it successfully, bigger controls are required. An optimal control policy represents a compromise between the two purposes. This dual feature is unique to the case of partial state information and not present in the case of complete state information. Partial information about the system will be contained in the information state (3.5) as a measure of the study of the system that characterizes its properties more and more precisely. Indeed a distinctive feature of DAC is the dependence of the rate of studying the system of the control policy [76].

### 3.3.3 Dynamic programming and control policy

Kumar and Varaiya [78] established that the optimal control that minimizes the performance index (3.2) is a *separated policy*, defined as follows.

**Definition 8 (Separated Policy: Kumar & Varaiya [78])** *A policy  $g = \{g_0, \dots, g_N\}$  is said to be separated if  $g_k$  depends on the measurements  $Y^k$  only through the information state, that is  $u_k = g_k(\pi_k(\cdot | Z^k))$ .*

The above definition signifies that in implementing a separated control law, the information state is first computed and then the controls chosen. The task of estimation and control are then separated. In the subsequent theorem of the SDP algorithm, an optimal control law for the problem shall be shown to be separated.

Let  $\Pi$  be the set of all probability row vectors  $\pi = \{\pi[1], \dots, \pi[I]\}$ , where  $\pi[i] \geq 0$  and  $\sum_i \pi[i] = 1$ . The problem formulated above can be solved by the following theorem that states the SDP algorithm using Bellman's equation.

**Theorem 6 (Kumar & Varaiya [78] Theorem (7.1))** Define recursively the value functions  $V_k(\boldsymbol{\pi})$ ,  $0 \leq k \leq N$  with the information state  $\boldsymbol{\pi}_k \in \boldsymbol{\Pi}$ ,

$$V_N(\boldsymbol{\pi}_N) := E_N\{c_N(x_N)|\boldsymbol{\pi}_N = \boldsymbol{\pi}\} \quad (3.8)$$

$$V_k(\boldsymbol{\pi}_k) := \min_{u \in \mathcal{U}} E_k\{c_k(x_k, u) + V_{k+1}(T_k(\boldsymbol{\pi}, y_{k+1}, u))|\boldsymbol{\pi}_k = \boldsymbol{\pi}\}, \quad (3.9)$$

where  $E_k$  signifies the expectation over the future information from time  $k$  onwards.

- Let  $g \in \mathbf{G}$ . Then

$$V_k(\boldsymbol{\pi}_k(Z^{g,k})) \leq J_k^g := E_k \left[ \sum_{l=k}^{N-1} c_l(x_l^g, u_l^g) + c_N(x_N^g) | Z^{g,k} \right],$$

the cost-to-go at time  $l = k$ .

- Let  $g$  be a separated control policy such that for all  $\boldsymbol{\pi} \in \boldsymbol{\Pi}$ ,  $g_k(\boldsymbol{\pi})$  achieves the minimum in (3.9). Then  $g$  is optimal in that it minimizes the performance index (3.2), and  $V_k(\boldsymbol{\pi}_k(Z^{g,k})) = J_k^g$  with probability 1.

The SDP algorithm in general requires heavy computational power reflecting the *curse of dimensionality* of the Bellman's equation (3.9). The larger the number of steps (i.e. time horizon) used in the SDP algorithm, the more demanding the computational power. When the effect of control on the future information state is included, via the  $T_k$  transformation (3.7), this complexity issue is exacerbated.

# Chapter 4

## ODAC Solutions to the Power Control

### Problem

In this chapter, the theory from Chapter 3 will be implemented to solve the problem of mobile wireless power control in a reduced complexity setting.

#### 4.1 Description of the problem

The power control problem in mobile wireless communications is reformulated according to Fel'dbaum's perspective [76] of the ODAC problem, depicted in the block diagram of Figure 4.1. In Fel'dbaum's framework, the BS and MS together act as the controller. In turn, the controlled object is the air interface that exhibits fading, whose *a priori* statistics are known.

The MS transmits a sequence of BPSK signal with power  $u_{k-1}^2$  through the communication channel, which is characterized by a single constant fading coefficient  $f$ , that is  $f_k = f$  for all  $k$ . The known *a priori* statistics of  $f$  is denoted as  $\pi_0$ . The output of the channel is the state  $x_k$  that is corrupted by the measurement AWGN noise  $w_k$  before

it reaches the BS which receives the signal as the measurement  $y_k$ . The reference SNR, denoted by  $\gamma^*$  is made known to the BS.

It is made clear at this point that we shall consider the problem with a reduced degree of complexity. In this setup, the communication link between the BS and MS is assumed to be perfect—the MS knows the measurements at the BS. This is indeed unrealistic but the assumption serves the purpose of examining the problem and its solutions from the perspective of the ODAC problem and helps draw heuristics from the solutions. As we shall see, the problem is of great difficulty even with the reduced complexity. In the end of the thesis, we shall consider the complete problem where the above assumption is eliminated.

The control, namely the MS transmitted power, bears a dual character: probing the channel to estimate the air interface, characterized by the fading coefficient, and applying the appropriate power level at which the MS should transmit the signal for reliable communications while optimizing energy. As we shall see, the control policy will be different depending on the *a priori* probability distribution of the fade, which is assumed known in advance. From this perspective and in relation to the block diagram in Figure 4.1, the problem now fits well into the description of a dual adaptive control problem which was explicated by Fel'dbaum in the 1960's [76]. Such problems have been proven notoriously difficult to solve and certainly no closed-form solution exists. However, we shall see that in this finite-state and finite-horizon setting, a solution can be computed, albeit with significant computational effort. Current commercial practice in mobile wireless power control, for example in GSM, continuously uses fixed-power training sequences to estimate the channel SNR and does not permit the adjustment of transmission power by more than 2 dB per trial. Such algorithm does not take into account the effect of the controls on the study of the fade, resulting in a waste of resources. Here in this idealized formulation the BS and MS seek to adjust the power in real-time to

minimize the transmission energy.

One of the new aspects is that unlike the current *ab initio* approach (i.e. completely uncertain fade value and training sequence based) in networks such as GSM, we have mentioned the assumption that the *a priori* a probability distribution of the fade prior to carrying out the power control algorithm. This will capture the existing approach as a special case but also refine it to accommodate improved fade knowledge as reflected in the distribution of the fade. We study the variation of the transmission power as the fade estimate is refined.

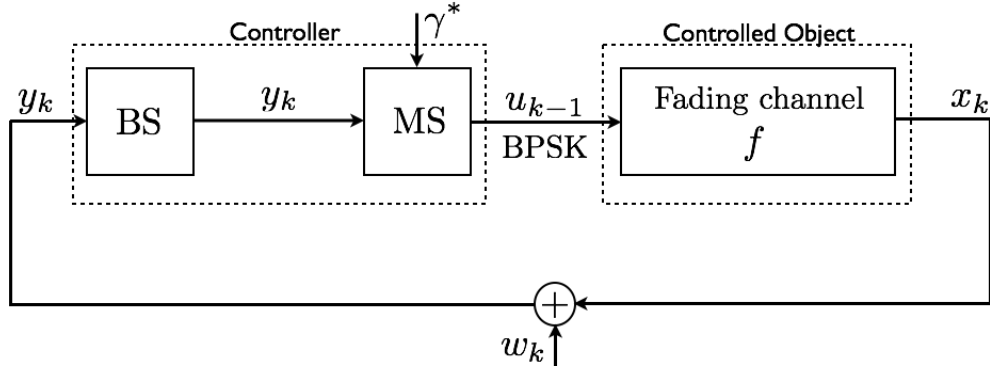


**Figure 4.1:** Power control in wireless communications redrawn following the dual adaptive control schema of Fel'dbaum [76]

In the framework of optimal dual adaptive control, the problem is classified as optimal stochastic control with an unknown constant parameter, i.e. the fading. The dynamics of this system are given by

$$\begin{aligned}
 x_k &= f u_{k-1}, \quad x_0 = f, \\
 &= f p_{k-1} a_{k-1}, \quad k = 1, 2, \dots \\
 y_k &= x_k + w_k,
 \end{aligned} \tag{4.1}$$

with the control constraint  $u_k \geq 0$  for all  $k$ . Here:

$f$  is the channel fade, which we presume to be constant over one packet transmission time,

$a_{k-1}$  is the BPSK training sequence,  $a_k \in \{-1, 1\}$ , known to both MS and BS.

$p_{k-1}$  is the amplitude, square root of the power, of the training signal. This is the control variable known solely to the MS.

$u_{k-1}$  is the transmitted signal chosen by the MS for the current packet. Since  $a_{k-1}$  is known to both ends, we identify  $u_{k-1}$  as the effective control variable.

$y_k$  is the received signal at the BS, and

$w_k$  is additive gaussian white noise of known variance  $\sigma_w^2$ .

Through out the rest of the thesis, we use  $[ \cdot ]$  for indices, subscript  $k$  for the discrete time index  $k$ . We impose the following assumptions.

### **Assumption 2**

(1.A) *The channel fade can take one of  $I < \infty$  distinct values,  $\{f[1], f[2], \dots, f[I]\}$ .*

(1.B) *The target SNR at the BS for message transmission is  $\gamma^* = 6.79\text{dB}$ , which results in a usable BER of  $10^{-3}$  for BPSK [101].*

(1.C) *There are  $I$  distinct transmission signals and powers corresponding to each possible fade value and  $\gamma^*$ .*

$$u^*[i]^2 = \frac{\sigma_w^2 \gamma^*}{f[i]^2}. \quad (4.2)$$

(1.D) *The time horizon for the problem is finite, denoted by  $N$ .*

Like any stochastic control problems, the problem being considered can be solved using SDP. This is also the tool Fel'dbaum used to analyze, but not fully solve, his very simple ODAC problems [76]. However the solution is very complex due to the rapid



growth in dimensions of the information state, that describes the evolution of the statistics of the fade as measurements are received and controls applied, as we shall see later. Here we shall constrain the problem to a finite time horizon  $N$  and finite state space of dimension  $I$ . The solutions in fact cannot be found analytically in closed-form but computationally, thanks to the aid of modern computers.

We seek to minimize the training and message power by posing the following problem in the category of stochastic optimal control.

### Stochastic optimal control problem

*With the problem described previously, minimize the performance index (3.2)*

$$J^g = E^g \left[ \sum_{k=0}^{N-1} c_k(x_k, u_k) + c_N(\pi_N) \right],$$

*over all admissible causal feedback control policies  $g \in \mathbf{G}$ ,*

$$u_k = g(Z^k) \in \{u^*[1], \dots, u^*[I]\},$$

*with:*

- initial probability mass function (pmf)  $\pi_0$  of the fade,  $f$ , and posterior pmf of the fade at time  $k$ ,  $\pi_k$ ,  $k = 1, \dots, N$ ,*
- history  $Z^k$  defined by (3.4):  $Z^k = (U^{k-1}, Y^k) = (u_0, y_1, u_1, y_2, \dots, u_{k-1}, y_k)$ ,*
- stage cost for  $k = 0, \dots, N - 1$ ,*

$$c_k(x_k, u_k) = \left( u_k^* - \frac{\sigma_w^2 \gamma^*}{f_k^2} \right)^2, \quad (4.3)$$

– terminal cost with  $i_N^* = \operatorname{argmax}_i \pi_N$ ,

$$c_N(\pi_N) = \left( u^*[i_N^*]^2 - \frac{\sigma_w^2 \gamma^*}{f[i_N^*]^2} \right)^2, \quad (4.4)$$

The expectation in the performance index (3.2) is over the  $\{w_k\}$  sequence and  $\pi_0$ .

The cost functions are chosen with the purpose of conserving the MS battery in mind. The terminal cost can be view as the cost resulting from choosing the terminal control  $u_N^*$  by certainty equivalent principle, whereby the control is selected as the most probable value present in the terminal-time information state  $\pi_N$ .

The solution to the above optimal control problem via SDP [102, 103] is well understood in principle but also extraordinarily computationally demanding, as will be demonstrated shortly. This formulation falls into the class of adaptive control, since the control depends on the estimation of a poorly known plant parameter.

It is worth remarking that, while Fel'dbaum posed a problem isomorphic to ours, he was unable to compute the solutions with the tools available in the 1960s. It is also noteworthy that this formulation has perfect feedback from BS to MS, which jointly comprise the controller. In the full problem discussed later, one needs to separate BS and MS, posit a noisy fading channel connected them, and have each solve a joint optimization problem. This is a degree of difficulty beyond the statement above.

Now that the problem has been properly formulated, we shall find its solutions using the SDP algorithm described in Chapter 3.

## 4.2 Implementation of the SDP algorithm

### 4.2.1 Information state and its update

Consider the system described by (4.1). Initially, all known information is the *a priori* pmf of the fade at time  $k = 0$ ,  $\pi_0$ . This is a distinct between our problem and the current approach in power control, where it is assumed that the channel is completely unknown every time the power control algorithm starts. The information state is the conditional probability vector of the state  $x_k$  at the MS given the available history (3.4). As measurements are received and controls applied, this conditional pmf updates to  $\pi_k$  via (3.7). This is the effect of the control on the future information about the system, a very interesting and useful feature of DAC. Since  $\{u_j : j = 1, \dots, k-1\}$  is known at the MS, the information state coincides with the conditional mass function of the fade. Therefore, we define the following as the information state for our problem.

$$\pi_k(Z^k) = \left[ P(f = f[1]|Z^k) \quad \dots \quad P(f = f[I]|Z^k) \right]. \quad (4.5)$$

By realizing the above fact, the information state can be updated from the *a priori* distribution of the fade  $\pi_0$ . Consider the information state update equation (3.7). Due to the AWGN channel with constant fade described by (4.1), the measurements  $y_k$  are distributed as  $N(fu_{k-1}, \sigma_w^2)$ . And so the conditional probabilities in  $D(y_k)$  from (3.6) are given by

$$p(y_k|x_k = i) = \frac{1}{\sqrt{2\pi}\sigma_w} \exp \left[ \frac{-(y_k - f[i]u_{k-1})^2}{2\sigma_w^2} \right]. \quad (4.6)$$

Furthermore, it is crucial to note that, since the fade is assumed to remain constant throughout the problem, the state transition matrix  $P(u_k)$  is taken as the identity matrix. This fact helps greatly with reducing the subsequent calculation. The information state

update (3.7) now reduces to

$$\boldsymbol{\pi}_{k+1}(\mathbf{Z}^{k+1}) = \frac{1}{\boldsymbol{\pi}_k D(y_{k+1}) \mathbf{1}} \boldsymbol{\pi}_k D(y_{k+1}), \quad (4.7)$$

$$:= T_k(\boldsymbol{\pi}_k(\mathbf{Z}^k), y_{k+1}, \mathbf{u}_k), \quad (4.8)$$

with the diagonal matrix  $D(y_{k+1})$  containing

$$D(y_{k+1})[i] = \frac{1}{\sqrt{2\pi}\sigma_w} \exp\left[-\frac{(y_{k+1} - f[i]u_k)^2}{\sigma_w^2}\right], \quad (4.9)$$

and  $\mathbf{1} = \begin{bmatrix} 1 & 1 & \dots & 1 \end{bmatrix}^T$ . Note that the denominator of (4.7) is just a normalization factor to ensure getting a probability. This is basically Bayes' Rule

$$\begin{aligned} P(f = f[i] | \mathbf{Z}^{k+1}) &= \frac{P(f = f[i], y_{k+1} | \mathbf{Z}^k)}{P(y_{k+1} | \mathbf{Z}^k)}, \\ &= \frac{P(y_{k+1} | \mathbf{Z}^k, f = f[i]) P(f = f[i] | \mathbf{Z}^k)}{P(y_{k+1} | \mathbf{Z}^k)}. \end{aligned}$$

The transformation  $T_k$  in (4.8) will appear in the solution via SDP, as it plays a vital role in computing the recursive Bellman's equation.

Since the information state update is based on the future measurements and controls, it can be traced back to  $\boldsymbol{\pi}_0$ . This is expressed as

$$\boldsymbol{\pi}_{k+1}(\mathbf{Z}^k) = \frac{\boldsymbol{\pi}_0 \prod_{l=1}^{k+1} D(y_l)}{\boldsymbol{\pi}_0 \prod_{l=1}^{k+1} D(y_l) \mathbf{1}}. \quad (4.10)$$

Here we can clearly see how the future measurements and controls affect the evolution of the fade's statistics. This evolution is a function of  $\boldsymbol{\pi}_0$ , and in turns, it affects the control policy. Therefore, the control policy is expect to depend greatly upon what we know about the channel beforehand, namely the *a priori* distribution of the fade. This

takes advantage of the study of the air interface to optimize the energy spent, formulated as the cost functions. This is far more advanced than the current approaches to power control where the study of the channel accumulated over time is ignored.

## 4.2.2 Duality of the power control problem

As mentioned before, the dual nature of the control signal in adaptive optimal control is that the control has two tasks: regulating the system behavior to minimize the cost, and probing or exciting the system to assist the active learning of unknown system parameters, thereby, in turn, improving control performance. Where the probing and regulating tasks are antithetical, the duality becomes evident and the nature of the solution exhibits sensitivity to the initial knowledge of the system –  $\pi_0$  in this case.

Figure 4.2 shows the quadratic cost function (4.3) versus control value  $u[i]$ , where these values are separated by 2dBm, as is used in practical mobile wireless systems such as PCS-1900. The graph is centered on the correct value  $u^*[i]$ .

The two features are immediately apparent.

- (i) The power penalty for incorrect selection of power grows quadratically with distance from  $u^*$ .
- (ii) In the practical dBm scale, the penalty for choosing too high a power is significantly greater than that for choosing dBm-equivalent too low a power.

Thus there is a penalty for incorrect power choice and this penalty is diminished for cautious lower power selections.

Equation (4.9) describes a random,  $w_k$ -dependent update of each element of the information state in response to the received measurement  $y_k$ . Examining (4.9) further,

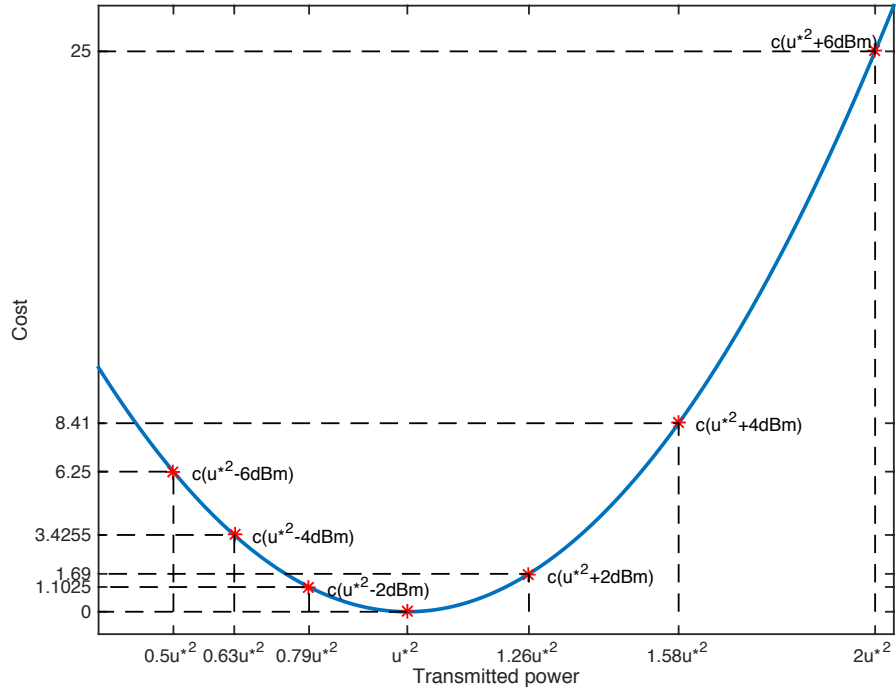


**Figure 4.2:** Quadratic cost (4.3) associated with a fixed value of  $u^* = \frac{\sigma_w^2 \gamma^*}{f^2}$  and different values of power separated by 2dBm increments.

we have the following.

$$\begin{aligned} E_w [D(y_{k+1})[i]] = & \\ & \int_{-\infty}^{\infty} \frac{1}{\sqrt{2\pi}\sigma_w} \exp \left[ -\frac{1}{2\sigma_w^2} (w_{k+1} + f^* u_k - f[i] u_k)^2 \right] \\ & \times \frac{1}{\sqrt{2\pi}\sigma_w} \exp \left[ -\frac{1}{2\sigma_w^2} w_{k+1}^2 \right] dw_{k+1}. \end{aligned} \quad (4.11)$$

Define  $\tilde{f}_i \triangleq f^* - f[i]$  and rewrite the argument of the exponential as follows by completing the square.

$$\begin{aligned} w_{k+1}^2 + (w_{k+1} + f^* u_k - f[i] u_k)^2 & \\ = \left( \sqrt{2} w_{k+1} + \frac{1}{\sqrt{2}} \tilde{f}_i [i] u_k \right)^2 + \frac{1}{2} \tilde{f}_i^2 [i] u_k^2. & \end{aligned}$$

Whence (4.11) becomes

$$\begin{aligned}
& E_w [D(y_{k+1})[i]] \\
&= \frac{1}{\sqrt{2\pi}\sigma_w} \exp\left(-\frac{1}{4\sigma_w^2} \tilde{f}^2[i]u_k^2\right) \times \\
& \int_{-\infty}^{\infty} \frac{1}{\sqrt{2\pi}\sigma_w} \exp\left[-\frac{1}{2\sigma_w^2} \left(\sqrt{2}w_{k+1} + \frac{1}{\sqrt{2}}\tilde{f}[i]u_k\right)^2\right] dw_{k+1}, \\
&= \frac{1}{\sqrt{2\pi}\sigma_w} \exp\left(-\frac{1}{4\sigma_w^2} \tilde{f}^2[i]u_k^2\right) \times \\
& \int_{-\infty}^{\infty} \frac{1}{\sqrt{2\pi}\sigma_w} \exp\left[-\frac{1}{2\sigma_w^2} \left(z + \frac{1}{\sqrt{2}}\tilde{f}[i]u_k\right)^2\right] \frac{dz}{\sqrt{2}}, \\
&= \frac{1}{2\sqrt{\pi}\sigma_w} \exp\left(-\frac{1}{4\sigma_w^2} \tilde{f}^2[i]u_k^2\right).
\end{aligned}$$

In other words,

$$E_w [D(y_{k+1})[i]] = \frac{1}{2\sqrt{\pi}\sigma_w} \exp\left(-\frac{1}{4\sigma_w^2} (f - f[i])^2 u_k^2\right). \quad (4.12)$$

Here the expectation is over  $w_{k+1}$ . Equation (4.12) illustrates the reliance on large values of  $u_k^2$  in achieving rapid refinement of the information state  $\pi_{k+1}$ . This is the dual feature of ODAC present in the problem: the stage cost is better regulated for small  $u_k^2$  while the information state is better resolved for large  $u_k^2$ . The ODAC solution via SDP algorithm strikes a balance between the two competing features to enhance the system performance in terms of energy spent.

### 4.2.3 Dynamic programming and control policy

The core difficulty in solving (3.9) for  $V_k$  and  $u^*$  lies in the application of the information state update  $T_k(\pi, y, u)$  prospectively forwards across the horizon from time  $k$  to  $N$ . Within the expectation  $E_k\{\cdot\}$ , one must account for the effect of choice of

$u_{k+j}$  for  $j = 0, \dots, N - k$  on the future values of  $\pi_{k+j}$ . Not only is Bellman's *curse of dimensionality* evident in the explosion in  $N$  of the number of feasible controls to be considered, but also the corresponding information state updates and expectation values must be computed. It is the inclusion of these many integrals over the future gaussian densities which dominates the computational burden.

With the formulation of the terminal stage cost (4.4), the terminal value function (3.8) is given by

$$V_N(\pi_N) = c_N(\pi_N) \quad (4.13)$$

The subsequent value functions (3.9) can be expressed as

$$V_k(\pi_k) := \min_{u_k \in \mathbf{U}} \left\{ \sum_i c_k(i, u_k) \pi_k[i] + \int_{y_{k+1}} V_{k+1}(T_k(\pi_k, y_{k+1}, u_k)) p(y_{k+1} | \pi_k, u_k) dy_{k+1} \right\}. \quad (4.14)$$

It is noteworthy that with the state being a discrete random variable, the value functions can also be derived using Fel'dbaum's formulation [76] with the consideration of the delay in the system's plant. Fel'dbaum calls these functions the auxiliary functions which are then to be treated with the SDP algorithm to find the optimal control policy. But since Fel'dbaum's system does not have a delay in the plant, his solution uses  $Y^k$  in the value function at time  $k + 1$  instead of  $Y^{k+1}$ .

The conditional pdf  $p(y_{k+1} | \pi_k, u_k)$  is a mixture of normal densities, which can be



written as

$$\begin{aligned} p(y_{k+1}|\boldsymbol{\pi}_k, u_k) &= \sum_j p(y_{k+1}|x_{k+1} = j)p(x_{k+1} = j|\boldsymbol{\pi}_k, u_k) \\ &= \sum_j \sum_i p(y_{k+1}|x_{k+1} = j)\boldsymbol{\pi}_k[i]P_{ij}(u_k) \end{aligned}$$

As discussed before, the state transition matrix  $P_{ij}(u_k)$  is a unit matrix. Thus, the above becomes

$$p(y_{k+1}|\boldsymbol{\pi}_k, u_k) = \sum_i p(y_{k+1}|f = f[i])\boldsymbol{\pi}_k[i]. \quad (4.15)$$

**Remark 4** *The density (4.15) is identical to the normalization factor that appears in the information state update (4.7). And so the integral in (4.14) can be reduced to a simpler form. Equation (4.13) remains unaltered.*

To obtain the expression for  $V_{N-1}(\boldsymbol{\pi}_{N-1})$ , we first write the terminal value function  $V_N$  as a function of  $\boldsymbol{\pi}_{N-1}$

$$V_N(T_{N-1}(\boldsymbol{\pi}_{N-1}, y_N, u_{N-1})) = c_N \left( \frac{\boldsymbol{\pi}_{N-1} D(y_N)}{\boldsymbol{\pi}_{N-1} D(y_N) \underline{\mathbf{1}}} \right).$$

For preceding,  $k < N$ , value functions, according to the above remark, the cancelation of the normalization  $\boldsymbol{\pi}_{N-1} D(y_N) \underline{\mathbf{1}}$  and the density mixture  $p(y_N|\boldsymbol{\pi}_{N-1}, u_{N-1})$  occurs when combined in (4.14). Thus

$$\begin{aligned} V_{N-1}(\boldsymbol{\pi}_{N-1}) &= \min_{u_{N-1} \in \mathbf{U}} \left\{ \sum_i c_{N-1}(i, u_{N-1}) \boldsymbol{\pi}_{N-1}[i] \right. \\ &\quad \left. + \int_{y_N} c_N \left( \frac{\boldsymbol{\pi}_{N-1} D(y_N)}{\boldsymbol{\pi}_{N-1} D(y_N) \underline{\mathbf{1}}} \right) dy_N \right\}. \end{aligned} \quad (4.16)$$

Now if we were to solve a one-step SDP algorithm, the solution for the optimal

control  $u_0^*$  could be found quite easily in closed form. The resulting control is termed the *cautious controller* [1]. While it still takes into account the parameter uncertainties, the gain of this controller will decrease if the variance of the parameter increases. As a result, the estimate of the parameter becomes poorer in the next step, making further increase in its variance. Following this trend, the magnitude of the control signal becomes very small. This is called the *turn-off phenomenon*.

In computing the subsequent value functions, the cancelation of the normalization and the density mixture always occurs because they both are independent of the control over which the minimization is conducted. The subsequent value functions can be found recursively by

$$\begin{aligned}
V_{N-k}(\boldsymbol{\pi}_{N-k}) = & \min_{u_{N-k} \in \mathbf{U}} \left\{ \sum_i c_{N-k}(i, u_{N-k}) \boldsymbol{\pi}_{N-k}[i] \right. \\
& + \int_{y_{N-k+1}} \min_{u_{N-k+1} \in \mathbf{U}} \left\{ \sum_i c_{N-k+1}(i, u_{N-k+1}) \boldsymbol{\pi}_{N-k}[i] D(y_{N-k+1})[i] \right. \\
& + \cdots + \left\{ \sum_i c_{N-1}(i, u_{N-1}) \boldsymbol{\pi}_{N-k}[i] D(y_{N-k+1})[i] \cdots D(y_{N-1})[i] \right. \\
& \left. \left. + \int_{y_N} c_N \left( \frac{\boldsymbol{\pi}_{N-k} D(y_{N-k+1}) \cdots D(y_N)}{\boldsymbol{\pi}_{N-k} D(y_{N-k+1}) \cdots D(y_N) \mathbf{1}} \right) dy_N \right\} dy_{N-1} \right\} \cdots dy_{N-k+1} \left. \right\}
\end{aligned} \tag{4.17}$$

The main difficulty in carrying out the SDP algorithm with the above value functions is the nested minimizations and integrations over the future measurements that affect the future information state. The dimensionality grows rather very rapidly even with a short time horizon  $N$ . This curse of dimensionality ensures that this computation explodes in complexity with horizon as we compute the succeeding value functions. Apparently the worst of them all is the initial value function  $V_0$ . There are some methods that trade the curse of dimensionality for the curse of complexity such as [104], but they

are not helpful here because we are also facing with the integrations over the infinite values of the set of measurements, that are gaussian. To deal with the integrals, we shall confine the set of possible measurements to a finite feasible range and use an approximation method, for example, the trapezoidal rule.

To briefly demonstrated Bellman's *curse of dimensionality* with the exponential increase in the number of controls to be explored as the horizon grows backwards in time, and how it is exacerbated by the nested computation of successive integral terms, consider the following overview of the simulation that is to come later. A computational implementation was developed with:

- four values for fade  $f$  with corresponding 4-vector  $\pi_k$ ,
- four control values  $\{u_k[i], i = 1, 2, 3, 4\}$ ,
- horizons  $N = 2, 3$  or 4 steps.
- integrals approximated by the trapezoidal rule with 21 points.

Matlab's `tic` and `toc` functions were used to generate approximate run time estimates with the following results.

Horizon	Computation time (s)
4-step	3300
3-step	42
2-step	1

This example will be revisited in detail in Section 4.4.

We make two observations about the stochastic dynamic programming solution.

**Remark 5** *The computation of the initial control value,  $u_0^*$ , is significantly more costly in calculation time than is the computation of any subsequent control value. Indeed, the computation time is dominated by the initial control value.*

This is evident since subsequent control calculations involve reduced-horizon dynamic programs.

**Remark 6** *The initial control calculation is a deterministic function of the initial information state. That is,  $u_0^*(\pi_0)$ .*

Based on the above remarks, in the next section we shall explore some heuristics of the problem and derive some alternative control policies to compare to ODAC.

## 4.3 Heuristics and alternative control laws

### 4.3.1 Heuristics

We build on the observations above in Remarks 5 and 6 to support the following heuristics to simplify the computational burden of the SDP algorithm.

**Heuristic 1** *Compute the initial optimal control value  $u_0^*(\pi_0)$  off-line as a precomputed function of the initial information state vector  $\pi_0$ . Then use a look-up table for this value followed by a reduced-horizon optimal control calculation or another control law.*

**Heuristic 2** *Propagate the information state from the end of  $t^{\text{th}}$  data packet,  $\pi_N^t$ , to the next packet initiation,  $\pi_0^{t+1}$ , to improve control performance and deal with a change in the communication channel. This can be accomplished by a Markov probability transition matrix,  $P_{jk}^\pi = P(f_{t+1} = f[k] | f_t = f[j])$ , that is*

$$\pi_0^{t+1} = \pi_N^t P_{jk}^\pi, \quad (4.18)$$

where  $P_{jk}^\pi$  can be found by the knowledge of the channel, e.g. Rayleigh fading channel.

While we do not simulate this second heuristic as it is out of the scope of this research, it is important to note two properties connected with the information state which justify attention to its propagation between packets. Clearly, the refinement of the information states presents a challenge to the control performance because of duality of the optimal control. So providing a concentrated information state is beneficial. Secondly, it is apparent from (4.7) that a zero element anywhere in  $\pi_k$  cannot be removed at subsequent times; likewise for a one element. Accordingly, it is possible that the information state might become degenerate and this degeneracy needs to be removed before the next packet via (4.18).

### 4.3.2 Alternative control laws

Beside our main focus on the ODAC solution, we shall also consider the following alternative suboptimal control laws.

**CE:** based on CE principle. Here the information state  $\pi_k$  is updated as usual using (4.7) based on the received signal  $y_k$ , but  $u_k$  is chosen to be the maximal *a posteriori* probability control.

$$u_k^{\text{CE}} = u^* \left( \underset{i}{\operatorname{argmax}} \{ \pi_k[i] \} \right), \text{ for all } k = 0, \dots, N \text{ and } i \in I. \quad (4.19)$$

This is a low computational complexity (but familiar) suboptimal adaptive controller.

**H:** based on Heuristic 1 with optimal  $u_0^*(\pi_0)$  precomputed followed by CE policy through the remainder of the horizon. Since the computation of  $u_0^*$  takes place off-line and CE control is low complexity, this controller too is low complexity. But it differs from CE in possessing an optimal initial step which makes up most of the computational power and time.

**ODAC-100:** based on optimal dual adaptive control with a variation of the cost function achieved by replacing terminal cost

$$c_N(\boldsymbol{\pi}_N) \leftarrow 100 c_N(\boldsymbol{\pi}_N).$$

This alters the original cost function by emphasizing the refinement of the information state by the terminal time. Since, in our scenario, we have a training sequence with optimally chosen powers but known to both MS and BS, the expectation is that non-adaptive power control or non-optimal CE adaptive power control algorithm will proceed after the training signal, where every effort has been made with SDP to estimate channel as precise as possible. This new cost function attempts to capture the penalty for poor fade estimates at time  $N$ . ODAC-100 will not in general be optimal for the original ODAC problem since it does not follow the terminal cost function specified by the optimal policy. Nevertheless because of the additional penalty, it should exhibit greater probing effects.

## 4.4 Computational results

Using `matlab`, we simulate the optimal stochastic control problem with the following parameters.

**Horizon**  $N = 4$ .

**Fade**  $f$  takes values in the set  $\{-17, -7, -3, 0\}$ dB.

**Noise** sequence  $\{w_k : k = 0, \dots, 4\}$  is taken over 10 independent realizations and is the same for each control law. Performance plots are averaged over the 10 realizations.

**Noise** power  $\sigma_w^2 = -5$ dBm.

**Power** for signal transmission takes values from a set with each power associated with the corresponding fade value as in (4.2) with the target SNR  $\gamma^* = 6.79\text{dB}$ .

$$\{u^{*2}[1], u^{*2}[2], u^{*2}[3], u^{*2}[4]\} = \{18.5, 8.9, 4.5, 1.5\} \text{ dBm.}$$

**Initial Information State** 4-vector  $\pi_0$  is taken to be

$$\pi_0 = [0.35, 0.15, 0.1, 0.4]. \quad (4.20)$$

**Integration** is conducted in (4.17) using a 21-point trapezoidal rule spanning  $\pm$ five standard deviations of the Gaussian density.

**Control laws** ODAC, CE, H, and ODAC-100 are computed and compared using the ODAC empirical performance index.

$$J^g = c_4(\pi_4) + \sum_{k=0}^3 \sum_{i=1}^4 c_k(i, u_k[i]) \pi_k[i], \quad (4.21)$$

where  $g$  is one of the four chosen control laws, with  $c_k$  from (4.3) and the terminal cost function  $c_N = c_4$  from (4.4).

#### 4.4.1 Performance and computation time

The empirical performance index (4.21) associated with the *a priori* information (4.20) and each control policy is tabulated in Table 4.1 for each possible value of the true fade  $f$ . Table 4.2 indicates the time taken for a simulation with one realization of the noise to complete for each control scheme and with differing time horizons.

Observations can be made based on Tables 4.1 and 4.2.

- ODAC outperforms the other control laws according to (3.2), although it does

**Table 4.1:** Average empirical performance ( $\times 10^4$ ) of the control policies and differing real fade values,  $f[i]$ . The performance is computed using the ODAC cost (4.21).

Actual fade:	$f[1]$	$f[2]$	$f[3]$	$f[4]$
ODAC	21	25	15	14
ODAC-100	25	35	19	14
CE	36	34	35	32
H	21	26	15	14

**Table 4.2:** Computation time of the control laws with a single realization of the measurement noise and differing time horizons.

Time horizon	ODAC & ODAC-100	CE	H
4-step	3300s	7ms	7ms
3-step	42s	0.3ms	0.3ms
2-step	1s	0.2ms	0.2ms

this at very considerable computational and complexity cost. The optimality of ODAC is in terms of expectations and definitely need not be evident with every noise realization. Indeed, within the ten realizations there are few where even CE outperforms ODAC for those specific noise realizations.

- ODAC-100, even though a result of the full stochastic dynamic programming algorithm, is suboptimal for the ODAC cost. The balance between probing and regulation leans towards probing when compared to ODAC.
- CE displays its suboptimality, reflecting its lack of probing or, equivalently, undue focus on regulation.
- As expected from its construction, the performance of policy H falls in between ODAC and CE, being very close to ODAC. However, its advantage is that its computational complexity is very close to that of CE, making it much more applicable and realistic compared to ODAC.



- Computational time for SDP increases extremely rapidly with increasing SDP time horizon, indicating the computational burden in solving the Bellman's equation (4.17) that is notoriously known for its curse of dimensionality.
- The computational times of ODAC and H and CE are different by a factor of nearly 500,000 in the case of 4-step SDP. This demonstrates the benefit of choosing  $u_0^*$  based on  $\pi_0$ , an example of which is presented in Section 4.3.

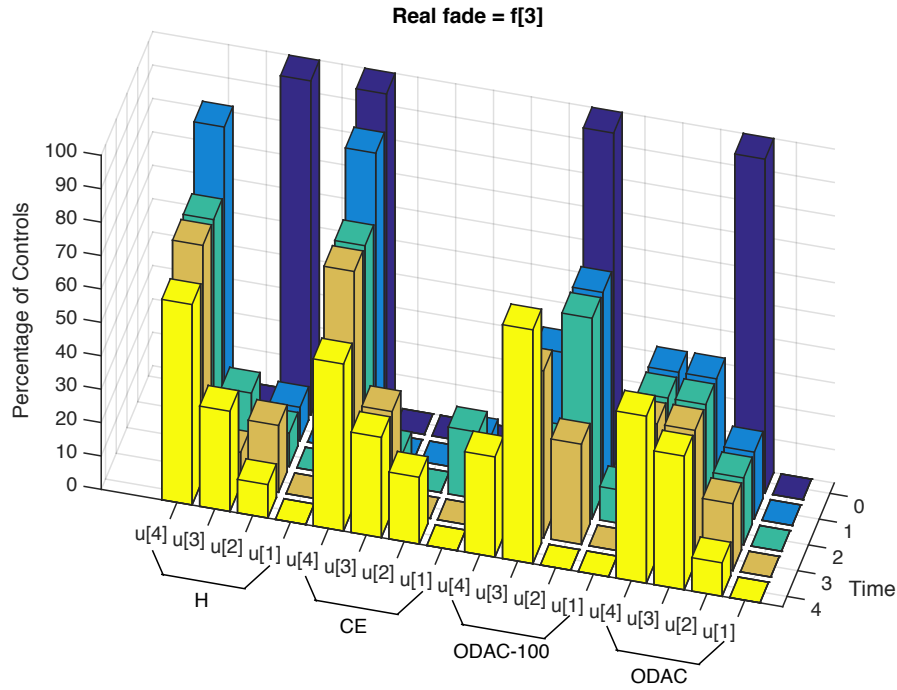
#### 4.4.2 Examination of control laws

Figure 4.3 is a collection of 20 histograms of the optimal control sequences,  $u_0^*$  through  $u_4^*$ , averaged over the 10 different channel noise realizations. The histograms are indexed by time 0-4 (also indicated by color) and by control law H, CE, ODAC-100, ODAC. Fade  $f[3] = -3\text{dB}$  is the actual fade of the channel and from (4.20),

$$\pi_0 = [0.35, 0.15, 0.1, 0.4].$$

We offer the following observations regarding Figure 4.3.

- The histograms in Figure 4.3 for time 0 demonstrate Remark 6, that the initial control  $u_0^*$  for ODAC is a function solely of  $\pi_0$  and does not depend on the noise realization. This also holds for the other three control policies, although each controller selects its own value of  $u_0^*$ . This is shown by a single value of the initial control for each policy occurring for every realization.
- As expected, ODAC-100 is the most reliable in terms of selecting the correct power level by the terminal time, followed by ODAC. This reflects the choice of the terminal cost function in ODAC-100 to emphasize probing.



**Figure 4.3:** Histograms of control values averaged over 10 realizations of the noise for each adaptive control scheme vs. time. The real fade is equal to  $f[3] = -3\text{dB}$ .

- This example has a particularly poorly informed  $\pi_0$  in (4.20). The actual fade value has a priori probability 0.1. Indeed,  $\pi_0$  is rather uninformative and we see that ODAC, (and therefore) H and ODAC-100 select larger control values early than does CE. This is probing to resolve the actual fade. This is costly but to obtain full benefits of probing a long time horizon must be used [84].

All other histograms corresponding with the rest of the real fade values in the set of the fade,  $f$ , are plotted in Figure 4.4, Figure 4.5 and Figure 4.6 for  $f[1]$ ,  $f[2]$  and  $f[4]$ , respectively. Notice that  $f[4]$  has the largest value of probability as in  $\pi_0$  (4.20). As a result, the optimal control value  $u[4]$  is much easier to be chosen by all the control policies compared to previous cases. In general, looking at the plots of histograms of the controls, one can see that the larger value the fade probability is in  $\pi_0$  (4.20), the easier it is for the control policies to choose the correct transmitted power  $u^*$ . Therefore the difference between ODAC and ODAC-100 and CE and H is less evident than in the case

where the probability of the real fade is low.

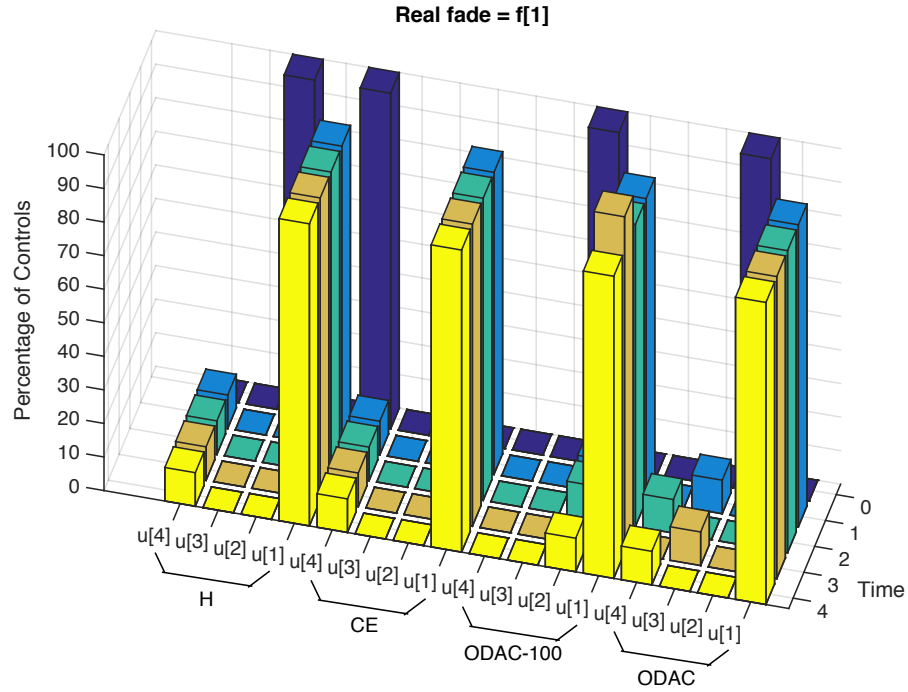


**Figure 4.4:** Histograms of control values averaged over 10 realizations of the noise for each adaptive control scheme vs. time. The real fade is equal to  $f[1] = -17\text{dB}$ .

Figure 4.7 depicts the evolution of the information states for the above trial, again averaged over the same 10 realizations of the noise but for two different values of the real fade:  $f[3]$  (upper) and  $f[4]$  (lower).

The two collections of histograms in Figure 4.7 illustrate, for each control policy, the evolution of the information state averaged over 10 different noise sequences, with differing real fade values. Note that  $f[3]$  has low a priori probability in (4.20), while  $f[4]$  has maximal a priori probability. This highlights the control value of the quality of the initial information state. From a mobile communications perspective, where fade estimation is part of every transmitted packet, the propagation of  $\pi_N$  from one packet to provide as accurate as possible value of  $\pi_0$  for the next is important. This demonstrates the substance of Heuristic 2.

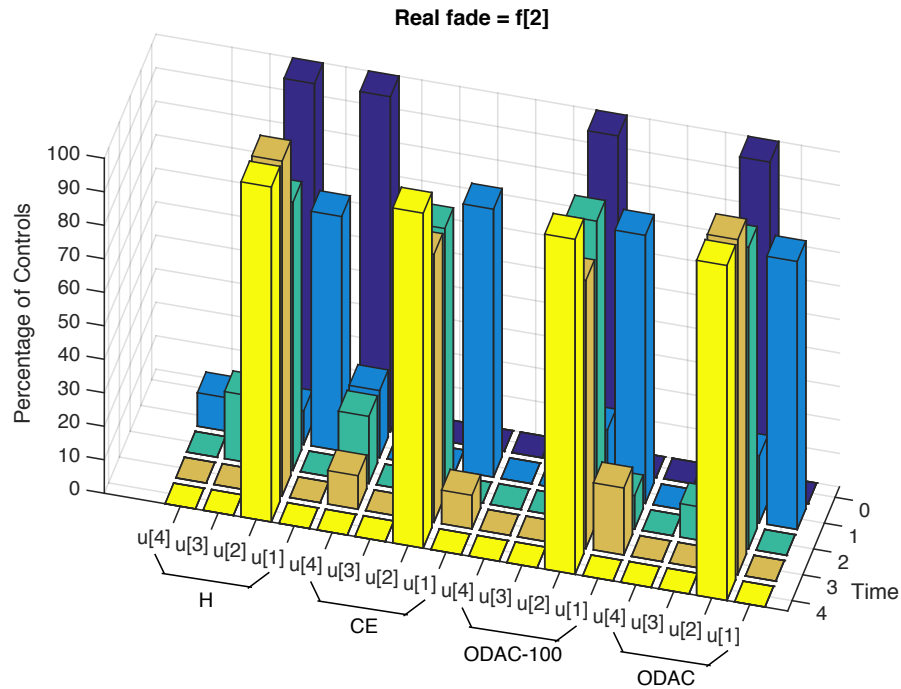


**Figure 4.5:** Histograms of control values averaged over 10 realizations of the noise for each adaptive control scheme vs. time. The real fade is equal to  $f[2] = -7\text{dB}$ .

For the rest of the real fade values, Figure 4.8 shows the plot of the evolution of the information states averaged over the same 10 realizations of the noise but for two different values of the real fade:  $f[1]$  (upper) and  $f[2]$  (lower).

## 4.5 Conclusion

In this chapter, we realize that the mobile wireless power control problem in communication system is stochastic optimal control problem. The problem is found to exhibit features of dual adaptive control: for probing, the MS transmitter tends to use big control (transmitted power) values to refine the study of the channel to aid the power control process; on the other hand, for regulation, the MS tends to select small control values to minimize the cost functions, which take into account the total energy spent on transmission to make the adaptation possible. The two aspects however are in conflict. A

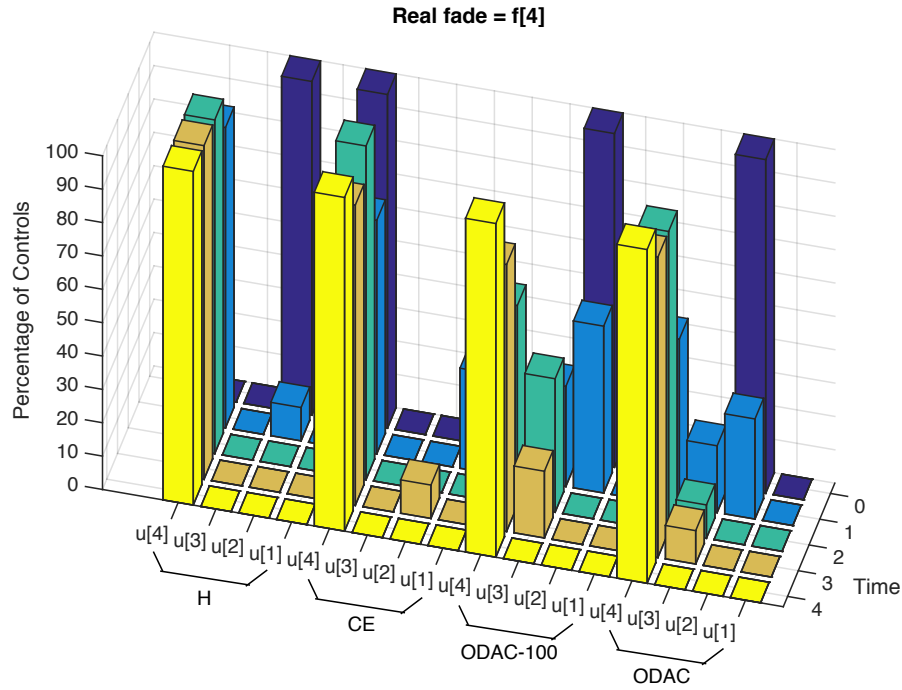


**Figure 4.6:** Histograms of control values averaged over 10 realizations of the noise for each adaptive control scheme vs. time. The real fade is equal to  $f[4] = 0\text{dB}$ .

good control policy must strike a balance between the dual characters.

We have considered the problem in a simplified setting, where the MS and BS can share their information about the system. Further, it is assumed that some *a priori* information of the fading is known in advance. Belonging to stochastic optimal control and dual adaptive control, the problem can be solved by the SDP algorithm, with the aid of the information state that describes the evolution of the statistics of the fade from the initial known information about the channel. This evolution is based on the future controls and measurements. Despite its primitive form, this is among the first times ODAC has been applied to understand a real-life commercial application of great significance, while the other applications of DAC have been suboptimal. The dual feature of the problem manifests on the optimal controller ODAC that strikes a balance between the two makes for a minimization of the performance index (4.21).

Once the solutions to the power control problem in the framework of ODAC

are obtained, we draw heuristics based on our findings. From the heuristics, we derive some other control policies that potentially help reduce the computational complexity of the ODAC solutions due the notorious curse of dimensionality appearing in Bellman's equation. The other control policies considered here do not have the dual feature which result in higher performance indices, especially in the case of CE that does not offer probing at all. One can alter the balance of the dual feature by adjusting the penalties on estimation and regulation, depending on the nature of the problem. The adjustment will inevitably result in a higher performance index but might be more suitable to the purposes of the desirable control policy.

The superior performance of ODAC, however, comes at a cost of computational complexity and time, which grows extremely rapidly with the time horizon in the SDP algorithm, which we have demonstrated in Table 4.2. This can be greatly alleviated with the realization that  $u_0^*$  is the most expensive and time consuming to compute, but on the other hand is a deterministic function only of the *a priori* information,  $\pi_0$ . Following this observation, rules can be devised to select  $u_0$  based on  $\pi_0$ . This helps reduce the computational time by an enormous amount, e.g. a factor of 500,000 in our example. This, in turn, implies a step forward in implementing the power control algorithm we have proposed to real-life applications in communication systems, even though the computational time is still far too high to be usable. This fact demonstrates what it takes to be optimal in power control.

Chapter 4, in full, is currently being prepared for submission for publication of the material, by M. H. Ha and R. R. Bitmead. The dissertation author was the primary investigator and author of this material.

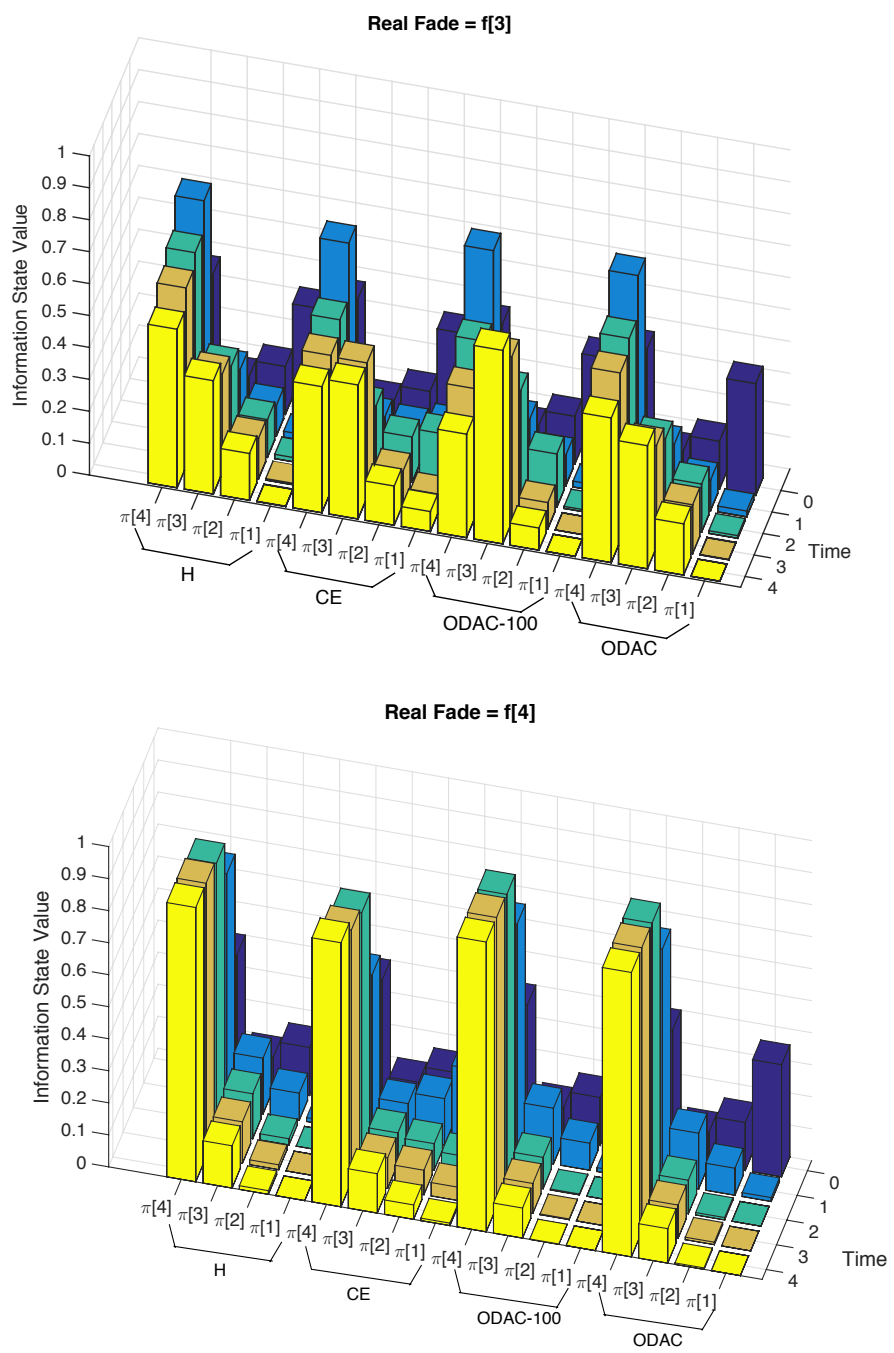


**Figure 4.7:** Evolution of the information state averaged over 10 realizations of the noise for each adaptive control scheme vs. sample time. Upper plot: real fade is  $f[3]$ . Lower plot: real fade is  $f[4]$ .

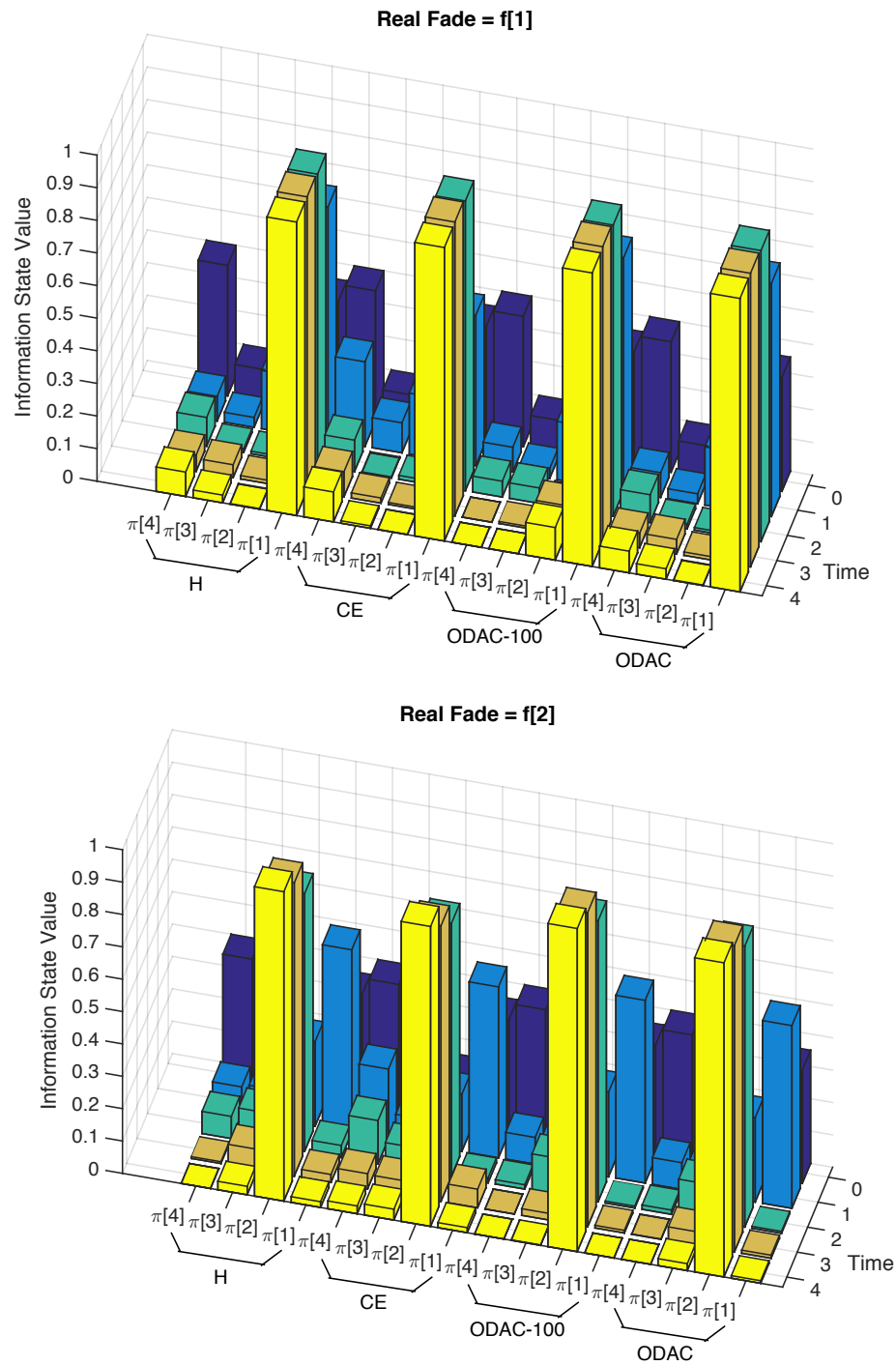


**Figure 4.8:** Evolution of the information state averaged over 10 realizations of the noise for each adaptive control scheme vs. sample time. Upper plot: real fade is  $f[1]$ . Lower plot: real fade is  $f[2]$ .



# Chapter 5

## Conclusion & Future Direction

### 5.1 Conclusion

Throughout Chapter 2, realizing that power control in communication systems is an adaptive system, we have examined the total energy cost in power control, including the energy cost of adaptation, spent by the MS transmitter. We have posed a power control under the setting of a communication system with a complex channel and complex signal, corrupted by circularly symmetric complex noise. Using a number of pilot tones, the LS estimate of the channel is computed. Based on the channel estimate, the signal and then noise powers are calculated, that allows the SNR estimate to be determined. There exists a conundrum in the algorithm, in which to minimize the variance of the SNR estimate, the MS transmitter should use an infinite number of pilot symbols transmitted at zero power. Using the SNR estimate, which is an  $\mathcal{F}$  distribution, an appropriate transmitted power level for the actual message data symbols can be chosen to overcome the fading environment, which concludes the power control algorithm. We have then formulated the total energy cost of the whole power control process, including the energy cost of adaptation. Based on the statistics of the SNR estimate, this total energy cost is calculated,

factoring in 3 cases: the transmitter chooses a satisfactory transmitted power level, a power level higher than necessary and one that is too low. While the second results in wasted energy, the last case necessitate a retransmission, which in turn includes also the re-estimate of SNR, basically a restart of the whole power control process.

The total energy cost of power control is then analyzed via simulations. It was found to exhibits a pathological behavior, in which to conserve the energy, the transmitter should use an infinite number of pilot tones at zero transmitted power to obtain the smallest energy cost possible. This behavior is the same as the optimal strategy to minimize the variance of the SNR estimate. However, when the MS transmitter is assumed to have a velocity, the total energy cost is modified to take into account the change in the channel condition due to the MS mobility. The above pathological behavior of the total energy cost disappears when the MS mobility is introduced. In this case, there exists an optimal pilot length  $K$  and pilot transmitted power  $P_0$  that results in the smallest minimum of the total energy cost across the range of the pilot transmitted power.

In the end of Chapter 2, we have also propose a non-data-aided, or blind adaptation, technique, that is to eliminate the use of pilot sequences, to apply to the power control problem. It is, however, found that in the setting of mobile wireless communication, the blind adaptation algorithm takes too long to compute the BER of the link, making it unimplementable.

In the next chapters, realizing that the mobile wireless power control problem is at its core a stochastic dual adaptive optimal control problem, we have demonstrated an application of SDP to a much simplified version of the problem, where it is assumed that the MS and BS can share their information about the system. This greatly simplifies the solutions obtained via SDP, with the aid of the information state that describes the evolution of the statistics of the fade from the initial known information about the channel. This evolution is based on the future measurements and controls. Despite its primitive

form, this is among the first times ODAC has been applied to understand a real-life commercial application of great significance. The dual feature of the problem manifests on probing, that tends to use big control (transmitted power from the MS) values to refine the information state, and regulation, that tends to select small control values to minimize the cost functions, which take into account the total energy spent on transmission to make the adaptation possible. The optimal controller ODAC that strikes a balance between the two makes for a minimization of the performance index (4.21).

Once the solutions to the power control problem in the framework of ODAC are obtained, we draw heuristics based on our findings. From the heuristics, we derive some other control policies that potentially help reduce the computational complexity of the ODAC solutions due the notorious curse of dimensionality appearing in Bellman's equation. The other control policies considered here do not have the dual feature which result in higher performance indices, especially in the case of CE that does not offer probing at all. One can alter the balance of the dual feature by adjusting the penalties on estimation and regulation, depending on the nature of the problem. The adjustment will inevitably result in a higher performance index but might be more suitable to the purposes of the desirable control policy.

The superior performance of ODAC, however, comes at a cost of computational complexity and time, which grows extremely rapidly with the time horizon in the SDP algorithm, which we have demonstrated in Table 4.2. This can be greatly alleviated with the realization that  $u_0^*$  is the most expensive and time consuming to compute, but on the other hand is a deterministic function only of the *a priori* information,  $\pi_0$ . Following this observation, rules can be devised to select  $u_0$  based on  $\pi_0$ . This helps reduce the computational time by an enormous amount, e.g. a factor of 500,000 in our example. This, in turn, implies a step forward in implementing the power control algorithm we have proposed to real-life applications in communication systems, even though the

computational time is still far too high to be usable. This fact demonstrates what it takes to be optimal in power control.

## 5.2 Future direction

For future work, we shall go back to the formulation presented in Section 4.1 and consider a more realistic problem. By this, we remove the assumption that the communication link between the MS and BS is perfect. The two are no longer able to share their information about the system. The MS and BS can now be seen as two separate controllers that communicate via some link denoted as  $t_k$ . This is a much harder problem since the signaling between MS and BS is difficult to be incorporated to the ODAC scenario, and requires knowledge in other fields beyond regular adaptive and stochastic optimal control.

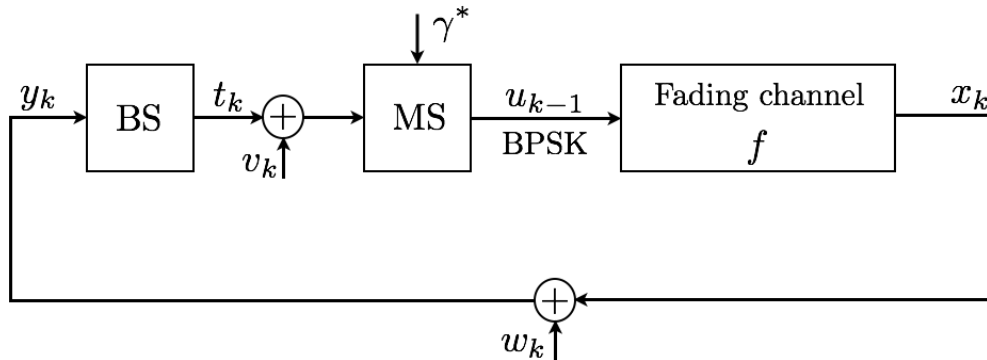


**Figure 5.1:** The full-scale problem in power control. The MS and BS are no longer able to share their information. The communication link between the two can be described by  $t_k$ , corrupted by AWGN  $v_k$ .

The full problem described above is demonstrated in Figure 5.1. The control signals of the MS and BS can be seen as  $u_{k-1}$  and  $t_k$ , respectively. We now need to formulate the dynamics of the two separately. Taking into account the noise in-between

the MS and BS,  $v_k$ , the dynamics of the MS can be expressed as

$$\begin{cases} x_k^{MS} = t_k \\ y_k^{MS} = t_k + v_k, \end{cases} \quad (5.1)$$

and of the BS

$$\begin{cases} x_k^{BS} = x_k = f u_{k-1} \\ y_k^{BS} = x_k + w_k = f u_{k-1} + w_k. \end{cases} \quad (5.2)$$

The objective is to minimize a performance index that is in a similar form to (4.21) but also takes  $t_k$  into account. While this still falls in the framework of dual adaptive control, we are not certain if the solutions to this problem can still be obtained via the SDP algorithm, since the complexity is beyond what we have considered here.

This stochastic optimal control problem greatly resembles Witsenhausen's counterexample [105] that has remained unsolved since its formulation - some recent articles related to Witsenhausen's counterexample are [106, 107, 108, 109]. However, it is even more complex than Witsenhausen's counterexample in the sense that the BS does not have access to perfect observations of the state  $x_k$ , as it is assumed in Witsenhausen's counterexample, and the control signal  $u_{k-1}$  of the MS is costly, more so than that of the BS in terms of the battery life of the MS. Witsenhausen's counterexample assumes the inverse of the latter statement. The derivation of the signaling solution  $t_k$  makes it even harder, not to mention the methodology in implementing  $t_k$  into the framework of stochastic optimal control.

Suppose that the MS and BS both have their own information state, denoted  $\pi_k^{MS}$  and  $\pi_k^{BS}$  respectively, with a mutual *a priori* information  $\pi_0$  which is the given initial distribution of the fade,  $f$ . The information states are updated following (5.1) and (5.2),

that is, it is updated based on the future measurements and controls of both the MS and BS. If the optimal controls could be obtained via SDP employed for both the MS and BS, the implementation of the algorithm for the MS is different from that for the BS. The two SDP algorithms have to be carried out online and simultaneously, as they greatly depend upon the solutions of the other. The combined algorithm, beside its anticipated profound complexity to derive, requires tremendous computational power that is far more demanding than the example we have presented previously.

Furthermore, we shall face a great difficulty in that the information state of the MS must include the knowledge about the BS, which contains knowledge about the MS itself, which in turn includes the knowledge about the BS. This beliefs propagation grows rather very rapidly. This complexity may render the problem intractable in the framework of SDP. This could be dealt with using the notion of bounded rationality [110] in stochastic cooperative game theory.

In [111], the authors considered a multi-agent setup, where the agents neglect the fact that they are mutually dependent through the environment. However, by interacting with the environment, they in turn alter the empirical observation of the others. This model allows each agent to face a Markov decision process instead of a partially observable Markov decision process, whose implementation is intractable due to beliefs propagation. Given enough an amount of measurements, each agent then develops its own model based on empirical observations that changes the environment. Due to the changes, the agents then compute new models and adjust their actions. This is best demonstrate in Figure 5.2. It has been shown that a convergence exists for this process, which the authors called empirical evidence equilibrium. However, due to the assumptions that the agents do not communicate with each other and that they need a large enough number of empirical observations, the formulation does not fit into our problem where the MS and BS are connected via the transmission  $t_k$ , and implementation time is crucial. Nevertheless, this

scheme is feasible if one could collect the data and carry out the algorithm offline long enough for the policies to converge to the empirical evidence equilibrium.

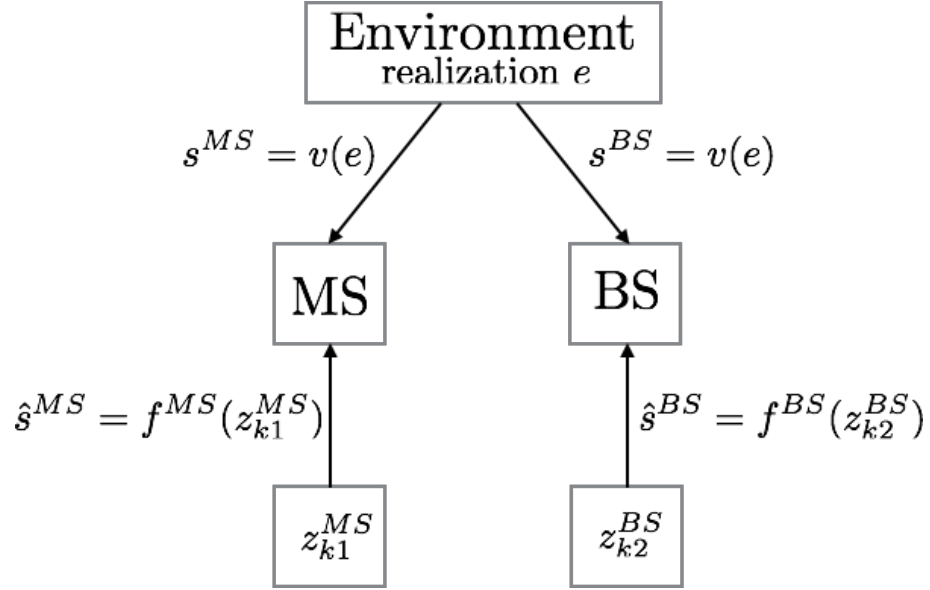


**Figure 5.2:** Full-scale power control in mobile wireless communications in the framework of [111]. Here  $z_{k1}^{MS}$  and  $z_{k2}^{BS}$  represent the vectors containing the last  $k1$  and  $k2$  observed signals of the MS and  $k2$  of the BS, respectively. Based on the depth- $k1$  and  $k2$  consistency, the MS and BS continuously reformulate their respective models of the environment and change their actions accordingly.  $k1$  and  $k2$  must be large enough for the policies to converge.

There have been attempts to deal with similar power control problems using a different than the traditional 2dBm step size in MS transmitted power. For example, the MS transmitted power is changed by a power of 2dBm steps based on the number of consecutive requests from BS to change the transmitted power in one direction [112]. In [113], the MS changes the transmitted power at a step size formulated as the product of a basic step sized based on its velocity, and a weighing factor chosen by a seemingly random rule based on 3 most recent consecutive command bits sent from the BS. In [114], the authors used a fixed step size based on the difference between the actual link SNR and the target SNR collected over a certain period of time. The common feature

of these papers is that there is no solid foundation for choosing the adaptive schemes, and certainly their control policies are not optimal. Nevertheless, they attempt to solve problems that are similar to our full-scale problem. However, the anticipation is that their solutions would be a special case of the solutions to our problem, if it would ever be obtained.

Much similar to the ODAC problem solved here that has led to heuristics, so too in the full-scale problem shall we need an heuristic solution. Once this is done, the adaptation in power control of communication systems will gain a huge advance compared to what has been being done currently.



# Bibliography

- [1] K. Åström and B. Wittenmark, *Adaptive Control*. Reading, Massachusetts: Addison-Wesley, 1989.
- [2] A. Mehrotra, *GSM System Engineering*, ser. Mobile Communications. Norwood, MA: Artech House, Inc., 1997.
- [3] K. Åström, “Theory and applications of adaptive control - A survey,” *Automatica*, vol. 19, no. 5, pp. 471–486, 1983.
- [4] L. W. Taylor and E. J. Adkins, “Adaptive control and the X-15,” in *Proc. Princeton University Conf. on Aircraft Flying Qualities*, Princeton University, 1965.
- [5] J. A. Aseltine, A. R. Mancini, and C. W. Sature, “A survey of adaptive control systems,” *IRE Trans.*, vol. AC-6, 1958.
- [6] O. R. Jacobs, “A review of self-adjusting systems in automatic control,” *Journal of Electronics and Control*, vol. 10, p. 311, 1961.
- [7] R. B. Asher, D. Adrisani, and P. Dorato, “Bibliography on adaptive control systems,” *IEEE Proc.*, vol. 64, p. 1126, 1976.
- [8] K. S. Narendra and R. V. Monopoli, *Applications of adaptive control*. New York: Academic Press, 1980.
- [9] C. J. Harris and S. A. Billings, *Self-tuning and adaptive control: Theory and applications*. London: Peter Peregrinus, 1981.
- [10] H. Unbehauen, *Methods and applications in adaptive control*. Berlin: Springer, 1980.
- [11] ETSI, *Digital cellular telecommunications system (phase 2+); Radio transmission and reception (3GPP TS45.005)*, v10.3.0 release 10 ed., ETSI, France, Jan. 2012.
- [12] ———, *Digital cellular telecommunications system (phase 2+); Radio subsystem link control (3GPP TS05.08)*, v8.23.0 release 1999 ed., ETSI, France, Dec. 2005.

- [13] C. U. Saraydar, N. B. Mandayam, and D. J. Goodman, "Efficient power control via pricing in wireless data networks," *IEEE Trans. Comm.*, vol. 50, no. 2, pp. 291–303, Feb. 2002.
- [14] V. Shah, N. B. Mandayam, and D. J. Goodman, "Power control for wireless data based on utility and pricing," in *Proc. IEEE PIMRC Conf.*, 1998, pp. 1427–1432.
- [15] H. Ji and C. Huang, "Non-cooperative uplink power control in cellular radio systems," *Wireless Networks*, vol. 4, no. 3, pp. 233–240, April 1998.
- [16] T. Elbatt and A. Ephremides, "Joint scheduling and power control for wireless ad-hoc networks," *IEEE Trans. on Wireless Comm.*, vol. 3, no. 1, pp. 74–85, Jan. 2004.
- [17] F. Meshkati, H. V. Poor, S. C. Schwartz, and N. B. Mandayam, "An energy-efficient approach to power control and receiver design in wireless data networks," *IEEE Trans. Comm.*, vol. 53, no. 11, pp. 1885–1894, Nov. 2005.
- [18] D. Feng, C. Jiang, G. Lim, L. Cimini, G. Feng, and G. Y. Li, "A survey of energy-efficient wireless communications," *IEEE Comm. Surveys and Tutorials*, vol. 15, no. 1, pp. 167–178, 2013.
- [19] V. P. Singh and K. Kumar, "Literature survey on power control algorithms for mobile ad-hoc networks," *Wireless Pers. Comm.*, vol. 60, pp. 679–685, 2011.
- [20] D. Tse and P. Viswanath, *Fundamentals of wireless communication*. Cambridge Univ. Press, 2005.
- [21] A. Goldsmith, *Wireless Communications*. Cambridge University Press, 2005.
- [22] D. L. Goeckel, "Adaptive coding for time-varying channels using outdated fading estimates," *IEEE Trans. on Comm.*, vol. 47, no. 6, pp. 844–855, June 1999.
- [23] S. G. Chua and A. Goldsmith, "Variable-rate variable-power MQAM for fading channels," *IEEE 46th Veh. Tech. Conf.*, vol. 2, pp. 815–819, 1996.
- [24] K. Balachandran, S. R. Kadaba, and S. Nanda, "Channel quality estimation and rate adaptation for cellular mobile radio," *IEEE JSAC*, vol. 17, no. 7, pp. 1244–1256, July 1999.
- [25] Y. Chi, A. Gomaa, N. Al-Dhahir, and A. R. Calderbank, "Training sequence design and tradeoffs for spectrally-efficient multi-user MIMO-OFDM systems," *IEEE Trans. on Wireless Comm.*, vol. 10, no. 7, pp. 2234–2245, July 2011.
- [26] R. M. Gagliardi and C. M. Thomas, "PCM data reliability monitoring through estimation of signal-to-noise ratio," *IEEE Trans. on Comm. Tech.*, vol. Com-16, no. 3, pp. 479–486, June 1968.

- [27] S. Adireddy, L. Tong, and H. Viswanathan, "Optimal placement of training for frequency selective block-fading channels," *IEEE Trans. Inform. Theory*, vol. 48, pp. 2338–2353, Aug. 2002.
- [28] B. Hassibi and B. M. Hochwald, "How much training is needed in multiple-antenna wireless links?" *IEEE Trans. Inform. Theory*, vol. 49, no. 4, pp. 951–963, April 2003.
- [29] S. Ohno and G. B. Giannakis, "Optimal training and redundant precoding for block transmissions with application to wireless OFDM," *IEEE Trans. Comm.*, vol. 50, no. 12, pp. 2113–2123, Dec. 2002.
- [30] M. Dong and L. Tong, "Optimal design and placement of pilot symbols for channel estimation," *IEEE Trans. Signal Processing*, vol. 50, no. 12, pp. 3055–3069, Dec. 2002.
- [31] R. Negi and J. Cioffi, "Pilot tone selection for channel estimation in a mobile wireless OFDM system," *IEEE Trans. Comm. Elec.*, vol. 44, pp. 1122–1128, Aug. 1998.
- [32] F. Ling, "Optimal reception, performance bound, and cutoff rate analysis of references-assisted coherent CDMA communications with applications," *IEEE Trans. Comm.*, vol. 47, pp. 1583–1592, Oct. 1999.
- [33] I. Barhumi, G. Leus, and M. Moonen, "Optimal training design for MIMO OFDM systems in mobile wireless channels," *IEEE Trans. Signal Processing*, vol. 51, no. 6, pp. 1615–1624, June 2003.
- [34] M. Engels, *Wireless OFDM systems: How to make them work*. Springer Science and Business Media, 2006.
- [35] P. Hoeher, S. Kaiser, and P. Robertson, "Two-dimensional pilot-symbol-aided channel estimation by Wiener filtering," in *Proc. ICASSP*, Munich, Germany, April 1997, pp. 1845–1848.
- [36] J. J. van de Beek, O. Edfors, M. Sandell, S. K. Wilson, and P. O. Borjesson, "On channel estimation in OFDM system," in *Proc. IEEE 45th V.T.C Conf.*, Chicago, IL, 1995, pp. 815–819.
- [37] S. Coleri, M. Ergen, A. Puri, and A. Bahai, "Channel estimation techniques based on pilot arrangement in OFDM systems," *IEEE Trans. on Broadcasting*, vol. 48, no. 3, pp. 223–229, Sept. 2002.
- [38] F. Sanzi, S. Jeltin, and J. Speidel, "A comparative study of iterative channel estimators for mobile OFDM systems," *IEEE Trans. Wireless Comm.*, vol. 2, no. 5, pp. 849–859, Sept. 2003.

- [39] M. Morelli and U. Mengali, "A comparison of pilot-aided channel estimation methods for OFDM systems," *IEEE Trans. Signal Processing*, vol. 49, no. 12, pp. 3065–3073, Dec. 2001.
- [40] O. Edfors, M. Sandell, J. J. van de Beek, S. K. Wilson, and P. O. Borjesson, "OFDM channel estimation by singular value decomposition," *IEEE Trans. Comm.*, vol. 46, no. 7, pp. 931–939, July 1998.
- [41] M. Hsieh and C. Wei, "Channel estimation for OFDM systems based on comb-type pilot arrangement in frequency selective fading channels," *IEEE Trans. Consumer Elec.*, vol. 44, no. 1, pp. 217–225, Feb. 1998.
- [42] *Mobile Radio Communications*. London, England: Pentech Press Limited, 1992.
- [43] J. Rinne and M. Renfors, "Pilot spacing in orthogonal frequency division multiplexing systems on practical channels," *IEEE Trans. Consumer Elec.*, vol. 42, pp. 959–962, Nov. 1996.
- [44] Y. Li, L. J. C. Jr., and N. R. Sollenberger, "Robust channel estimation for OFDM systems with rapid dispersive fading channels," *IEEE Trans. Comm.*, vol. 46, pp. 902–915, July 1998.
- [45] Y. Le, "Pilot-symbol-aided channel estimation for OFDM in wireless systems," *IEEE Trans. Veh. Tech.*, vol. 48, pp. 1207–1215, July 2000.
- [46] H. J. Su and E. Geraniotis, "Improved performance of a PSAM system with iterative filtering and coding," in *Proc. 36th Annu. Allerton Conf. Comm.*, Sept. 1998, pp. 156–166.
- [47] T. Keller and L. Hanzo, "Adaptive multicarrier modulation: a convenient framework for time-frequency processing in wireless communications," in *Proc. IEEE*, vol. 88, no. 5, May 2000, pp. 611–640.
- [48] T. A. Summers and S. G. Wilson, "SNR mismatch and online estimation in turbo decoding," *IEEE Trans. Comm.*, vol. 46, pp. 421–423, April 1998.
- [49] K. Balachandran, S. R. Kadaba, and S. Nanda, "Channel quality estimation and rate adaptation for cellular mobile radio," *IEEE Jour. on Selected Areas in Comm.*, vol. 17, pp. 1244–1256, July 1999.
- [50] R. B. Kerr, "On signal and noise level estimation in a coherent PCM channel," *IEEE Trans. Aerosp. Elec. Syst.*, vol. AES-2, pp. 450–454, July 1966.
- [51] M. K. Simon and A. Mileant, "SNR estimation for the baseband assembly," in *JPL, Telecomm. and Data Acquisition Prog. Rep.*, Pasadena, CA, May 1986, pp. 42–85.
- [52] T. R. Benedict and T. T. Soong, "The joint estimation of signal and noise from the sum envelope," *IEEE Trans. Inform. Theory*, vol. IT-13, pp. 447–454, July 1967.

- [53] R. Matzner, "An SNR estimation algorithm for complex baseband signals using higher order statistics," *Facta Universitatis (Nis)*, no. 6, pp. 41–52, 1993.
- [54] R. Matzner and F. Engleberger, "An SNR estimation algorithm using fourth-order moments," in *Proc. IEEE Int'l Symp. on Info. Theory*, Trondheim, Norway, June 1994, p. 119.
- [55] D. R. Pauluzzi and N. C. Beaulieu, "A comparison of SNR estimation techniques for the AWGN channel," *IEEE Trans. on Comm.*, vol. 48, no. 10, pp. 1681–1691, Oct. 2000.
- [56] S. Boumard, "Novel noise variance and snr estimation algorithm for wireless MIMO OFDM systems," in *Proc. IEEE Global. Telecomm. Conf.*, Dec 2003, pp. 1330–1334.
- [57] X. Xu, Y. Jing, and X. Yu, "Subspace-based noise variance and snr estimation for OFDM systems," in *Proc. IEEE Mobile Radio Applications Wireless Comm. Networking Conf.*, Mar. 2005, pp. 23–26.
- [58] G. Ren, H. Zhang, and Y. Chang, "SNR estimation algorithm based on the preamble for OFDM systems in frequency selective channels," *IEEE Trans. Comm.*, vol. 57, no. 8, pp. 2230–2234, Aug. 2009.
- [59] H. Arslan and S. Reddy, "Noise power and SNR estimation for OFDM based wireless communication systems," in *Proc. of 3rd IASTED Intl. Conf. Wireless and Optical Comm.*, Alberta, Canada, 2003.
- [60] M. Zivkovic and R. Mathar, "Preamble-based snr estimation in frequency selective channels for wireless OFDM systems," in *Veh. Tech. Conf. VTC Spring 2009*, Barcelona, Spain, April 2009, pp. 1–5.
- [61] Y. Li, "Blind SNR estimation of OFDM signals," in *IEEE 2010 Intl. Conf. on Microwave and Millimeter Wave Tech.*, Australia, 2010, pp. 1792–1796.
- [62] R. G. Gallager, *Principles of Digital communication*, 1st ed. Cambridge, 2008.
- [63] M. Abramowitz and I. A. Stegun, *Handbook of mathematical functions*, 9th ed., ser. Applied Mathematics Series 55. Washington D.C.: National Bureau of Standards, U.S. Government Printing Office, Nov. 1970.
- [64] D. Tse and P. Viswanath, *Fundamentals of wireless communication*. Cambridge University Press, 2005.
- [65] J. H. Stapleton, *Linear statistical models*. John Wiley & Sons, 1995.
- [66] W. G. Cochran, "The distribution of quadratic forms in a normal system, with applications to the analysis of covariance," *Mathematical Proc. of the Cambridge Philosophical Society*, vol. 30, no. 2, pp. 178–191, April 1934.

- [67] *Linear algebra and linear models*, 2nd ed. Springer, 2000.
- [68] P. Billingsley, *Probability and measure*. New York, NY: John Wiley & Sons, 1979.
- [69] R. Clarke, “A statistical theory of mobile radio reception,” *Bell Systems Technical Journal*, pp. 957–1000, July-Aug. 1968.
- [70] M. Schwartz, *Mobile Wireless Communications*. Cambridge University Press, 2005.
- [71] M. Siddiqui, “Statistical inference for Rayleigh distributions,” *Radio Science Journal of Research NBS/USNC-URSI*, vol. 68D, no. 9, pp. 1005–1010, Sept. 1964.
- [72] M. Saily, G. Sebire, and E. Riddington, *GSM/EDGE evolution and performance*. Wiley, 2011.
- [73] J. P. M. de Sa, *Applied statistics using SPSS, STATISTICA, MATLAB and R*. Springer, 2007.
- [74] A. Fel’dbaum, “Dual-control theory,” *Automn. Remote Control*, vol. 21, pp. 874–880, 1960.
- [75] ———, “Dual-control theory,” *Automn. Remote Control*, vol. 22, pp. 1–12, 109–121, 1961.
- [76] ———, *Optimal Control Systems*. New York, NY: Academic Press, 1965.
- [77] B. Wittenmark, “Adaptive dual control methods: An overview,” *Proceedings of the 5<sup>th</sup> IFAC Symposium on Adaptive Control and Signal Processing* Budapest, pp. 67–72, 1995.
- [78] P. R. Kumar and P. Varaiya, *Stochastic Systems: Estimation, Identification, and Adaptive Control*. Englewood Cliffs, NJ: Prentice-Hall, 1986.
- [79] K. J. Åström and B. Wittenmark, *Adaptive Control*, 2<sup>nd</sup> ed. Don Mills, Canada: Addison - Wesley, 1995.
- [80] R. Bellman, *Adaptive Control Processes*. Princeton: Princeton University Press, 1966.
- [81] Y. Bar-Shalom and E. Tse, “Caution, probing, and the value of information in the control of uncertain systems,” *Annals of Economic and Social Measurement*, vol. 5, no. 3, pp. 323–337, 1976.

- [82] K. Astrom, "Optimal control of Markov processes with incomplete state information," *Journal of Mathematical Analysis and Applications*, vol. 10, pp. 174–205, 1965.
- [83] J. Sternby, "A simple dual control problem with an analytical solution," *IEEE Transactions on Automatic Control*, vol. 21, no. 6, pp. 840–844, Dec. 1976.
- [84] K. Astrom and A. Helmersson, "Dual control of an integrator with unknown gain," *Computers and Mathematics with Applications*, vol. 12A, no. 6, pp. 653–662, 1986.
- [85] T. Bohlin, "Optimal dual control of a simple process with unknown gain," in *Technical Paper PT 18.196, IBM Nordic Laboratory*, Lidings, Sweden, 1969.
- [86] B. Bernhardsson, "Dual control of a first-order system with two possible gains," *Intl. J. of Adaptive Control and Signal Processing*, vol. 3, pp. 15–22, 1989.
- [87] N. Filatov and H. Unbehauen, *Adaptive dual control*. New York: Springer, 2004.
- [88] R. Milito, C. S. Padilla, R. A. Padilla, and D. Cadorin, "An innovations approach to dual control," *IEEE Transactions on Automatic Control*, vol. 27, pp. 132–137, 1982.
- [89] B. Wittenmark and C. Elevitch, "An adaptive control algorithm with dual features," in *Proc. 7th IFAC/IFORS Symp. on Identification and System Parameter Estimation*, York, UK, 1985, pp. 587–592.
- [90] B. Lindoff, J. Holst, and B. Wittenmark, "Analysis of approximations of dual control," *International Journal of Adaptive Control and Signal Processing*, vol. 13, pp. 593–620, 1999.
- [91] E. Tse and Y. Bar-Shalom, "Actively adaptive control for nonlinear stochastic systems," *Proc. of the IEEE*, vol. 64, no. 8, pp. 1172–1181, 1976.
- [92] K. Åström and B. Wittenmark, "Problems of identification and control," *Journal of Mathematical Analysis and Applications*, vol. 34, pp. 90–113, 1971.
- [93] B. Allison, J. Ciarniello, P. Tessier, and G. Dumont, "Dual adaptive control of chip refiner motor load," *Automatica*, vol. 31, no. 8, pp. 1169–1184, 1995.
- [94] A. Ismail and G. Dumont, "Dual adaptive control of paper coating," *IEEE Trans. on Control Systems Technology*, vol. 11, no. 3, pp. 289–309, 2003.
- [95] M. Bugeja and S. Fabri, "Dual adaptive dynamic control of mobile robots using neural networks," *IEEE Trans. on Systems, Man, and Cybernetics, Part B*, vol. 39, no. 1, pp. 129–141, 2009.

- [96] N. Filatov and H. Unbehauen, “Nonlinear adaptive control of a laboratory-scale vertical take-off aircraft,” in *Proc. EURACO Workshop II on Robust and Adaptive Control of Integrated Systems*, Herrsching, Germany, 1996, pp. 27–34.
- [97] R. Silva, N. Filatov, J. Lemos, and H. Unbehauen, “Feedback/feedforward dual adaptive control of a solar collector field,” in *Proc. IEEE Int’l Conf. on Control App.*, Trieste, Italy, 1998, pp. 309–313.
- [98] T. Knohl, W. Xu, and H. Unbehauen, “Dual adaptive neural control and its application to Hammerstein systems,” in *Proc. Int’l Conf. of Control, Automation, Robotics and Vision*, Singapore, 2000, p. paper 116.
- [99] Y. Bar-Shalom, “Stochastic dynamic programming: caution and probing,” *IEEE Trans. Automat. Contr.*, vol. AC-26, no. 5, pp. 1184–1195, Oct. 1981.
- [100] D. P. Bertsekas, *Dynamic Programming and Optimal Control, Vol. 1*. Belmont, MA: Athena Scientific, 1995.
- [101] E. A. Lee and D. G. Messerschmitt, *Digital Communication*, 2nd ed. The Netherlands: Kluwer Academic Publishers, 1990.
- [102] D. P. Bertsekas, *Dynamic Programming and Stochastic Control*. New York, NY: Academic Press, 1976.
- [103] ———, *Dynamic Programming - Deterministic and Stochastic Models*. Englewood Cliffs, NJ: Prentice Hall, 1987.
- [104] F. Fahroo, L. Y. Wang, and G. Yin, Eds., *Recent advances in research on unmanned aerial vehicles*, ser. Lecture Notes in Control and Information Sciences. Springer, 2013, vol. 444.
- [105] H. Witsenhausen, “A counterexample in stochastic optimum control,” *SIAM J. Control*, vol. 6, pp. 131–147, 1968.
- [106] J. Lee, E. Lau, and Y. Ho, “The Witsenhausen counterexample: A hierarchical search approach for nonconvex optimization problems,” *IEEE Transactions on Automatic Control*, vol. 46, pp. 382–397, 2001.
- [107] P. Grover and A. Sahai, “Vector Witsenhausen counterexample as assisted interference suppression,” *Int. J. Syst., Control Comm. (Special Issue on Information Processing and Decision Making in Distributed Control Systems)*, vol. 2, pp. 197–237, 2010.
- [108] C. H. Papadimitriou and J. N. Tsitsiklis, “Intractable problems in control theory,” *SIAM J. Control Optimization*, vol. 24, no. 4, pp. 639–654, 1986.



- [109] M. Baglietto, T. Parisini, and R. Zoppoli, “Numerical solutions to the Witsenhausen counterexample by approximating networks,” *IEEE Trans. Automat. Contr.*, vol. 46, no. 9, pp. 1471–1577, 2001.
- [110] A. Rubinstein, *Modeling bounded rationality*. Cambridge, MA: MIT Press, 1998.
- [111] N. Dubebout and J. S. Shamma, “Empirical evidence equilibria in stochastic games,” in *IEEE 51st Annual Conference on Decision and Control*, Maui, Hawaii USA, Dec. 2012, pp. 5780–5785.
- [112] M. G. Cea, G. C. Goodwin, and T. Wigren, “Model predictive zooming power control in future cellular systems under coarse quantization,” in *IEEE Veh. Tech. Conf. (VTC Fall)*, Quebec City, QC, Sept. 2012, pp. 1–5.
- [113] H. Lee and D. Cho, “A new adaptive power control scheme based on mobile velocity in wireless mobile communication systems,” in *IEEE VTS 53rd V.T.C, VTC2001 Spring*, vol. 4, 2001, pp. 2878–2882.
- [114] M. R. Khan and P. C. Jain, “A simple modified fixed step size power control algorithm for CDMA cellular systems,” in *International Multimedia, Signal Processing and Communication Technologies, IMPACT 09*, Aligarh, March 2009, pp. 134–137.